NASA CR 189122
USAAVSCOM TR-92-C-010
Report No. EDR 15982



2

# COOLED HIGH-TEMPERATURE RADIAL TURBINE PROGRAM

## II – FINAL REPORT

by Dr. Philip H. Snyder

ALLISON GAS TURBINE DIVISION
GENERAL MOTORS CORPORATION
P.O. Box 420
Indianapolis, IN 46206-0420

May 1992

Prepared for
Lewis Research Center
Contract NAS3-24230





National Aeronautics and
Space Administration

Lewis Research Center
Cleveland, Ohio 44135
AC 216 433-4000

# REPORT DOCUMENTATION PAGE

*Form Approved*
*OMB No. 0704-0188*



**1. AGENCY USE ONLY** *(Leave blank)*

**2. REPORT DATE**

**3. REPORT TYPE AND DATES COVERED**
Final Contractor Report

**4. TITLE AND SUBTITLE**
Cooled High-Temperature Radial Turbine Program II - Final Report

**5. FUNDING NUMBERS**
WU- 505-62-0K
505-68-10
NAS3-24230

**6. AUTHOR(S)**
Dr. Philip H. Snyder

**7. PERFORMING ORGANIZATION NAME(S) AND ADDRESS(ES)**
Allison Gas Turbine Division
General Motors Corporation
P. O. Box 420
Indianapolis, IN 46206-0420

**8. PERFORMING ORGANIZATION REPORT NUMBER**
15982

**9. SPONSORING/MONITORING AGENCY NAMES(S) AND ADDRESS(ES)**
NASA Lewis Research Center
Cleveland, Ohio 44135-3191
and
Propulsion Directorate
U.S. Army Aviation Systems Command
Cleveland, Ohio 44135-3191

**10. SPONSORING/MONITORING AGENCY REPORT NUMBER**
NASA CR- 189122
USAAVSCOM TR-92-C-010

**11. SUPPLEMENTARY NOTES**
Richard J. Roelke, Project Manager
NASA Lewis Research Center
Cleveland, OH 44135

**12a. DISTRIBUTION/AVAILABILITY STATEMENT**
Unclassified - Unlimited
Subject Category - STAR Category 07

**12b. DISTRIBUTION CODE**

**13. ABSTRACT** *(Maximum 200 words)*

The objective of this program was the design and fabrication of a air-cooled high-temperature radial turbine (HTRT) intended for experimental evaluation in a warm turbine test facility at the Lewis Research Center. The rotor and vane were designed to be tested as a scaled version (rotor diameter of 14.4 inches diameter) of a 8.021 inch dia diameter rotor designed to be capable of operating with a rotor inlet temperature (RIT) of 2300°F, a nominal mass flow of 4.56 lbm/sec, a work level of equal or greater than 187 Btu/lbm, and an efficiency of 86% or greater. The rotor was also evaluated to determine it's feasibility to operate at 2500°F RIT. The rotor design conformed to the rotor blade flow path specified by NASA for compatibility with their test equipment. Fabrication was accomplished on three rotors, a bladeless rotor, a solid rotor, and an air-cooled rotor.

**14. SUBJECT TERMS**
Turbine, Radial Inflow, Cooled Rotor, Rotorcraft Engine

**15. NUMBER OF PAGES**
88

**16. PRICE CODE**

| 17. SECURITY CLASSIFICATION OF REPORT | 18. SECURITY CLASSIFICATION OF THIS PAGE | 19. SECURITY CLASSIFICATION OF ABSTRACT | 20. LIMITATION OF ABSTRACT |
|---|---|---|---|
| Unclassified | Unclassified | Unclassified | |

NSN 7540-01-280-5500

Standard Form 298 (Rev. 2-89)
Prescribed by ANSI Std. Z39-18
298-102

TABLE OF CONTENTS

LIST OF TABLES

## LIST OF FIGURES

## 1.0 Summary

This is the final report for work on this contract and covers the results of the Tasks V and VII. The original effort was structured with four tasks. Task I, was entitled Design Goals and Requirements and consisted of the aerodynamic and structural design of an air-cooled vane and rotor. Work on this task was reported in NASA CR-179606, reference 1. Task II comprised a total test rig design. This partially completed task was subsequently canceled. Task III, also cancelled, was to have accomplished fabrication of equipment designed to Task II. Task IV was directed at preparation of technical, financial, and schedular reporting.

Tasks V, VI, and VII were added to the original program to accomplish the redirected program goals. Task V, entitled Turbine Design, consisted of the aerodynamic design of an uncooled vane and the aerodynamic, heat transfer, and structural design of an air cooled rotor. Results of this task were summarized in an AIAA paper, reference 2, and are reported in detail herein. Effort on Task VI comprised test rig interface work required to ensure compatibility of the cooled radial turbine rotor designed in Task V with the LeRC designed test rig, and was accomplished through close coordination with NASA LeRC test equipment personnel. Based on detailed turbine test rig drawings, the compatibility of the NASA test rig with the research rotor was established. Included was a critical speed analysis, squeeze film damper analysis, fragment containment casing study, and rotor cooling air supply assessment. The results of these engineering studies are documented in separate analysis reports and are not part of this final report. Task VII accomplished the rotor fabrication. Following NASA approvals, detailed drawings were make and parts were released for fabrication. A bladeless rotor, a solid-bladed rotor, and an air-cooled rotor were fabricated. The bladeless rotor was machined from solid stock. The solid and hollow rotor were cast at the Howmet Turbine Components Corporation, LaPort Division. The bladed rotors were balanced and spin tested before delivery to NASA LeRC.

## 2.0 Introduction

Requirements for advanced turbine engines call for increased specific power and improved specific fuel consumption (SFC). Results of basic gas turbine cycle studies have in general shown these requirements can be met through the use of increased turbine inlet temperatures and increased cycle pressure ratios. The result is a significant reduction in core equivalent mass flow rates and hence a commensurate reduction in core flow passage dimensions. For axial turbines, small passage dimensions are usually associated with low aspect ratio airfoils giving rise to secondary flow losses and increased tip clearances, both of which reduce stage efficiencies. Past studies have shown that radial turbines offer lower sensitivity to the efficiency penalties of reduced passage dimensions and, hence, result in designs having higher turbine efficiencies at low equivalent flow values. In addition, radial turbines offer the potential of high loading per stage. This gives rise to the possible reduction in number of stages which can result in cost benefits. The use of a radial turbine in the gasifier section thus becomes attractive in the design of small turbine engines.

The development of high temperature capabilities in radial turbines has recently been pursued via ceramic blading. However prior to the development of a mature ceramic radial turbine technology, the use of the air cooled metallic radial turbine has been proposed for advanced engines with high power-to-weight and improved SFC requirements.

The addition of cooling to the blades of a metal radial turbine has provided a significant challenge. The investment cast and HIP-bonded approach developed as part of a previous Army contract (reference 3) has demonstrated the greatest promise in meeting coolant passage constraints while yielding rotors demonstrating adequate life. The rotor developed for that program is shown just prior to the HIP bond process in Figure 2.0-1. The design reported here builds upon that work. This study adds to the design approach by developing a second generation investment cast and HIP-bonded cooled metal rotor design capable of commercial fabrication and promising acceptable efficiency and rotor life. The current program seeks to enhance rotor aerodynamics, further improve cooling performance, and furnish the test rotors necessary to provide definitive experimental aerodynamic and heat transfer information on cooling of a high temperature radial turbine rotor.

This report presents the results of work performed on the Cooled High-Temperature Radial Turbine Program conducted by the Allison Gas Turbine Division of General Motors and funded by the NASA Lewis Research Center under NASA contract NAS3-24230. The objective of this program was to design and fabricate two radial turbine rotors for the experimental investigation of the cooled, high-temperature radial turbine (HTRT) concept. This vane/rotor system was designed to operate at a rotor inlet temperature (RIT) of 2300$^{o}$F and a cycle pressure ratio of 14:1 with rotor flow of 4.6 lbm/sec. An addendum to the design task was to also evaluate the cooling design effectiveness and rotor life operating at 2500°F RIT.

Design goals were high aerodynamic performance ($\eta_{TT}$>86%), a rotor life of 5000 hours, a low-cycle fatigue (LCF) life of 6000 cycles, and the utilization of fabrication capabilities and material properties available within the next 10 years. The rotor design features improved cooling effectiveness and blade angle distribution compared to prior Allison advanced radial turbine design efforts. The stator was designed assuming ceramic technology eliminating the need for stator cooling. Effort included the fabrication of two bladed rotors intended for instrumentation and test at the NASA Lewis Research Center warm turbine test facility.

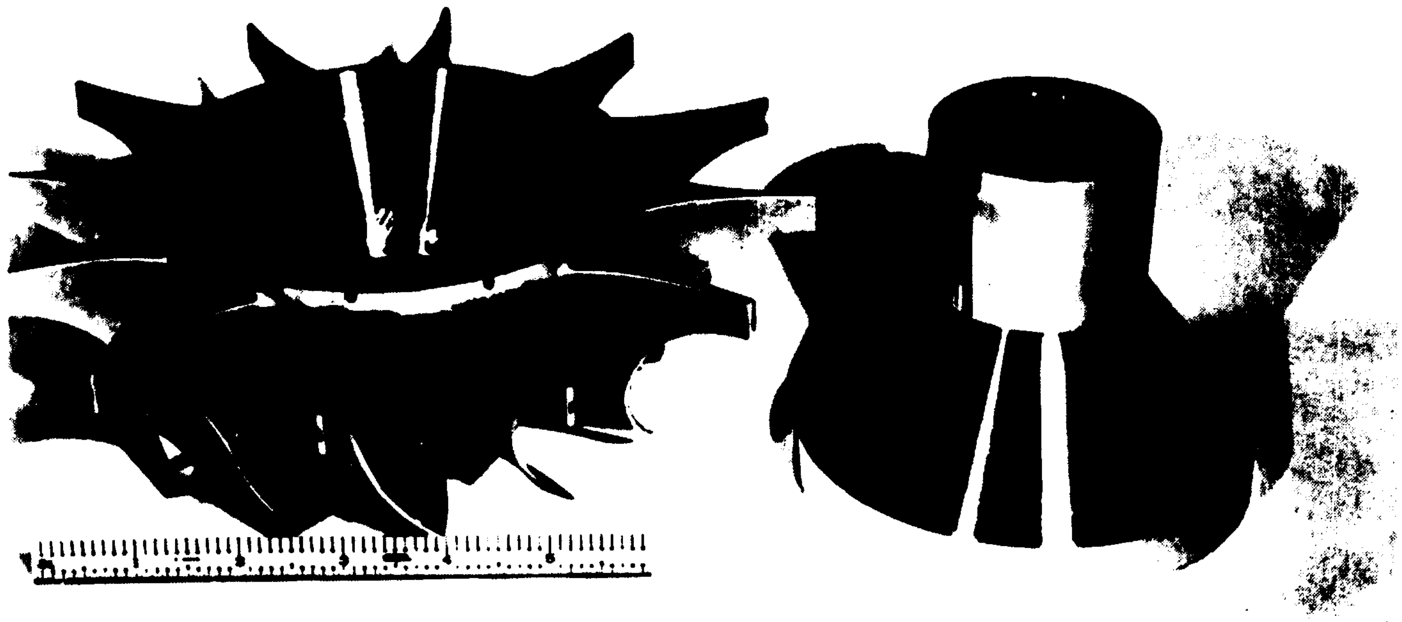

INVESTMENT CAST BLADE SHELL POWERED METAL HUB

FIGURE 2.0-1 DUAL ALLOY HIP BONDED RADIAL TURBINE ROTOR

## 3.0 RESULTS AND DISCUSSION

### 3.1 Turbine Design

#### 3.1.1 Engine Configuration Cycle

The radial-inflow turbine design is based on a hypothetical engine configuration incorporating the design requirements of Table 3.1-1. The cycle is selected to satisfy these criteria at intermediate rated power (IRP) as presented in Table 3.1-2. The gas generator incorporates a compressor of 14.4:1 pressure ratio with 4.75 lbm/sec airflow. Shaft power is 920 hp with an SFC of 0.44 lb.hp.hr. Part power (75% IRP) conditions are presented in Table 3.1-3. Engine cycle data at idle is shown in Table 3.1-4.

Table 3.1-1. HTRT Design Point Conditions.

| | |
|---|---|
| Rotor Inlet Total Temperature ($^{O}F$) | 2300 |
| Vane Inlet Total Pressure (psia) | 200 |
| Total-to-total Expansion Ratio | 3.66 |
| Actual Flow (lbm/sec) | 4.56 |
| Equivalent Flow (lbm/sec) | 0.80 |
| Power Output (hp) | 1191 |
| Corrected Work ($\Delta H/\theta_c$) | 34.2 |
| Mechanical Speed (rpm) | 61,900 |
| Direction of rotation as viewed from the rear of the turbine | CCW |
| Rotor Diameter (inches) | 8.02 |
| Rotor Tip Speed (ft/sec) | 2166 |
| Specific Speed ($rpm/ft^{3/4}sec^{1/2}$) | 62.2 |
| Blade-jet Speed Ratio | 0.66 |
| Adiabatic Efficiency (T-to-T, %) | 87.0 |

Cooling flows for the gasifier turbine section are set at 5.7%. The vane is uncooled assuming ceramic construction, the rotor cooling is divided between internal passage (4.3%), hub film (0.5%) and hub bore (1.0%).

The engine general arrangement shown in Figure 3.1-1 is a carry over from the Task I effort. The gas generator turbine rotor bore diameter has been sized to allow passage of the power turbine extension drive shaft, which is capable of transmitting in excess of 1000 shp.

#### 3.1.2 Meanline Velocity Diagram and Aerodynamic Design.

Design studies conducted as part of the Task I work have served as a basis for the turbine design reported here. Table 3.1-5 presents design point values for the radial turbine. The design reflects selection of the operating point within the optimal range in terms of specific speed and blade-jet speed ratio. Average exit swirl values were set to zero for design point operation. The design does not attempt to be fully optimal and does reflect limitations imposed by rig hardware design constraints. This limitation set the vane inner and outer radii and width, the rotor tip diameter and width, the outer shroud contour, and the exit tip and hub diameters.

TABLE 3.1-2 ENGINE CYCLE, INTERMEDIATE RATED (IRP)

| ALT | DTAMB | VEL | XM | KTAS | KIAS | DEFF | ERAM | RPR | PAMB | P1-ID | TAMR-R | TAMR-F | T1-F | RC-OA | EFF-OA | CASE |
|---|---|---|---|---|---|---|---|---|---|---|---|---|---|---|---|---|
| 0. | 0.0 | 0.0 | 0.0 | 0.0 | 0.0 | 0.9900 | 0.9900 | 0.990 | 14.696 | 14.696 | 518.67 | 59.00 | 59.00 | 14.40 | 0.8111 | 1.0 |

| ID | T-R | P-PSIA | W-COR | WD | R | EFF | FAR | AREA | XMN | PS-PSIA | THETA | DELTA | H | SF-N,1 | NSI | (N |
|---|---|---|---|---|---|---|---|---|---|---|---|---|---|---|---|---|
| LPC | 518.7 | 14.549 | 4.791 | 4.743 | 14.4000 | 0.8111 | 0.0 | 0.0 | 0.0 | 0.0 | 1.000 | 0.990 | 124.0 | 0.9796 | 0 | 1 |
| BURN | 1229.0 | 209.511 | 0.479 | 4.438 | 0.9850 | 0.9900 | 0.0 | 4.2 | 0.200 | 203.884 | 2.369 | 14.256 | 298.7 | 0.5585 | 0 | 2 |
| COOL | 2760.0 | 206.368 | 0.747 | 4.550 | 0.0 | 0.0 | 0.02534 | 0.0 | 0.0 | 0.0 | 5.321 | 14.042 | 746.1 | 0.0 | 0 | 3 |
| LPT | 2760.0 | 206.368 | 0.769 | 4.550 | 3.6652 | 0.8650 | 0.02534 | 0.0 | 0.0 | 0.0 | 5.145 | 14.042 | 746.1 | 1.0480 | 0 | 4 |
| DELP | 2144.6 | 56.309 | 2.415 | 4.550 | 0.9850 | 0.0 | 0.02534 | 21.6 | 0.200 | 54.858 | 4.135 | 3.831 | 562.0 | 0.5838 | 0 | 5 |
| COOL | 2144.6 | 55.460 | 2.452 | 4.550 | 0.0 | 0.0 | 0.02534 | 0.0 | 0.0 | 0.0 | 4.135 | 3.774 | 562.0 | 0.0 | 0 | 6 |
| PT | 2109.7 | 55.460 | 2.599 | 4.746 | 3.4341 | 0.8870 | 0.02427 | 0.0 | 0.0 | 0.0 | 3.954 | 3.774 | 551.2 | 1.0290 | 0 | 7 |
| COOL | 1629.1 | 16.150 | 7.655 | 4.746 | 0.0 | 0.0 | 0.02427 | 0.0 | 0.0 | 0.0 | 3.141 | 1.099 | 414.0 | 0.0 | 0 | 8 |
| DELP | 1623.5 | 16.150 | 7.756 | 4.817 | 1.0000 | 0.0 | 0.02390 | 68.8 | 0.200 | 15.728 | 3.130 | 1.099 | 412.3 | 0.0 | 0 | 9 |
| NOZZ | 1623.5 | 16.150 | 7.756 | 4.817 | 1.0989 | 0.0 | 0.02390 | 1.0 | 0.0 | 0.0 | 3.130 | 1.099 | 412.3 | 0.0 | 0 | 10 |
| THB | 1586.1 | 14.696 | 8.424 | 4.817 | 1.0989 | 0.0 | 0.02390 | 38.5 | 0.403 | 14.696 | 3.058 | 1.000 | 401.9 | 1.0000 | 0 | 11 |
| EX9 | 1586.1 | 14.696 | 8.424 | 4.817 | 1.0000 | 0.0 | 0.02390 | 38.5 | 0.403 | 14.696 | 3.058 | 1.000 | 401.9 | 0.0 | 0 | 12 |

ES= 1 NVAR= 2 MATRX= 0 LOOP= 9 EMAX= 0.00005 NLIM= 3 3

1= T (3), T (4) V= 3000.000, 2500.000, 0.0 E= 2760.000, 0.0 L=1
2= EFF (1), R (4) V= 1.000, 0.500, 0.0 E= 3.665, 0.0 L=1

## C O M P R E S S O R B L E E D I N F O R M A T I O N

| BLEED NO. | | 1 | 2 | 3 | 4 | 5 | 6 | 7 | 8 | 9 | 10 | 11 | 12 | TOTALS |
|---|---|---|---|---|---|---|---|---|---|---|---|---|---|---|
| MPR 1 | BLEED | 0.0 | 0.0414 | 0.0150 | 0.0080 | 0.0 | 0.0 | 0.0 | 0.0 | 0.0 | 0.0 | 0.0 | 0.0 | 0.0644 |
| ID | DEL-H | 1.0000 | 1.0000 | 1.0000 | 1.0000 | 1.0000 | 1.0000 | 1.0000 | 1.0000 | 1.0000 | 1.0000 | 1.0000 | 1.0000 | |
| LPC | FLOW | 0.0 | 0.196 | 0.071 | 0.038 | 0.0 | 0.0 | 0.0 | 0.0 | 0.0 | 0.0 | 0.0 | 0.0 | 0.305 |
| LPC | TEMP | 0.0 | 1229.0 | 1229.0 | 1229.0 | 0.0 | 0.0 | 0.0 | 0.0 | 0.0 | 0.0 | 0.0 | 0.0 | |
| LPC | PRESS | 0.0 | 209.51 | 209.51 | 209.51 | 0.0 | 0.0 | 0.0 | 0.0 | 0.0 | 0.0 | 0.0 | 0.0 | |
| LPC | IRF | 1 | 1 | 1 | 1 | 1 | 1 | 1 | 1 | 1 | 1 | 1 | 1 | |
| | NTC(N) N= | 3 | 6 | 8 | O/B | O/B | O/B | O/B | O/B | O/B | O/B | O/B | O/B | |

## C O M P O N E N T P E R F O R M A N C E

| N | ID | RETA | XN | XN-MAP | H.P. | HPX/PHP | SF(N,2) | FFF-MAP | R-MAP | W-MAP | SMRELL | FLOW ID | | EFF ID | | MAPTYP |
|---|---|---|---|---|---|---|---|---|---|---|---|---|---|---|---|---|
| 1 | LPC | 1.0000 | 100.000 | 100.000 | 1172.83 | 12.00 | 0.0 | 0.8280 | 3.0000 | 100.0000 | 0.0 | 0. | 0. | 0. | 0. | 1 |
| 4 | LPT | 0.0 | 100.000 | 100.000 | 1184.83 | 0.0 | 0.0 | 0.8254 | 3.8962 | 99.9999 | 0.0 | 0. | 0. | 0. | 0. | 1 |
| 7 | PT | 0.0 | 100.000 | 100.000 | 921.04 | 0.0 | 0.0 | 0.8620 | 3.2304 | 100.0000 | 0.0 | 0. | 0. | 0. | 0. | 1 |

## N O Z Z L E P E R F O R M A N C E

| NOZZLE | (N) | TYP | FG | FN | RJ | CFG | CD | AREA(TH) | V-EXIT | SF(TH,2) | SF(EX,2) | CFGT ID | | CDT ID | | MAPTYP |
|---|---|---|---|---|---|---|---|---|---|---|---|---|---|---|---|---|
| 1 (8-9) | 10 | 1 | 106.39 | 106.39 | 1.0989 | 0.9850 | 1.0000 | 38.48 | 721.3 | 5.239 | 0.0 | 0. | 0. | 0. | 0. | 1 |

## F I N A L E N G I N E P E R F O R M A N C E

| F-RAM | WA-ENG | WA-COR | EFF-PROP | FN-PROP | FN-TOT | SFC-TOT | EFF-TH | FHV | DTAMTP | WFE | NODISS | PWSDGF |
|---|---|---|---|---|---|---|---|---|---|---|---|---|
| 0.0 | 4.743 | 4.791 | 0.0 | 2302.6 | 2409.0 | 0.1680 | 0.3146 | 18400.0 | 0.0 | 404.8 | 1 | 1.00000 |

| PWSD | SFC | WFT | PWSD-R1 | FN | PWSD-EQ | SFC-EQ | PW/WA | DEFTIP | ERAMTP | HPXPT | FAR-ST | WFTGF |
|---|---|---|---|---|---|---|---|---|---|---|---|---|
| 921.0 | 0.4395 | 404.8 | 930.3 | 106.4 | 963.6 | 0.4201 | 194.189 | 0.0 | 0.0 | 0.0 | 0.067751 | 1.00000 |

# TABLE 3.1-3 ENGINE CYCLE, 75% POWER

| ALT | DTAMB | VEL | XM | KTAS | KIAS | DEFF | ERAM | RPR | PAMB | P1-ID | TAMB-R | TAMB-F | T1-F | RC-OA | EFF-OA | CASE |
|---|---|---|---|---|---|---|---|---|---|---|---|---|---|---|---|---|
| 0. | 0.0 | 0.0 | 0.0 | 0.0 | 0.0 | 0.9900 | 0.9900 | 0.990 | 14.696 | 14.696 | 518.67 | 59.00 | 59.00 | 12.40 | 0.8100 | 2.0 |

| (N) | ID | T-R | P-PSIA | W-COR | WD | R | EFF | FAR | AREA | XMN | PS-PSIA | THETA | DELTA | H | SF-N,1 | NSI | (N) |
|---|---|---|---|---|---|---|---|---|---|---|---|---|---|---|---|---|---|
| 1 | LPC | 518.7 | 14.549 | 4.361 | 4.317 | 12.4000 | 0.8100 | 0.0 | 0.0 | 0.0 | 0.0 | 1.000 | 0.990 | 124.0 | 0.9783 | 0 | 1 |
| 2 | BURN | 1176.5 | 180.412 | 0.476 | 4.039 | 0.9350 | 0.9700 | 0.0 | 4.3 | 0.200 | 175.556 | 2.268 | 12.276 | 285.3 | 0.5572 | 0 | 2 |
| 3 | COOL | 2516.0 | 177.706 | 0.752 | 4.126 | 0.0 | 0.0 | 0.02165 | 0.0 | 0.0 | 0.0 | 4.851 | 12.092 | 669.2 | 0.0 | 0 | 3 |
| 4 | LPT | 2516.0 | 177.706 | 0.772 | 4.126 | 3.7888 | 0.8650 | 0.02165 | 0.0 | 0.0 | 0.0 | 4.702 | 12.092 | 669.2 | 1.0480 | 0 | 4 |
| 5 | DELP | 1932.1 | 46.903 | 2.495 | 4.126 | 0.9850 | 0.0 | 0.02165 | 22.2 | 0.200 | 45.689 | 3.725 | 3.172 | 498.3 | 0.5796 | 0 | 5 |
| 6 | COOL | 1932.1 | 46.200 | 2.533 | 4.126 | 0.0 | 0.0 | 0.02165 | 0.0 | 0.0 | 0.0 | 3.725 | 3.144 | 498.3 | 0.0 | 0 | 6 |
| 7 | PT | 1902.9 | 46.200 | 2.680 | 4.305 | 2.8632 | 0.8870 | 0.02073 | 0.0 | 0.0 | 0.0 | 3.578 | 3.144 | 489.4 | 1.0290 | 0 | 7 |
| 8 | COOL | 1518.0 | 16.150 | 6.702 | 4.305 | 0.0 | 0.0 | 0.02073 | 0.0 | 0.0 | 0.0 | 2.927 | 1.099 | 382.0 | 0.0 | 0 | 8 |
| 9 | DELP | 1513.2 | 16.150 | 6.792 | 4.370 | 1.0000 | 0.0 | 0.02042 | 60.0 | 0.200 | 15.726 | 2.917 | 1.099 | 380.5 | 0.0 | 0 | 9 |
| 10 | NOZZ | 1513.2 | 16.150 | 6.792 | 4.370 | 1.0989 | 0.0 | 0.02042 | 1.0 | 0.0 | 0.0 | 2.917 | 1.099 | 380.5 | 0.0 | 0 | 10 |
| 11 | THB | 1477.4 | 14.696 | 7.375 | 4.370 | 1.0989 | 0.0 | 0.02042 | 33.5 | 0.404 | 14.696 | 2.848 | 1.000 | 370.8 | 1.0000 | 0 | 11 |
| 12 | EX9 | 1477.4 | 14.696 | 7.375 | 4.370 | 1.0000 | 0.0 | 0.02042 | 33.5 | 0.404 | 14.696 | 2.848 | 1.000 | 370.8 | 0.0 | 0 | 12 |

IDES= 1   NVAR= 1   MATRX= 0   LOOP= 11   EMAX= 0.00002   NLIN= 3

C 1= T (3), T (4) V= 3000.000, 2500.000, 0.0 E= 2516.000, 0.0 L=1

## C O M P R E S S O R   B L E E D   I N F O R M A T I O N

| | BLEED NO. | 1 | 2 | 3 | 4 | 5 | 6 | 7 | 8 | 9 | 10 | 11 | 12 | TOTALS |
|---|---|---|---|---|---|---|---|---|---|---|---|---|---|---|
| COMPR 1 | BLEED | 0.0 | 0.0414 | 0.0150 | 0.0080 | 0.0 | 0.0 | 0.0 | 0.0 | 0.0 | 0.0 | 0.0 | 0.0 | 0.0644 |
| NO. ID | DEL-H | 1.0000 | 1.0000 | 1.0000 | 1.0000 | 1.0000 | 1.0000 | 1.0000 | 1.0000 | 1.0000 | 1.0000 | 1.0000 | 1.0000 | |
| 1 LPC | FLOW | 0.0 | 0.179 | 0.065 | 0.035 | 0.0 | 0.0 | 0.0 | 0.0 | 0.0 | 0.0 | 0.0 | 0.0 | 0.278 |
| 1 LPC | TEMP | 0.0 | 1176.5 | 1176.5 | 1176.5 | 0.0 | 0.0 | 0.0 | 0.0 | 0.0 | 0.0 | 0.0 | 0.0 | |
| 1 LPC | PRESS | 0.0 | 180.41 | 180.41 | 180.41 | 0.0 | 0.0 | 0.0 | 0.0 | 0.0 | 0.0 | 0.0 | 0.0 | |
| 1 LPC | IRF | 1 | 1 | 1 | 1 | 1 | 1 | 1 | 1 | 1 | 1 | 1 | 1 | |
| | NTC(N) N= | 3 | 6 | 8 | O/B | O/B | O/B | O/B | O/B | O/B | O/B | O/B | O/B | |

## C O M P O N E N T   P E R F O R M A N C E

| N | ID | BETA | XN | XN-MAP | H.P. | HPX/PHP | SF(N,2) | EFF-MAP | R-MAP | W-MAP | SMPELL | FLOW ID | EFF ID | MAPTYP |
|---|---|---|---|---|---|---|---|---|---|---|---|---|---|---|
| 1 | LPC | 1.0000 | 100.000 | 100.000 | 985.72 | 12.00 | 0.0 | 0.8280 | 3.0000 | 100.0000 | 0.0 | 0. 0. | 0. 0. | 1 |
| 4 | LPT | 0.0 | 100.000 | 100.000 | 997.72 | 0.0 | 0.0 | 0.8254 | 3.8962 | 99.9999 | 0.0 | 0. 0. | 0. 0. | 1 |
| 7 | PT | 0.0 | 100.000 | 100.000 | 654.30 | 0.0 | 0.0 | 0.8620 | 3.2303 | 100.0000 | 0.0 | 0. 0. | 0. 0. | 1 |

## N O Z Z L E   P E R F O R M A N C E

| NOZZLE | (N) | TYP | FG | FN | RJ | CFG | CD | AREA(TH) | V-EXIT | SF(TH,2) | SF(EX,2) | CFGT ID | CDT ID | MAPTYP |
|---|---|---|---|---|---|---|---|---|---|---|---|---|---|---|
| PRI (8-9) | 10 | 1 | 93.55 | 93.55 | 1.0989 | 0.9850 | 1.0000 | 33.54 | 699.3 | 5.238 | 0.0 | 0. 0. | 0. 0. | 1 |

## F I N A L   E N G I N E   P E R F O R M A N C E

| F-RAM | WA-ENG | WA-COR | EFF-PROP | FN-PROP | FN-TOT | SFC-TOT | EFF-TH | FHV | DTAMTP | WFE | NODISS | PWSDGF |
|---|---|---|---|---|---|---|---|---|---|---|---|---|
| 0.0 | 4.317 | 4.361 | 0.0 | 1635.8 | 1729.3 | 0.1820 | 0.2874 | 18400.0 | 0.0 | 314.8 | 1 | 1.00000 |

| PWSD | SFC | WFT | PWSD-R1 | FN | PWSD-EQ | SFC-EQ | PW/WA | DEFTIP | ERAMTP | HPXPT | FAR-ST | WFTGF |
|---|---|---|---|---|---|---|---|---|---|---|---|---|
| 654.3 | 0.4811 | 314.8 | 660.9 | 93.5 | 691.7 | 0.4550 | 151.564 | 0.0 | 0.0 | 0.0 | 0.067751 | 1.00000 |

# TABLE 3.1-4 ENGINE CYCLE-IDLE

| ALT | DTAMB | VEL | XM | KTAS | KIAS | DEFF | ERAM | RPR | PAMB | P1-ID | TAMB-R | TAMB-F | T1-F | RC-OA | EFF-OA | CASE |
|---|---|---|---|---|---|---|---|---|---|---|---|---|---|---|---|---|
| 0. | 0.0 | 0.0 | 0.0 | 0.0 | 0.0 | 0.9900 | 0.9900 | 0.990 | 14.696 | 14.696 | 518.67 | 59.00 | 59.00 | 3.80 | 0.7200 | 3.0 |

| (N) | ID | T-R | P-PSIA | W-COR | WD | R | EFF | FAR | AREA | XMN | PS-PSIA | THETA | DELTA | H | SF-N,1 | NSI | (N) |
|---|---|---|---|---|---|---|---|---|---|---|---|---|---|---|---|---|---|
| 1 | LPC | 518.7 | 14.549 | 1.707 | 1.690 | 3.8000 | 0.7200 | 0.0 | 0.0 | 0.0 | 0.0 | 1.000 | 0.990 | 124.0 | 0.8696 | 0 | 1 |
| 2 | BURN | 850.3 | 55.288 | 0.538 | 1.581 | 0.9850 | 0.9900 | 0.0 | 4.7 | 0.200 | 53.778 | 1.639 | 3.762 | 204.1 | 0.5494 | 0 | 2 |
| 3 | COOL | 1539.0 | 54.458 | 0.742 | 1.597 | 0.0 | 0.0 | 0.00996 | 0.0 | 0.0 | 0.0 | 2.967 | 3.706 | 383.5 | 0.0 | 0 | 3 |
| 4 | LPT | 1539.0 | 54.458 | 0.754 | 1.597 | 2.9950 | 0.8550 | 0.00996 | 0.0 | 0.0 | 0.0 | 2.915 | 3.706 | 383.5 | 1.0358 | 0 | 4 |
| 5 | DELP | 1213.1 | 18.183 | 1.974 | 1.597 | 0.9930 | 0.0 | 0.00996 | 17.3 | 0.200 | 17.697 | 2.339 | 1.237 | 297.3 | 0.2619 | 0 | 5 |
| 6 | COOL | 1213.1 | 18.055 | 1.988 | 1.597 | 0.0 | 0.0 | 0.00996 | 0.0 | 0.0 | 0.0 | 2.339 | 1.229 | 297.3 | 0.0 | 0 | 6 |
| 7 | PT | 1198.4 | 18.055 | 2.083 | 1.667 | 1.1333 | 0.8460 | 0.00953 | 0.0 | 0.0 | 0.0 | 2.285 | 1.229 | 293.4 | 0.9814 | 0 | 7 |
| 8 | COOL | 1165.3 | 15.930 | 2.305 | 1.667 | 0.0 | 0.0 | 0.00953 | 0.0 | 0.0 | 0.0 | 2.247 | 1.084 | 284.9 | 0.0 | 0 | 8 |
| 9 | DELP | 1160.7 | 15.930 | 2.335 | 1.692 | 1.0000 | 0.0 | 0.00939 | 20.4 | 0.200 | 15.503 | 2.238 | 1.084 | 283.7 | 0.0 | 0 | 9 |
| 10 | NOZZ | 1160.7 | 15.930 | 2.335 | 1.692 | 1.0840 | 0.0 | 0.00939 | 1.0 | 0.0 | 0.0 | 2.238 | 1.084 | 283.7 | 0.0 | 0 | 10 |
| 11 | THB | 1136.0 | 14.696 | 2.504 | 1.692 | 1.0840 | 0.0 | 0.00939 | 12.4 | 0.371 | 14.696 | 2.190 | 1.000 | 277.3 | 1.0000 | 0 | 11 |
| 12 | EX9 | 1136.0 | 14.696 | 2.504 | 1.692 | 1.0000 | 0.0 | 0.00939 | 12.4 | 0.371 | 14.696 | 2.190 | 1.000 | 277.3 | 0.0 | 0 | 12 |

IDES= 1 NVAR= 1 MATRX= 1 LOOP= 4 EMAX= 0.00002 NLIM= 3

C 1= T (3), T .4) V= 2000.000, 1000.000, 0.0 E= 1539.000, 0.0 L=1

C O M P R E S S O R  B L E E D  I N F O R M A T I O N

| COMPR NO. | ID | BLEED NO. | 1 | 2 | 3 | 4 | 5 | 6 | 7 | 8 | 9 | 10 | 11 | 12 | TOTALS |
|---|---|---|---|---|---|---|---|---|---|---|---|---|---|---|---|
| 1 | | BLEED | 0.0 | 0.0414 | 0.0150 | 0.0080 | 0.0 | 0.0 | 0.0 | 0.0 | 0.0 | 0.0 | 0.0 | 0.0 | 0.0644 |
| | | DEL-H | 1.0000 | 1.0000 | 1.0000 | 1.0000 | 1.0000 | 1.0000 | 1.0000 | 1.0000 | 1.0000 | 1.0000 | 1.0000 | 1.0000 | |
| 1 | LPC | FLOW | 0.0 | 0.070 | 0.025 | 0.014 | 0.0 | 0.0 | 0.0 | 0.0 | 0.0 | 0.0 | 0.0 | 0.0 | 0.109 |
| 1 | LPC | TEMP | 0.0 | 850.3 | 850.3 | 850.3 | 0.0 | 0.0 | 0.0 | 0.0 | 0.0 | 0.0 | 0.0 | 0.0 | |
| 1 | LPC | PRESS | 0.0 | 55.29 | 55.29 | 55.29 | 0.0 | 0.0 | 0.0 | 0.0 | 0.0 | 0.0 | 0.0 | 0.0 | |
| 1 | LPC | IBF | 1 | 1 | 1 | 1 | 1 | 1 | 1 | 1 | 1 | 1 | 1 | 1 | |
| | | NTC(N) N= | 3 | 6 | 8 | O/B | O/B | O/B | O/B | O/B | O/B | O/B | O/B | O/B | |

C O M P O N E N T  P E R F O R M A N C E

| N | ID | BETA | XN | XN-MAP | H.P. | HPX/PHP | SF(N,2) | EFF-MAP | R-MAP | W-MAP | SHRELL | FLOW ID | EFF ID | MAPTYP |
|---|---|---|---|---|---|---|---|---|---|---|---|---|---|---|
| 1 | LPC | 1.0000 | 100.000 | 100.000 | 191.62 | 3.00 | 0.0 | 0.8280 | 3.0000 | 100.0000 | 0.0 | 0. 0. | 0. 0. | 1 |
| 4 | LPT | 0.0 | 100.000 | 100.000 | 194.62 | 0.0 | 0.0 | 0.8254 | 3.8961 | 99.9999 | 0.0 | 0. 0. | 0. 0. | 1 |
| 7 | PT | 0.0 | 100.000 | 100.000 | 20.16 | 0.0 | 0.0 | 0.8620 | 3.2303 | 99.9999 | 0.0 | 0. 0. | 0. 0. | 1 |

N O Z Z L E  P E R F O R M A N C E

| NOZZLE | (N) | TYP | FG | FN | RJ | CFG | CD | AREA(TH) | V-EXIT | SF(TH,2) | SF(EX,2) | CFGT ID | CDT ID | MAPTYP |
|---|---|---|---|---|---|---|---|---|---|---|---|---|---|---|
| PRI (8-9) | 10 | 1 | 29.19 | 29.19 | 1.0840 | 0.9850 | 1.0000 | 12.39 | 563.5 | 6.135 | 0.0 | 0. 0. | 0. 0. | 1 |

F I N A L  E N G I N E  P E R F O R M A N C E

| F-RAM | WA-ENG | WA-COR | EFF-PROP | FN-PROP | FN-TOT | SFC-TOT | EFF-TH | FHV | DTAMTP | WFE | NODISS | PWSDGF |
|---|---|---|---|---|---|---|---|---|---|---|---|---|
| 0.0 | 1.690 | 1.707 | 0.0 | 50.4 | 79.6 | 0.7120 | 0.0492 | 18400.0 | 0.0 | 56.7 | 1 | 1.00000 |

| PWSD | SFC | WFT | PWSD-R1 | FN | PWSD-EQ | SFC-EQ | PW/WA | DEFTIP | ERAMTP | HPXPT | FAR-ST | WFTGF |
|---|---|---|---|---|---|---|---|---|---|---|---|---|
| 20.2 | 2.8110 | 56.7 | 20.4 | 29.2 | 31.8 | 1.7801 | 11.930 | 0.0 | 0.0 | 0.0 | 0.067751 | 1.00000 |

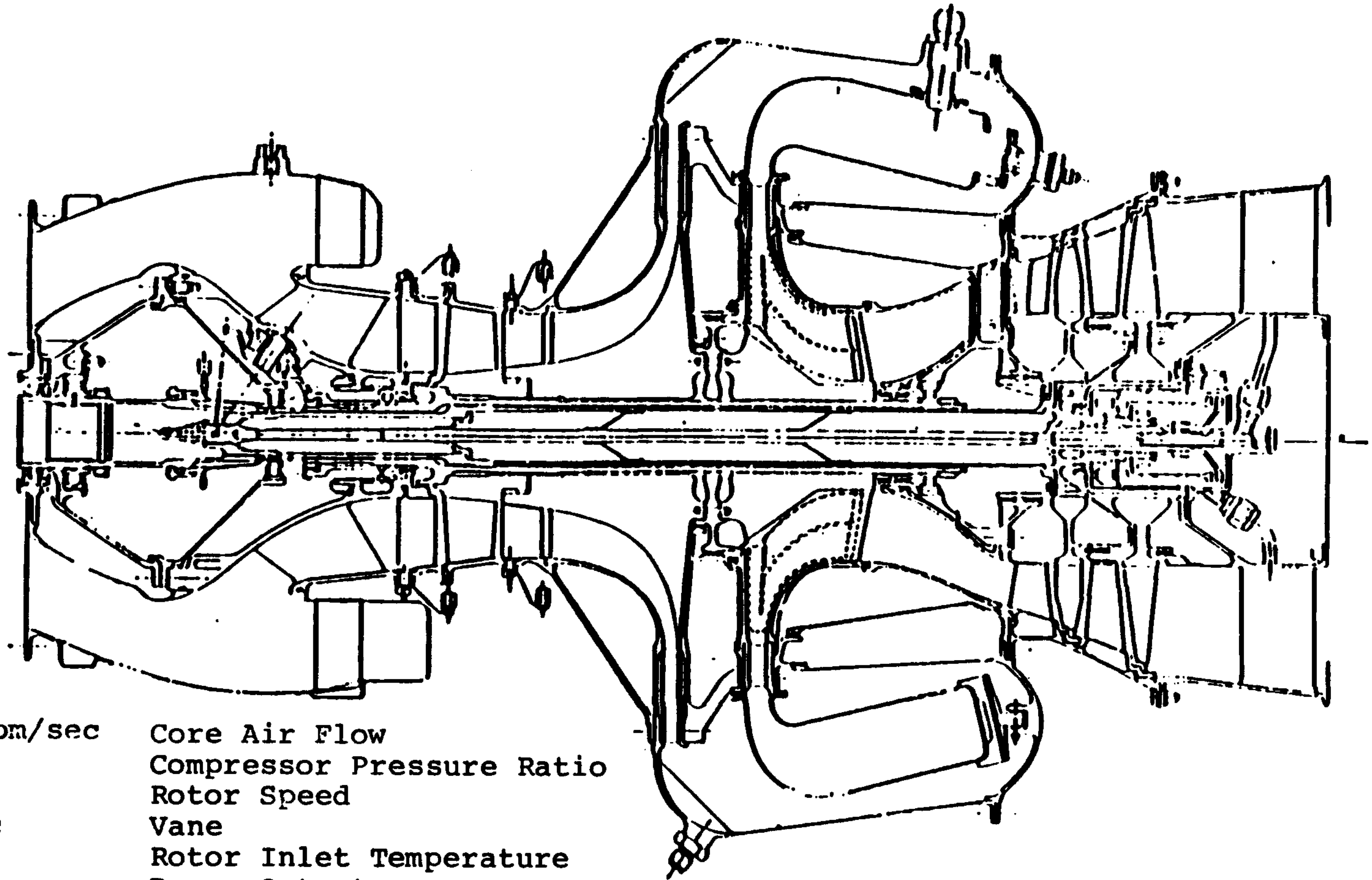

| | |
|---|---|
| 4.74 lbm/sec | Core Air Flow |
| 14.4 | Compressor Pressure Ratio |
| 61900 | Rotor Speed |
| Ceramic | Vane |
| 2300°F | Rotor Inlet Temperature |
| 920 hp | Power Output |
| 0.44 | SFC |

FIGURE 3.1-1 TYPICAL SMALL ENGINE INCORPORATING THE COOLED HTRT

TABLE 3.1-5 TURBINE PERFORMANCE AT INTERMEDIATE RATED POWER

| ACTUAL | | CORRECTED |
|---|---|---|
| W= 4.5596 | EFF-TT(ADIABATIC)=0.8700 | WRTHCE/D= 0.7939 |
| DELH(ADIABATIC)=186.846 | EFF-TS(ADIABATIC)=0.8396 | DELH/THC(ADIABATIC)= 36.243 |
| SPEED= 61900.00 | EFF-TT(NET)=0.8595 | N/RTHC= 27262.32 |
| HP(NET)=1190.780 | EFF-TS(NET)=0.8295 | HP/DRTHC= 38.5365 |
| TORQUE= 102.273 | RTOT= 3.6648 | TE/D= 7.843 |
| U/CT=0.6606 U/CS=0.6490 | RTOS= 3.8728 | SPEED-FLOW PAR= 360.72 |

CYCLE PARAMETERS

| STATION | T TOTAL | P TOTAL | T STATIC | P STATIC | GAMMA | CP | T RELATIVE |
|---|---|---|---|---|---|---|---|
| 00 | 2760.000 | 200.000 | | | | | |
| 0 | 2760.000 | 200.000 | 2754.596 | 198.298 | | | |
| 1 | 2760.000 | 191.892 | 2464.611 | 117.140 | 1.298 | 0.2992 | |
| 2 | 2760.000 | 191.206 | 2420.523 | 107.887 | 1.298 | 0.2992 | 2447.042 |
| 3 | 2133.769 | 54.574 | 2106.326 | 51.643 | 1.306 | 0.2926 | 2209.744 |

VELOCITY DIAGRAM

| STATION | U | V | VU | W | WU | VR | ALPHA | BETA |
|---|---|---|---|---|---|---|---|---|
| 0 | | 284.518 | 0.0 | | | 284.518 | 0.0 | |
| 1 | | 2103.479 | 2029.168 | | | 554.168 | 74.725 | |
| 2 | 2166.385 | 2254.997 | 2165.123 | 630.307 | -1.26 | 630.306 | 73.769 | -0.115 |
| 3 | 1066.914 | 634.135 | 11.742 | 1231.007 | -1055.17 | 634.026 | 1.061 | -58.999 |

| STATION | V/VCR | MV | W/WCR | MW |
|---|---|---|---|---|
| 0 | 0.1230 | 0.1148 | | |
| 1 | 0.9090 | 0.8974 | | |
| 2 | 0.9745 | 0.9708 | 0.2893 | 0.2713 |
| 3 | 0.3112 | 0.2917 | 0.5937 | 0.5662 |

GEOMETRY

| STATION | DIAMETER | BLADE HEIGH T | AREA |
|---|---|---|---|
| 0 | 11.0019 | 0.3439 | 11.8864 |
| 1 | 8.5584 | 0.3439 | 9.2464 |
| 2 | 8.0210 | 0.3439 | 8.6658 |
| 3 | 3.9502 | 1.2634 | 15.6789 |

LOSS ANALYSIS

| | DELH | DEL ETA | PRESS RECO V | OMEGA | E BAR |
|---|---|---|---|---|---|
| NOZZLE | 6.976 | 0.0325 | 0.9591 | 0.1094 | 0.0732 |
| VANELESS SPACE | 0.651 | 0.0030 | 0.9964 | | |
| INCIDENCE | 0.084 | 0.0004 | | | |
| AXIAL CLEARANCE | 3.269 | 0.0152 | | | |
| RADIAL CLEARANCE | 2.966 | 0.0138 | | | |
| ROTOR | 13.537 | 0.0630 | 0.8696 | 0.813 | 0.3968 |
| WINDAGE | 2.260 | 0.0105 | | | |
| EXIT | 8.031 | 0.0374 | | | |

GEOMETRIC PARAMETERS

| NOZZLE | ROTOR | |
|---|---|---|
| N O. OF BLADES=15.0 | NO. OF BLADES=13.0 | THETA TOTAL/L=0.0100 |
| SOLIDITY= 1.399 | SOLIDITY= 3.386 | AXIAL CLEARANCE=0.0300 |
| CHORD 2.509 | SPACING(EXIT-M)= 0.962 | RADIAL CLEARANCE=0.0100 |
| SPACING(EXIT)= 1.792 | SPACING(EXIT-H) 0.649 | BLADE INLET ANGLE= 0.0 |
| TR EDGE THICK=0.0200 | TR EDGE THICK=0.0650 | |

GENERAL PARAMETERS

| | | |
|---|---|---|
| SPECIFIC SPEED= 62.225 | D3 H/D3T=0.5153 | VANE THROAT AREA 2.3148 in.$^2$ |
| SPECIFIC DIAMETER= 1.6266 | D3M/D2=0.4925 | VANE THROAT WIDTH 0.4487 in. |
| AN SQRD= 0.41719E+09 | H1/D2=0.0429 | |
| UNTAPERED HUB STRESS= 77555.87 | D1/D2= 1.0670 | |
| BORE STRESS= 98557.69 | D0/D1= 1.2855 | |
| THROAT CHOKED W= 4.5616 | STATION 1 CHOKED W= 4.5616 | |
| PS REACTION= 0.3791 | VEL REACTION= 0.4996 | REY NO= 0.31795E+06 |

Development of a radial turbine taking full advantage of increased design capabilities awaits its application in a suitable engine program.

The meanline performance analysis at 100% IRP shown in Table 3.1-5 presents the relevant geometric, and aerodynamic performance data. Information is broken down into cycle parameter, velocity diagram, flow path/blade geometry, loss analysis, and general parameters. Station definition is as follows: 00-inlet, 0-vane inlet outer diameter, 1-vane exit diameter, 2-rotor inlet diameter, 3-rotor exit plane.

The Allison radial turbine aerodynamic analysis program was used to predict performance at two additional point, 75% power and idle. These results are presented in Tables 3.1-6 and 3.1-7.

Detailed aerodynamic design of the rotor was accomplished using 2-D and 3-D inviscid codes in conjunction with a 1-D boundary layer analyses. For the purpose of this study, the shroud contour and inducer width were predetermined for conformance to NASA rig hardware constraints. The meridional flow path is shown in Figure 3.1-2. The blade angle distribution and hub contour were design parameters subject to selection in providing the desired blade loading distributions.

The logarithmic blade thickness distributions used were based strongly on previous HIRT optimization studies. A region of constant wall thickness as shown in Figure 3.1-3 was employed which reflects casting technology constraint on the design. Blade metal normal thickness (total for the two side walls) distributions are shown in Figure 3.1-4.

Blade angle distribution was selected to achieve near constant aerodynamic loading on the blade for the mean and shroud contours, with minimal turning downstream of the rotor throat. Distributions of this type load the blade uniformly over its length and avoid diffusion on the blade suction surfaces. The selected blade angle distribution is shown in Figure 3.1-5 along with the AGT 100 power turbine design. The AGT 100 power turbine has demonstrated superior performance and was used as a guide in this design. Blade sections of the resulting design are shown and presented in Figures 3.1-6 and 7. The rotor was designed to produce a near zero exit swirl at design conditions. Figure 3.1-8 shows the exducer section exit swirl angle as a function of exducer span.

The resulting surface velocity distributions for the rotor are shown in Figure 3.1-9 through 3.1-11 as predicted by two methods, a meridional solution (2-D) and a blade to blade solution (quasi 3-D). Comparable results for the AGT 100 power turbine are shown in Figures 3.1-12 to 14. The three dimensional results were subsequently smoothed and a 1-D boundary layer solution was performed. Results are summarized in Figures 3.1-15 to 17. Figure 3.1-18 presents a summary of the results for the hub, mean, and tip streamlines.

Note that for the hub streamline, an excessive amount of diffusion was present over a significant portion of the blade. This was partly the result of specification of radial filament blading for the rotor as is common in radial turbine design practice.

# TABLE 3.1-6 TURBINE PERFORMANCE ESTIMATE AT 75% POWER

| ACTUAL | | CORRECTED |
|---|---|---|
| W= 4.2222 | EFF-TT(ADIABATIC)=0.8724 | WRTHCE/D= 0.7900 |
| DELH(ADIABATIC)=169.615 | EFF-TS(ADIABATIC)=0.8421 | DELH/THC(ADIABATIC)= 36.092 |
| SPEED= 61900.00 | EFF-TT(NET)=0.8602 | N/RTHC= 28553.68 |
| HP(NET)= 999.099 | EFF-TS(NET)=0.8303 | HP/DRTHC= 38.1146 |
| TORQUE= 85.971 | RTOT= 3.6271 | TE/D= 7.420 |
| U/CT=0.6943 U/CS=0.6821 | RTOS= 3.8297 | SPEED-FLOW PAR= 375.94 |

CYCLE PARAMETERS

| STATION | T TOTAL | P TOTAL | T STATIC | P STATIC | GAMMA | CP | T RELATIVE |
|---|---|---|---|---|---|---|---|
| 00 | 2516.000 | 177.700 | | | | | |
| 0 | 2516.000 | 177.700 | 2511.122 | 176.203 | | | |
| 1 | 2516.000 | 170.980 | 2264.778 | 108.081 | 1.298 | 0.2992 | |
| 2 | 2516.000 | 170.409 | 2227.512 | 100.202 | 1.298 | 0.2992 | 2251.759 |
| 3 | 1947.567 | 48.992 | 1922.905 | 46.401 | 1.306 | 0.2926 | 2014.461 |

VELOCITY DIAGRAM

| STATION | U | V | VU | W | WU | VR | ALPHA | BETA |
|---|---|---|---|---|---|---|---|---|
| 0 | | 270.295 | 0.0 | | | 270.295 | 0.0 | |
| 1 | | 1939.857 | 1871.326 | | | 511.061 | 74.725 | |
| 2 | 2166.385 | 2078.762 | 1996.706 | 602.698 | -169.68 | 578.319 | 73.847 | -16.352 |
| 3 | 1066.914 | 601.140 | 74.101 | 1158.256 | -992.81 | 596.555 | 7.081 | -58.999 |

| STATION | V/VCR | MV | W/WCR | MW |
|---|---|---|---|---|
| 0 | 0.1223 | 0.1142 | | |
| 1 | 0.8780 | 0.8634 | | |
| 2 | 0.9409 | 0.9329 | 0.2883 | 0.2705 |
| 3 | 0.3088 | 0.2894 | 0.5850 | 0.5576 |

GEOMETRY

| STATION | DIAMETER | BLADE HEIGH T | AREA |
|---|---|---|---|
| 0 | 11.0019 | 0.3439 | 11.8864 |
| 1 | 8.5584 | 0.3439 | 9.2464 |
| 2 | 8.0210 | 0.3439 | 8.6658 |
| 3 | 3.9502 | 1.2634 | 15.6789 |

LOSS ANALYSIS

| | DELH | DEL ETA | PRESS RECO V | OMEGA | E BAR |
|---|---|---|---|---|---|
| NOZZLE | 5.973 | 0.0307 | 0.9619 | 0.1077 | 0.0736 |
| VANELESS SPACE | 0.560 | 0.0029 | 0.9967 | | |
| INCIDENCE | 0.209 | 0.0011 | | | |
| AXIAL CLEARANCE | 3.014 | 0.0155 | | | |
| RADIAL CLEARANCE | 2.735 | 0.0141 | | | |
| ROTOR | 11.984 | 0.0616 | 0.8709 | 0.826 | 0.4017 |
| WINDAGE | 2.367 | 0.0122 | | | |
| EXIT | 7.217 | 0.0371 | | | |

GEOMETRIC PARAMETERS

| NOZZLE | ROTOR | |
|---|---|---|
| N O. OF BLADES=15.0 | NO. OF BLADES=13.0 | THETA TOTAL/L=0.0100 |
| SOLIDITY= 1.399 | SOLIDITY= 3.386 | AXIAL CLEARANCE=0.0300 |
| CHORD 2.509 | SPACING(EXIT-M)= 0.962 | RADIAL CLEARANCE=0.0100 |
| SPACING(EXIT)= 1.792 | SPACING(EXIT-H) 0.649 | BLADE INLET ANGLE= 0.0 |
| TR EDGE THICK=0.0200 | TR EDGE THICK=0.0650 | |

GENERAL PARAMETERS

| | | |
|---|---|---|
| SPECIFIC SPEED= 65.030 | D3 H/D3T=0.5153 | |
| SPECIFIC DIAMETER= 1.6357 | D3M/D2=0.4925 | |
| AN SQRD= 0.41719E+09 | H1/D2=0.0429 | |
| UNTAPERED HUB STRESS= 77555.87 | D1/D2= 1.0670 | |
| BORE STRESS= 98557.69 | D0/D1= 1.2855 | |
| THROAT CHOKED W= 4.2449 | STATION 1 CHOKED W= 4.2449 | |
| PS REACTION= 0.4098 | VEL REACTION= 0.5339 | REY NO= 0.31588E+06 |

TABLE 3.1-7 TURBINE PERFORMANCE ESTIMATE AT IDLE POWER

| ACTUAL | | CORRECTED |
|---|---|---|
| W= 1.6516 | EFF-TT(ADIABATIC)=0.8636 | WRTHCE/D= 0.7880 |
| DELH(ADIABATIC)= 84.171 | EFF-TS(ADIABATIC)=0.8399 | DELH/THC(ADIABATIC)= 29.281 |
| SPEED= 39059.00 | EFF-TT(NET)=0.8545 | N/RTHC= 23037.13 |
| HP(NET)= 194.617 | EFF-TS(NET)=0.8310 | HP/DRTHC= 30.9522 |
| TORQUE= 26.448 | RTOT= 2.7889 | TE/D= 7.443 |
| U/CT=0.6188 U/CS=0.6102 | RTOS= 2.8818 | SPEED-FLOW PAR= 302.56 |

CYCLE PARAMETERS

| STATION | T TOTAL | P TOTAL | T STATIC | P STATIC | GAMMA | CP | T RELATIVE |
|---|---|---|---|---|---|---|---|
| 00 | 1539.000 | 54.500 | | | | | |
| 0 | 1539.000 | 54.500 | 1536.031 | 54.043 | | | |
| 1 | 1539.000 | 52.253 | 1383.928 | 32.885 | 1.298 | 0.2992 | |
| 2 | 1539.000 | 52.062 | 1360.900 | 30.453 | 1.298 | 0.2992 | 1377.422 |
| 3 | 1257.072 | 19.542 | 1247.450 | 18.912 | 1.306 | 0.2926 | 1282.939 |

VELOCITY DIAGRAM

| STATION | U | V | VU | W | WU | VR | ALPHA | BETA |
|---|---|---|---|---|---|---|---|---|
| 0 | | 210.871 | 0.0 | | | 210.871 | 0.0 | |
| 1 | | 1524.081 | 1470.238 | | | 401.523 | 74.725 | |
| 2 | 1366.993 | 1633.327 | 1568.744 | 497.518 | 201.75 | 454.775 | 73.833 | 23.924 |
| 3 | 673.225 | 375.471 | 55.110 | 721.116 | -618.12 | 371.404 | 8.440 | -59.000 |

| STATION | V/VCR | MV | W/WCR | MW |
|---|---|---|---|---|
| 0 | 0.1220 | 0.1139 | | |
| 1 | 0.8820 | 0.8677 | | |
| 2 | 0.9452 | 0.9378 | 0.3043 | 0.2856 |
| 3 | 0.2401 | 0.2244 | 0.4564 | 0.4310 |

GEOMETRY

| STATION | DIAMETER | BLADE HEIGH T | AREA |
|---|---|---|---|
| 0 | 11.0019 | 0.3439 | 11.8864 |
| 1 | 8.5584 | 0.3439 | 9.2464 |
| 2 | 8.0210 | 0.3439 | 8.6658 |
| 3 | 3.9502 | 1.2634 | 15.6790 |

LOSS ANALYSIS

| | DELH | DEL ETA | PRESS RECO V | OMEGA | E BAR |
|---|---|---|---|---|---|
| NOZZLE | 3.985 | 0.0409 | 0.9584 | 0.1171 | 0.0791 |
| VANELESS SPACE | 0.376 | 0.0039 | 0.9963 | | |
| INCIDENCE | 1.177 | 0.0121 | | | |
| AXIAL CLEARANCE | 1.494 | 0.0153 | | | |
| RADIAL CLEARANCE | 1.356 | 0.0139 | | | |
| ROTOR | 4.645 | 0.0477 | 0.9025 | 0.962 | 0.4561 |
| WINDAGE | 0.888 | 0.0091 | | | |
| EXIT | 2.815 | 0.0289 | | | |

GEOMETRIC PARAMETERS

| NOZZLE | ROTOR | |
|---|---|---|
| N O. OF BLADES=15.0 | NO. OF BLADES=13.0 | THETA TOTAL/L=0.0100 |
| SOLIDITY= 1.399 | SOLIDITY= 3.386 | AXIAL CLEARANCE=0.0300 |
| CHORD 2.509 | SPACING(EXIT-M)= 0.962 | RADIAL CLEARANCE=0.0100 |
| SPACING(EXIT)= 1.792 | SPACING(EXIT-H) 0.649 | BLADE INLET ANGLE= 0.0 |
| TR EDGE THICK=0.0200 | TR EDGE THICK=0.0650 | |

GENERAL PARAMETERS

| | | |
|---|---|---|
| SPECIFIC SPEED= 54.346 | D3 H/D3T=0.5153 | |
| SPECIFIC DIAMETER= 1.7443 | D3M/D2=0.4925 | |
| AN SQRD= 0.16611E+09 | H1/D2=0.0429 | |
| UNTAPERED HUB STRESS= 30879.98 | D1/D2= 1.0670 | |
| BORE STRESS= 39242.02 | DO/D1= 1.2855 | |
| THROAT CHOKED W= 1.6646 | STATION 1 CHOKED W= 1.6576 | |
| PS REACTION= 0.3243 | VEL REACTION= 0.4006 | REY NO= 0.17953E+06 |

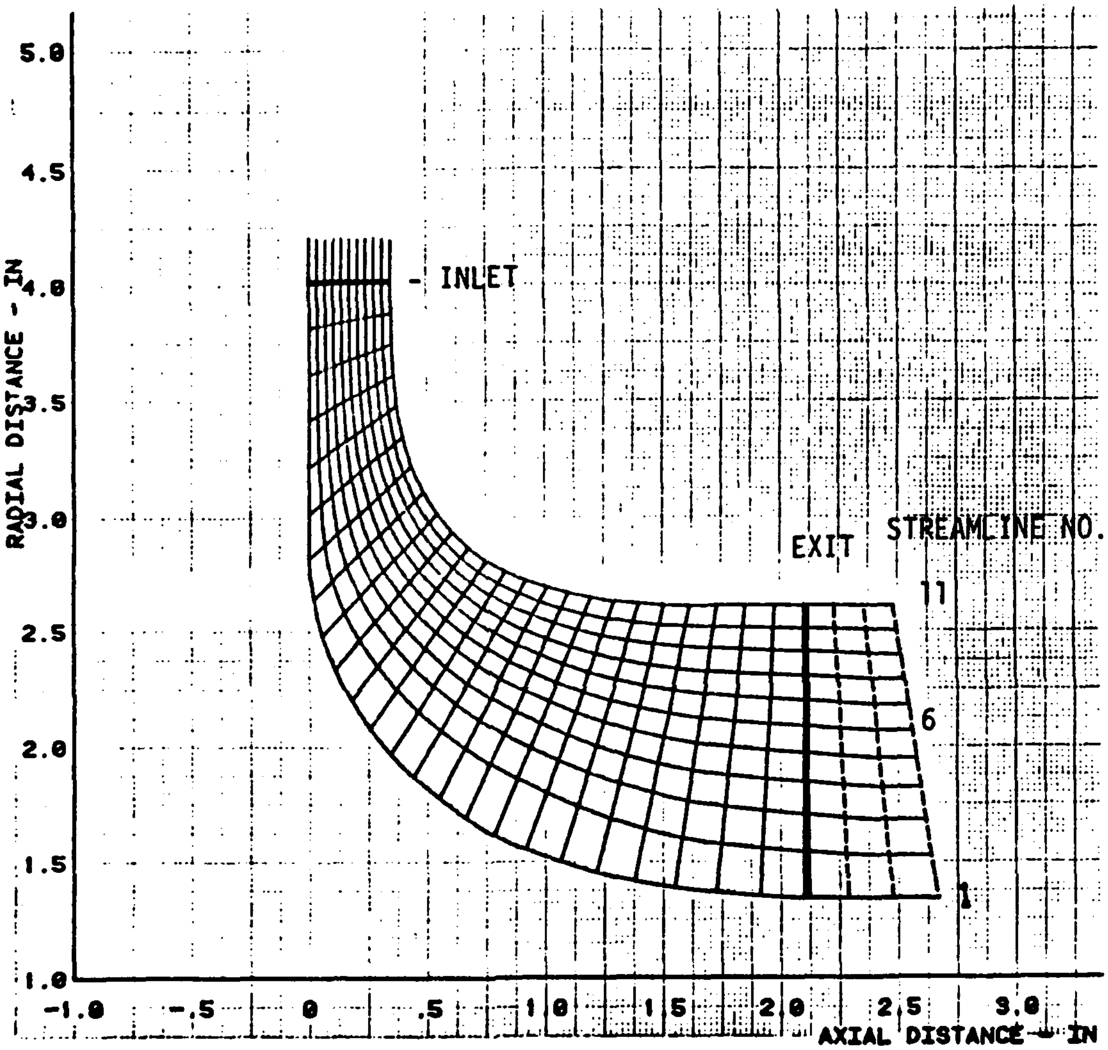


FIGURE 3.1-2 MERIDONIAL FLOWPATH

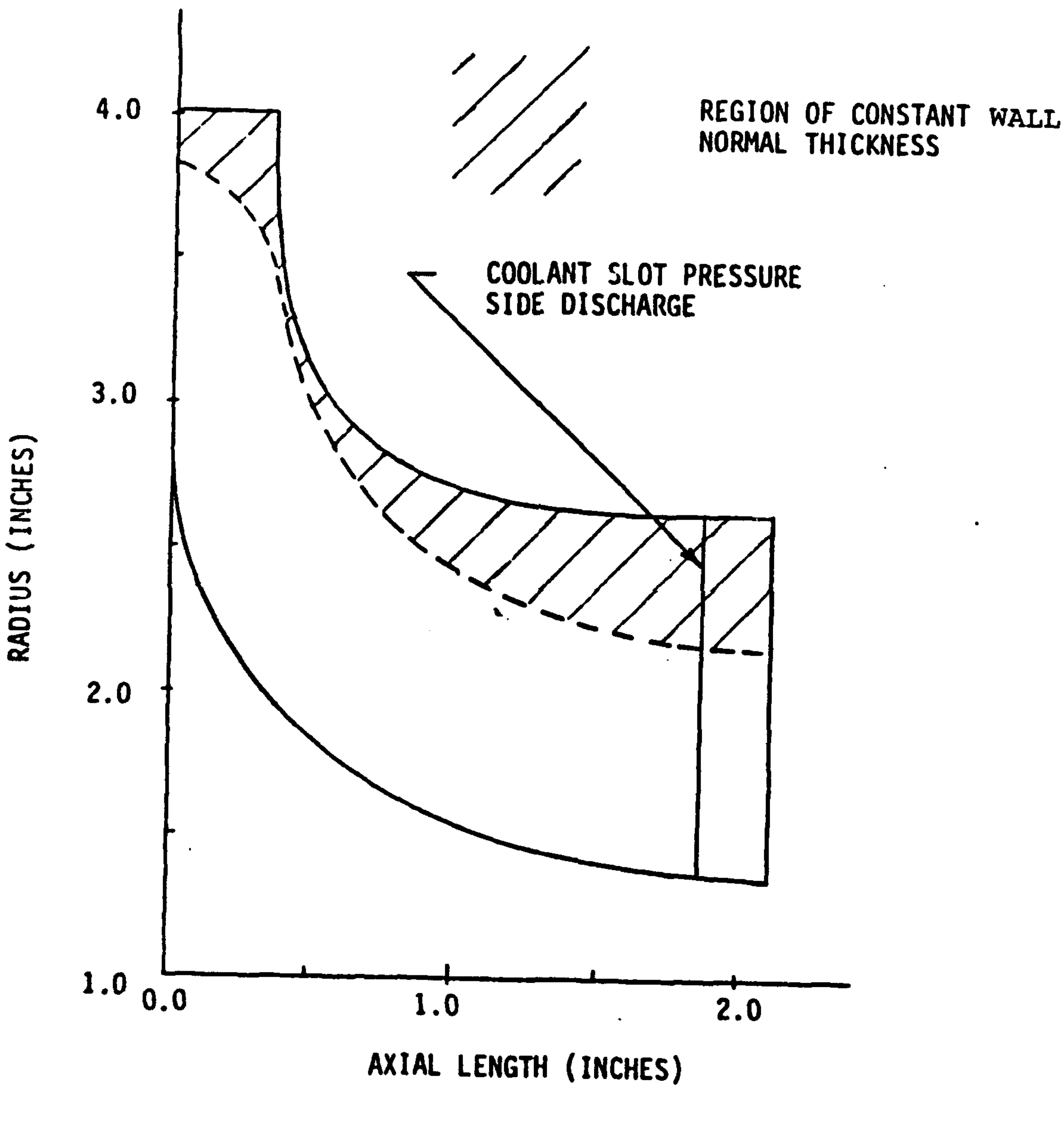


FIGURE 3.1-3 FLOWPATH WITH BLADE THICKNESS REGIONS

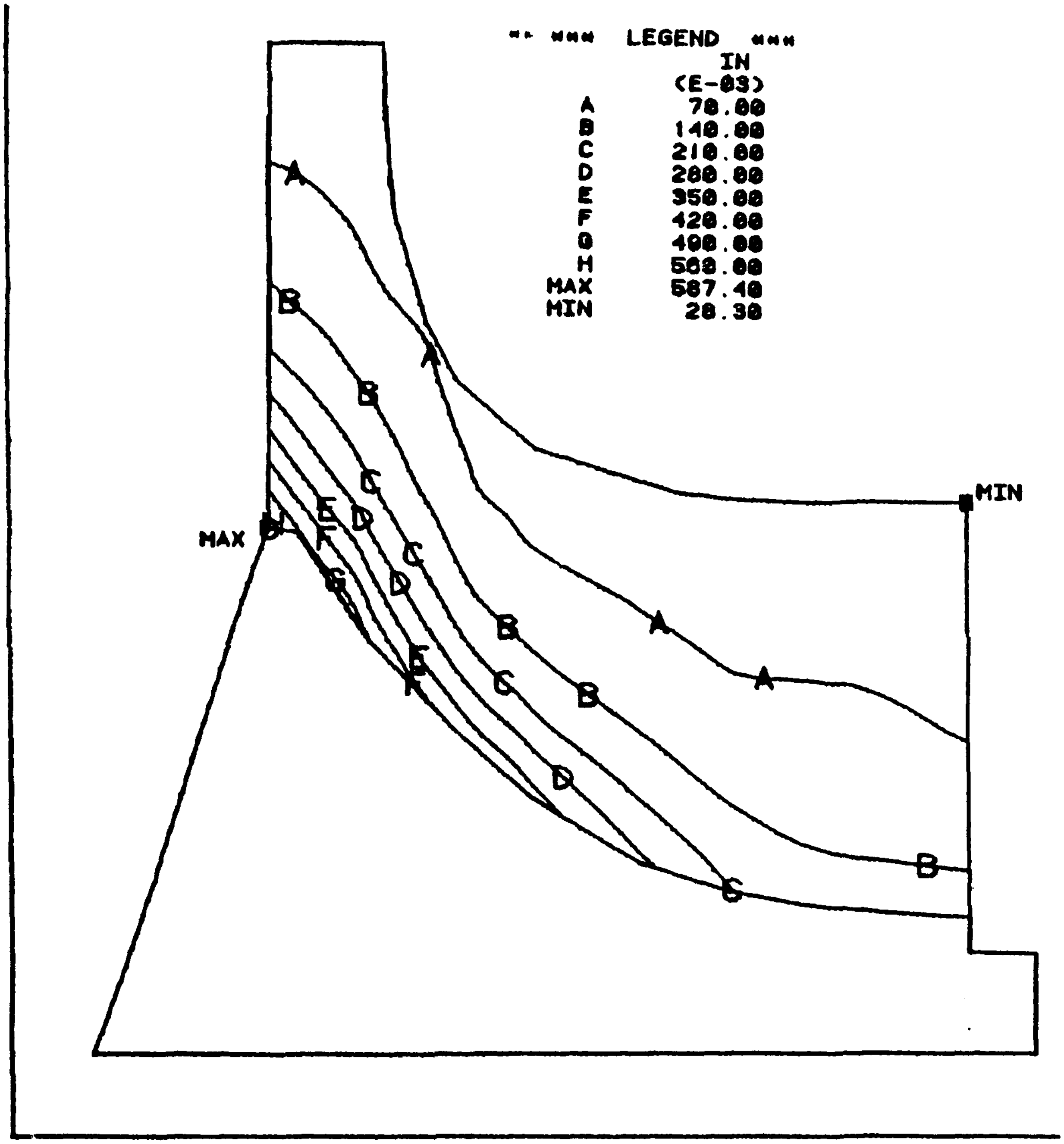


FIGURE 3.1-4 BLADE METAL NORMAL THICKNESS

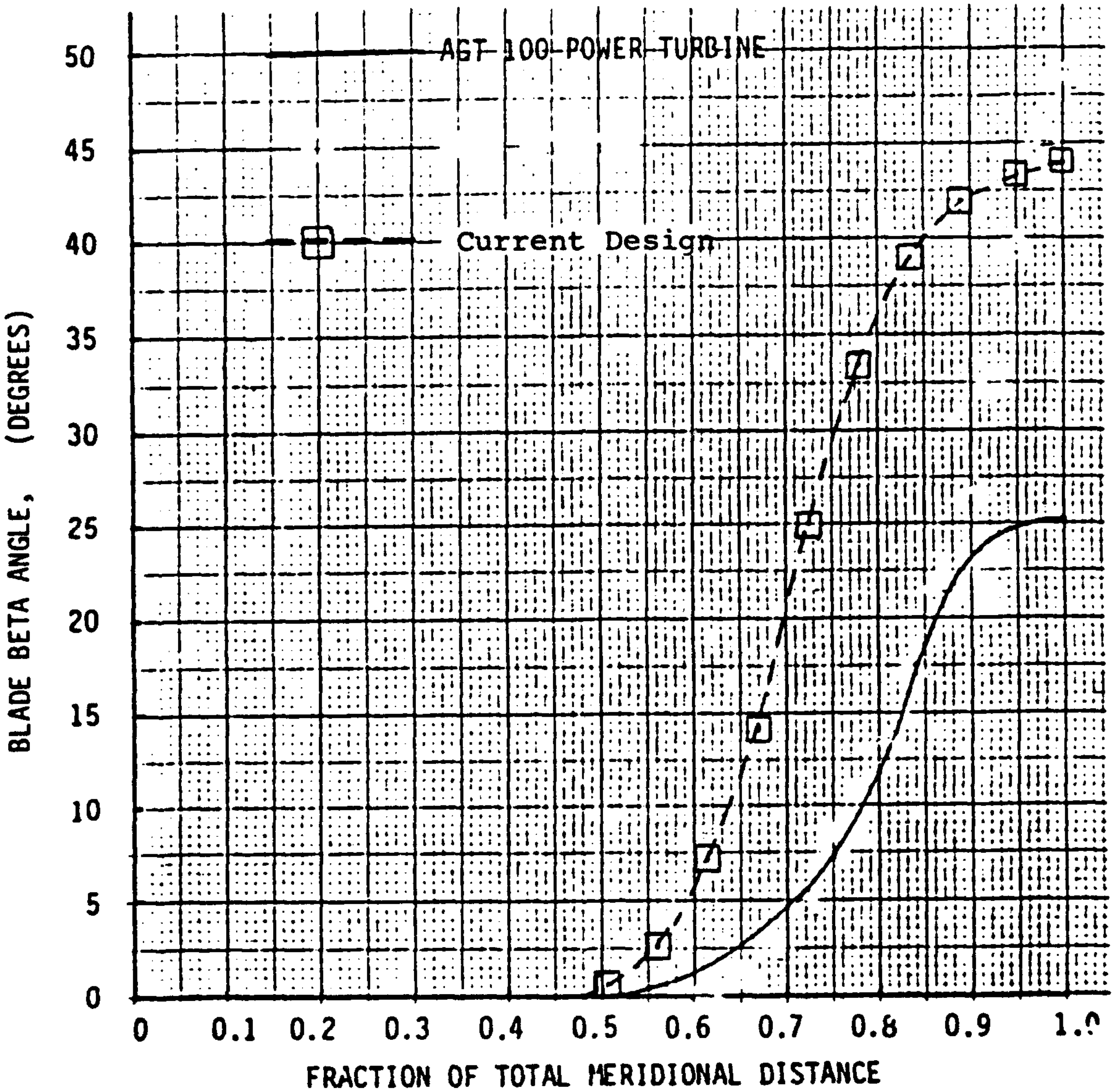


FIGURE 3.1-5 ROTOR BLADE ANGLE DISTRIBUTION

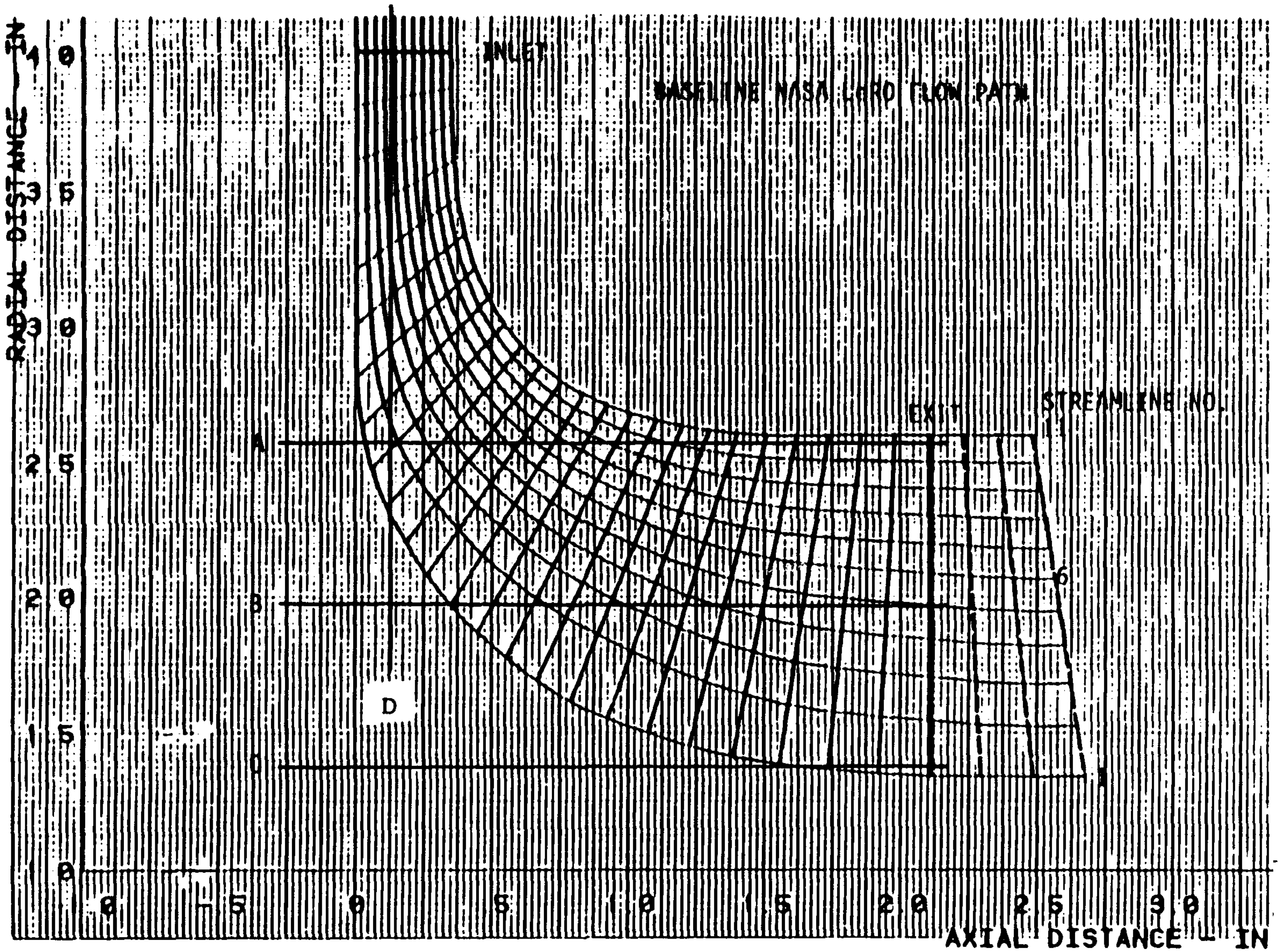


FIGURE 3.1-6 ROTOR STREAMLINE PREDICTIONS AND BLADE SECTION LOCATIONS

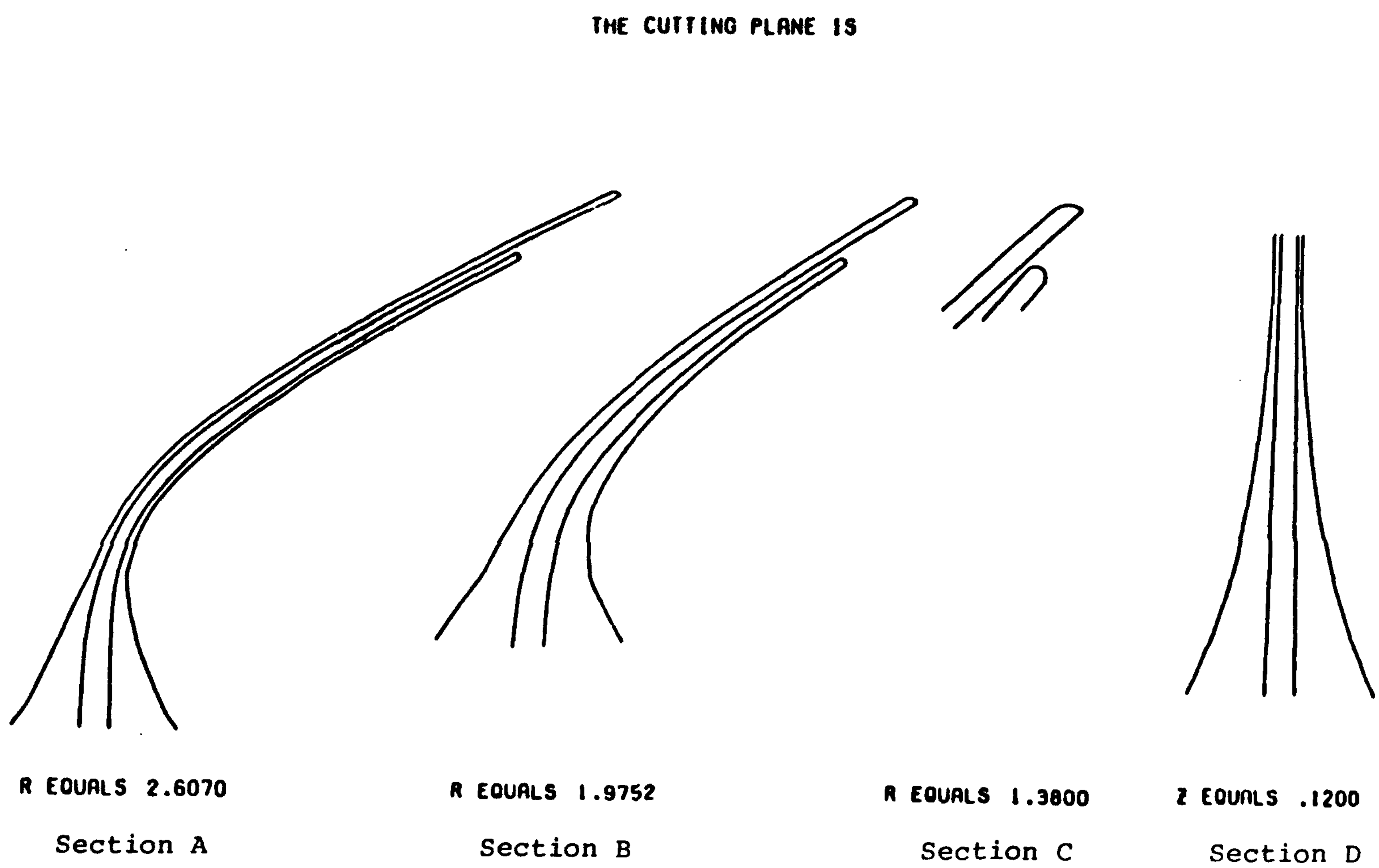


FIGURE 3.1-7 ROTOR BLADE SECTIONS

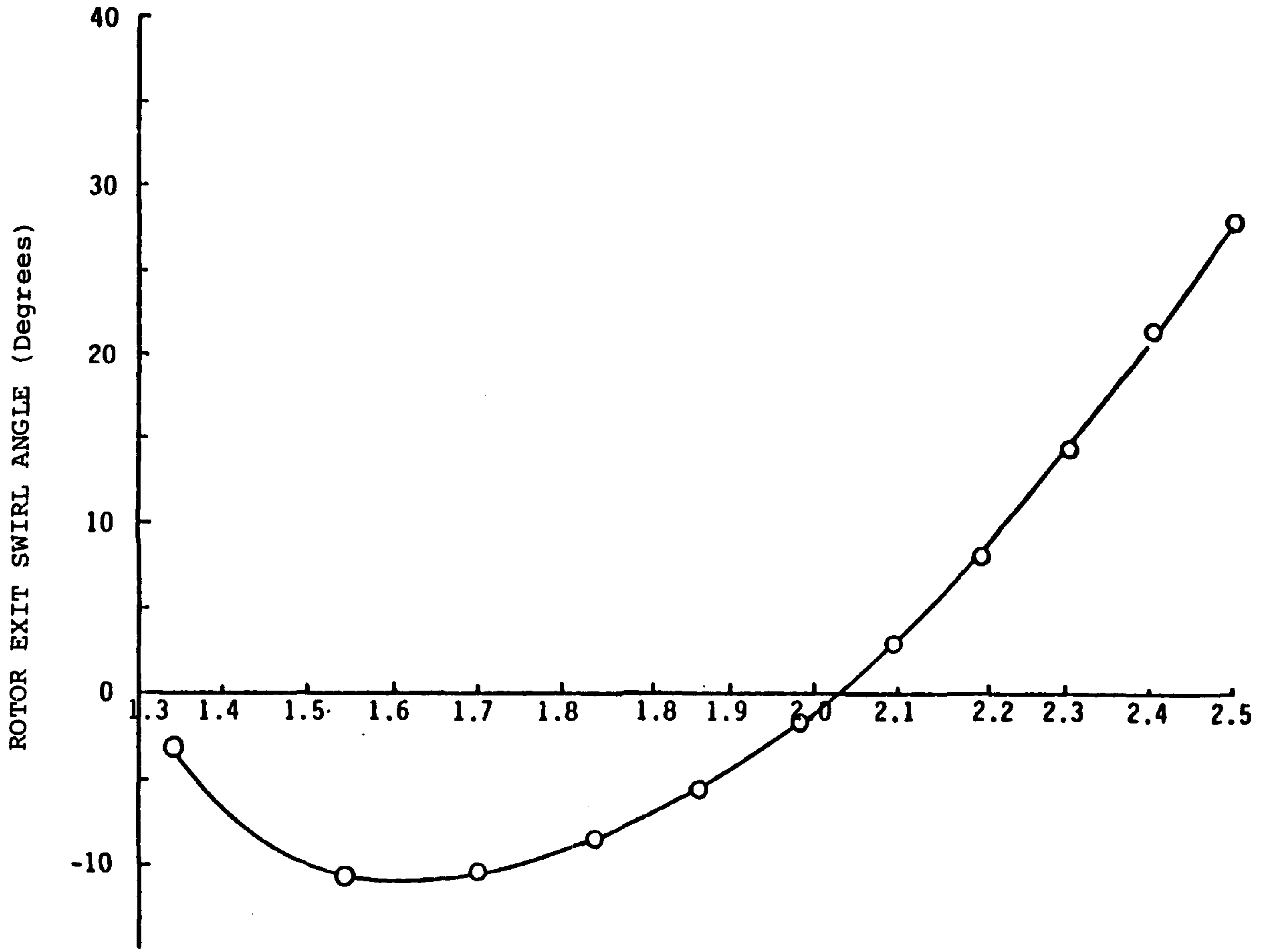


FIGURE 3.1-8 ROTOR EXIT SWIRL AT IRP

INITIAL FLOWPATH, STREAMLINE 1.

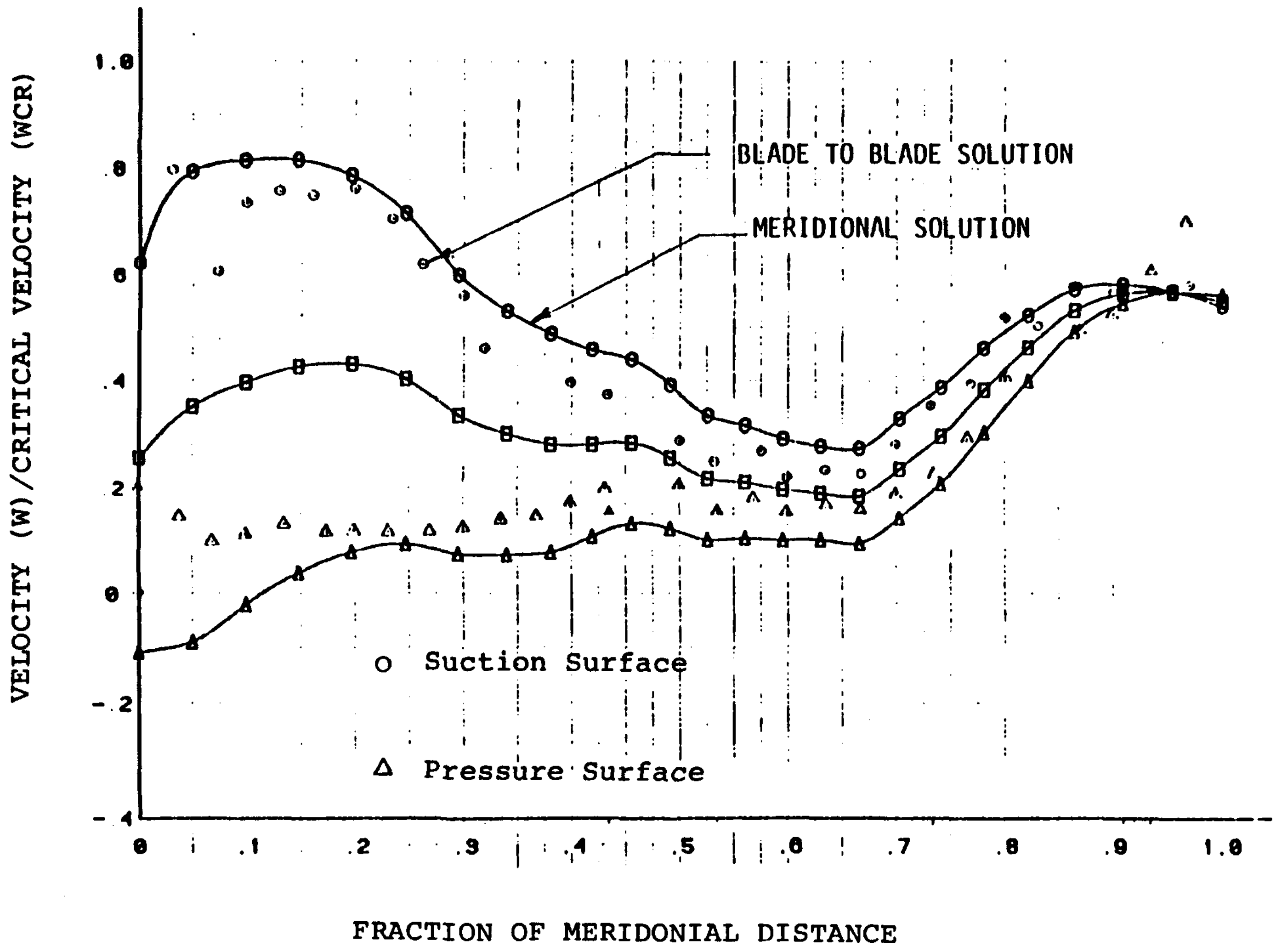


FIGURE 3.1-9 NASA HTRT ROTOR VELOCITY PROFILE, HUB STREAMLINE

INITIAL FLOW PATH, STREAMLINE 6

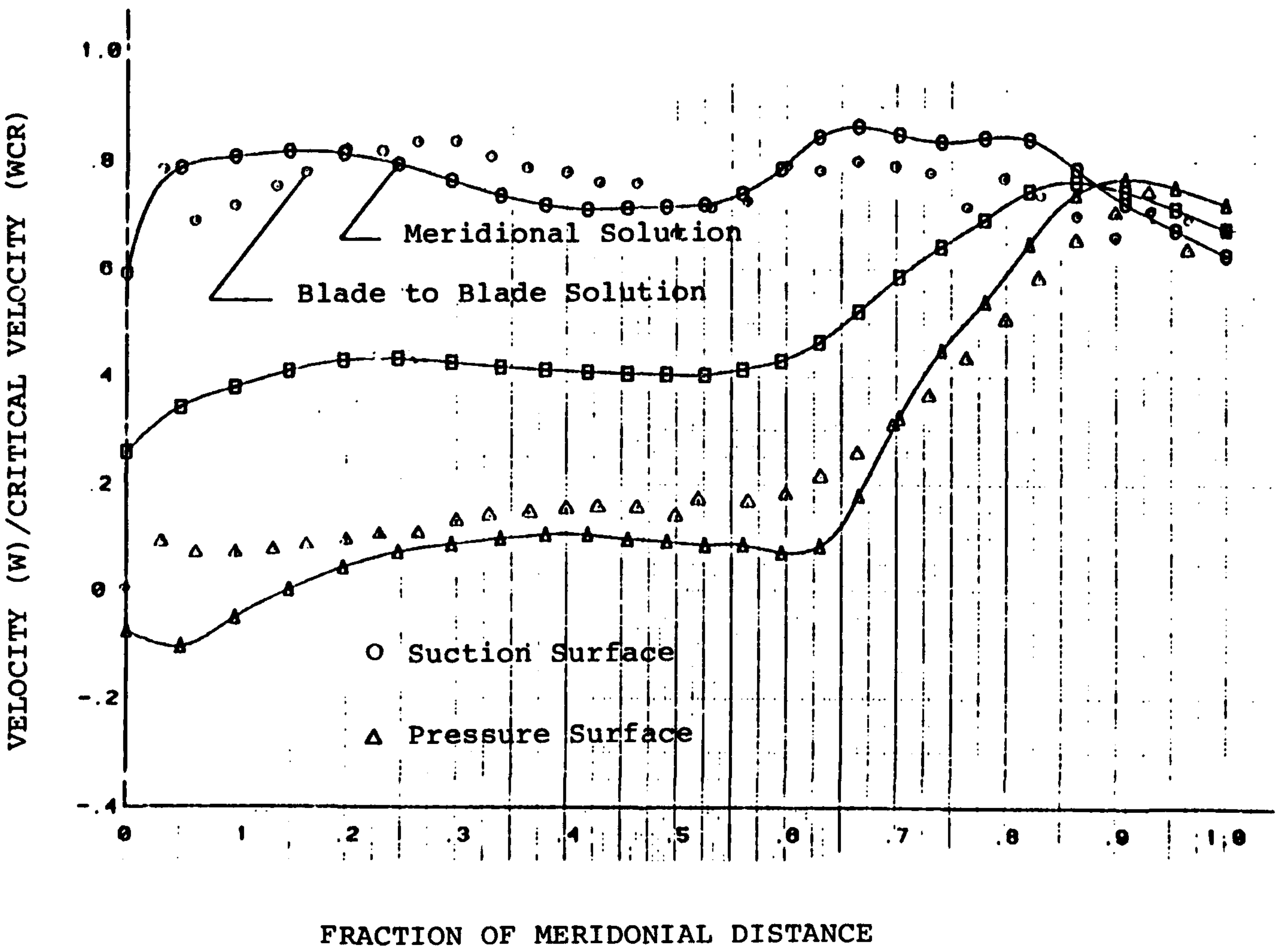


FIGURE 3.1-10 NASA HTRT ROTOR VELOCITY PROFILE, MEAN STREAMLINE

INITIAL FLOWPATH, STREAMLINE 11

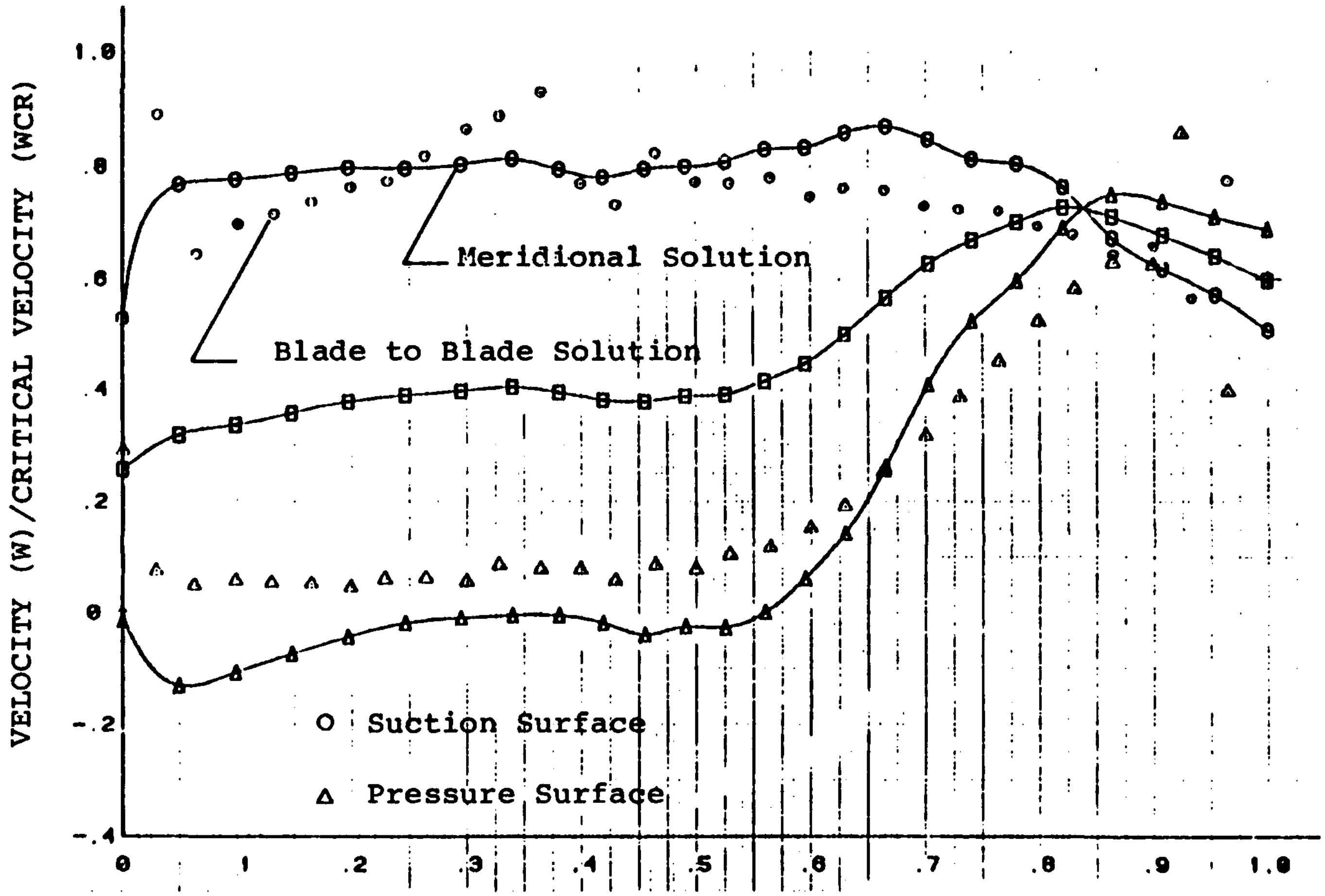


FIGURE 3.1-11 NASA HTRT ROTOR VELOCITY PROFILE, SHROUD STREAMLINE

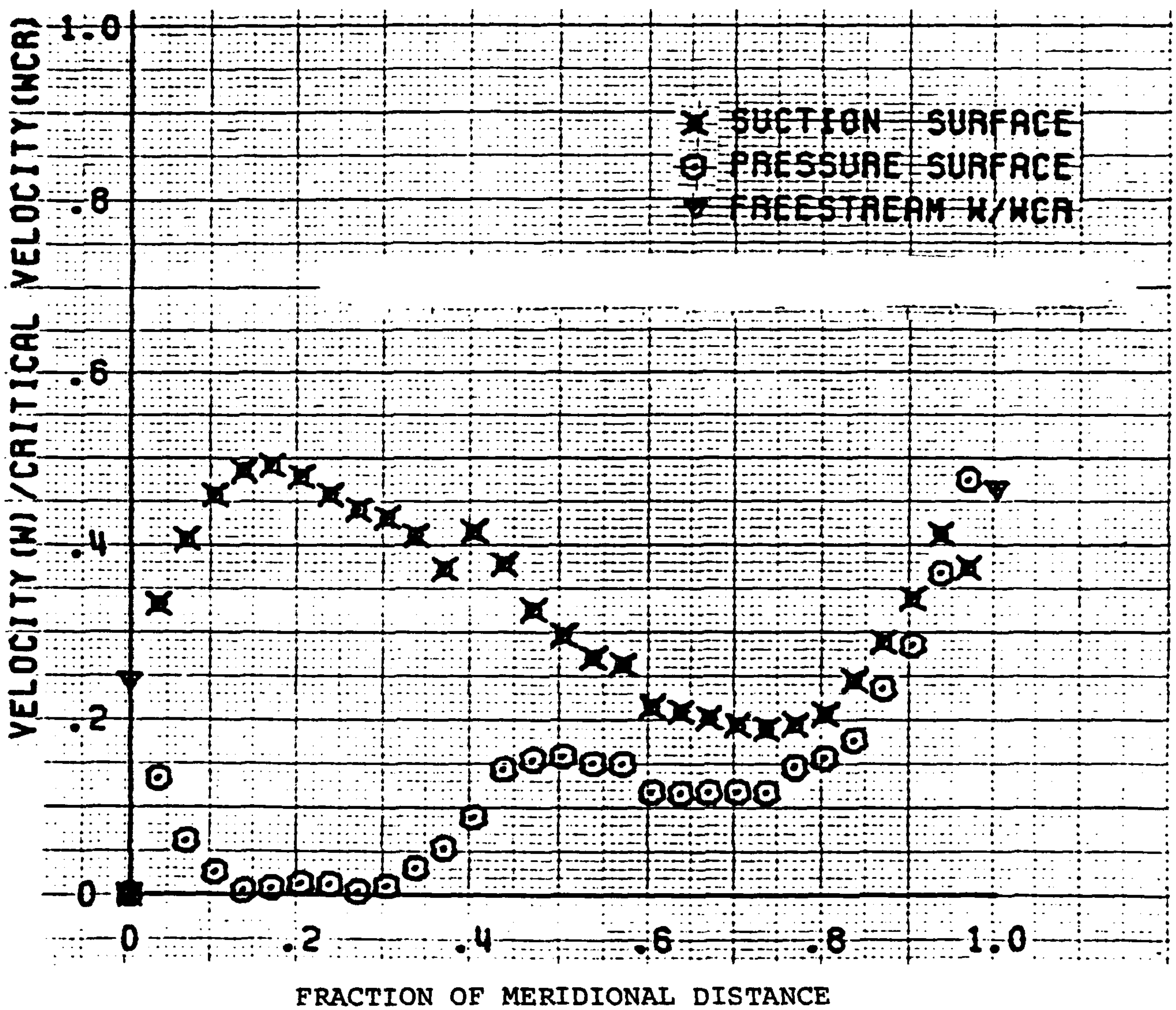


FIGURE 3.1-12 AGT100 POWER TURBINE ROTOR VELOCITY PROFILE, HUB STREAMLINE

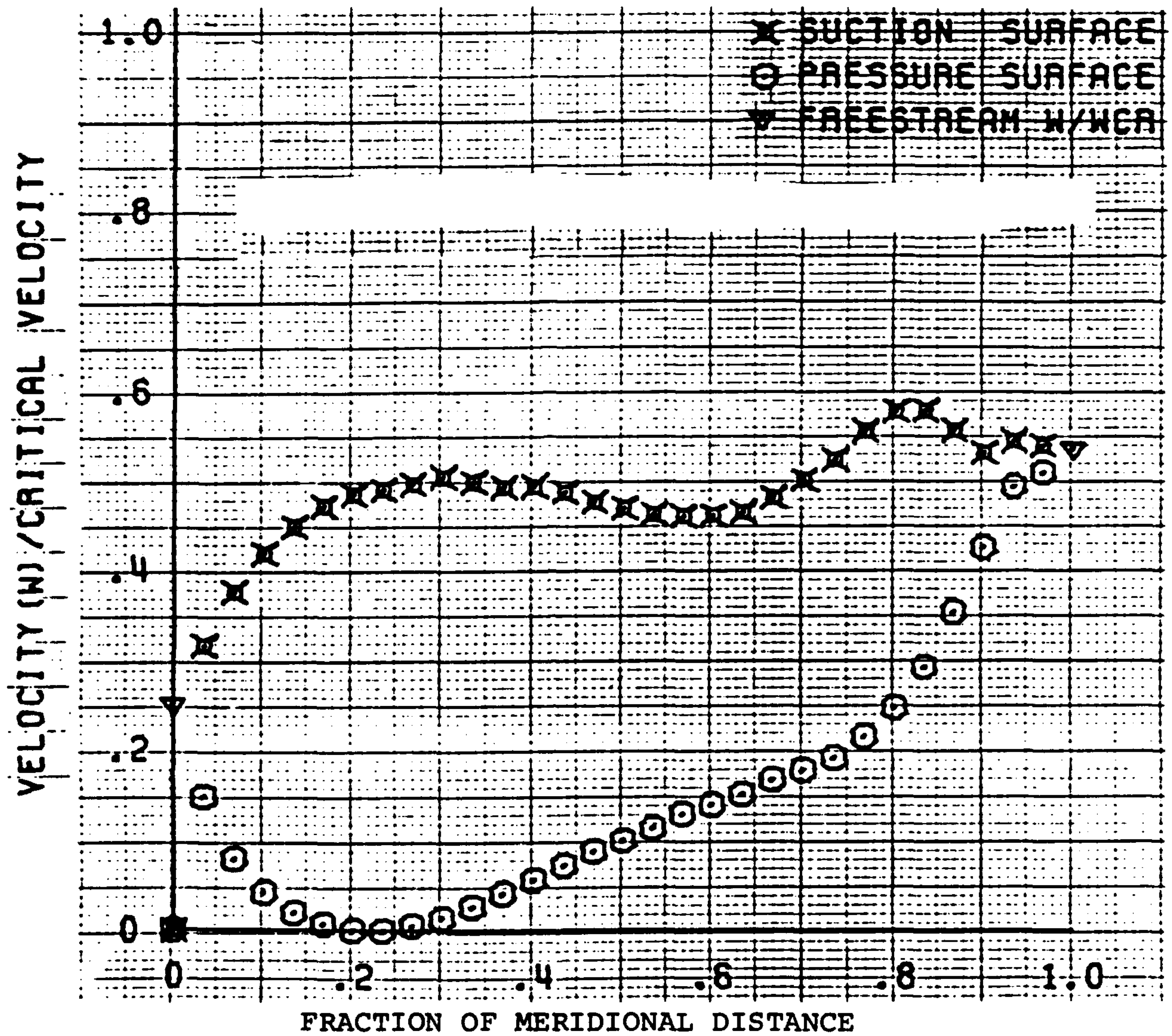


FIGURE 3.1-13 AGT100 POWER TURBINE ROTOR VELOCITY PROFILE, MEAN STREAMLINE

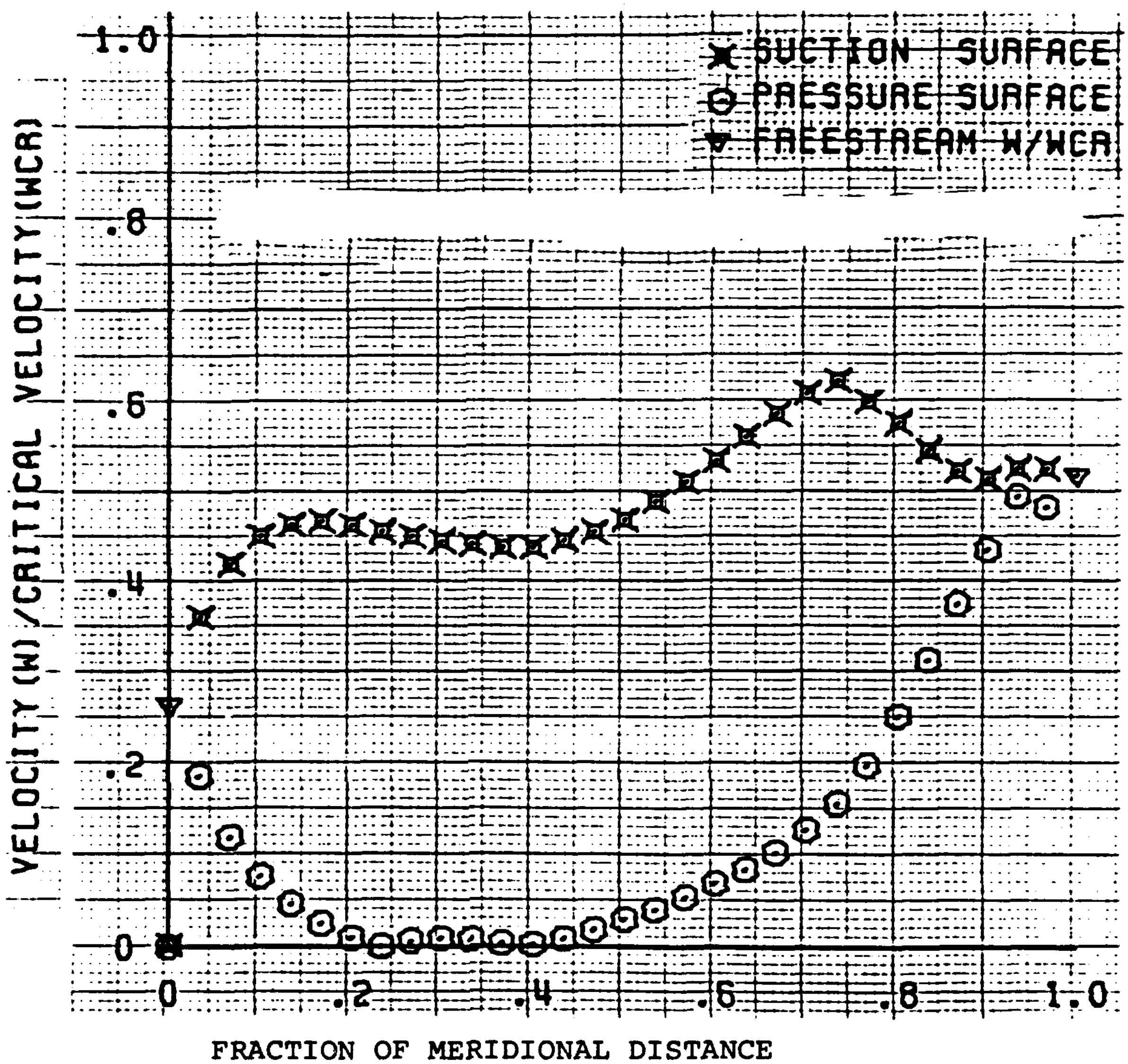


FIGURE 3.1-14 AGT100 POWER TURBINE ROTOR VELOCITY PROFILE, SHROUD STREAMLINE

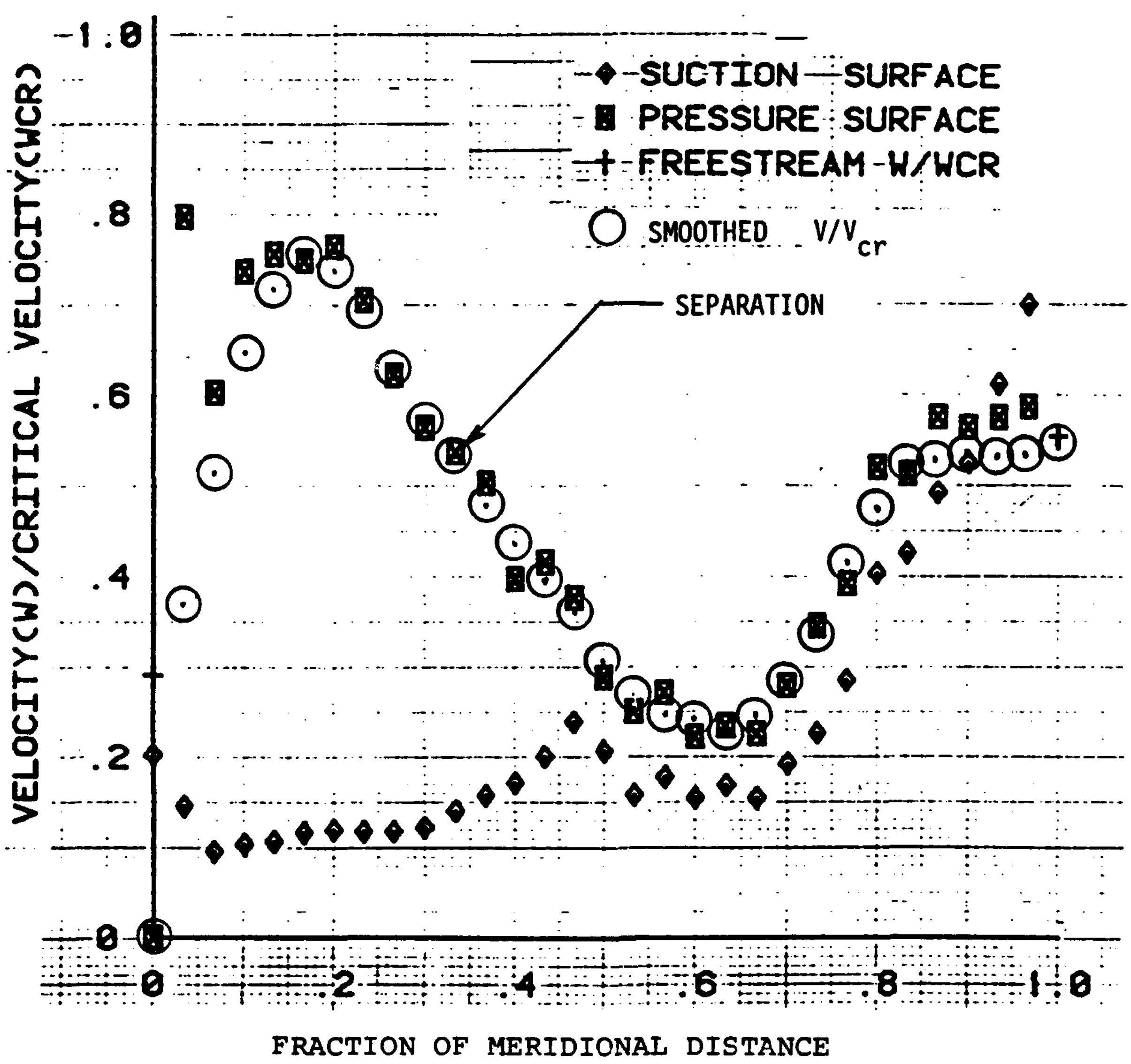


FIGURE 3.1-15 NASA HTRT ROTOR BOUNDARY LAYER ANALYSIS, HUB STREAMLINE

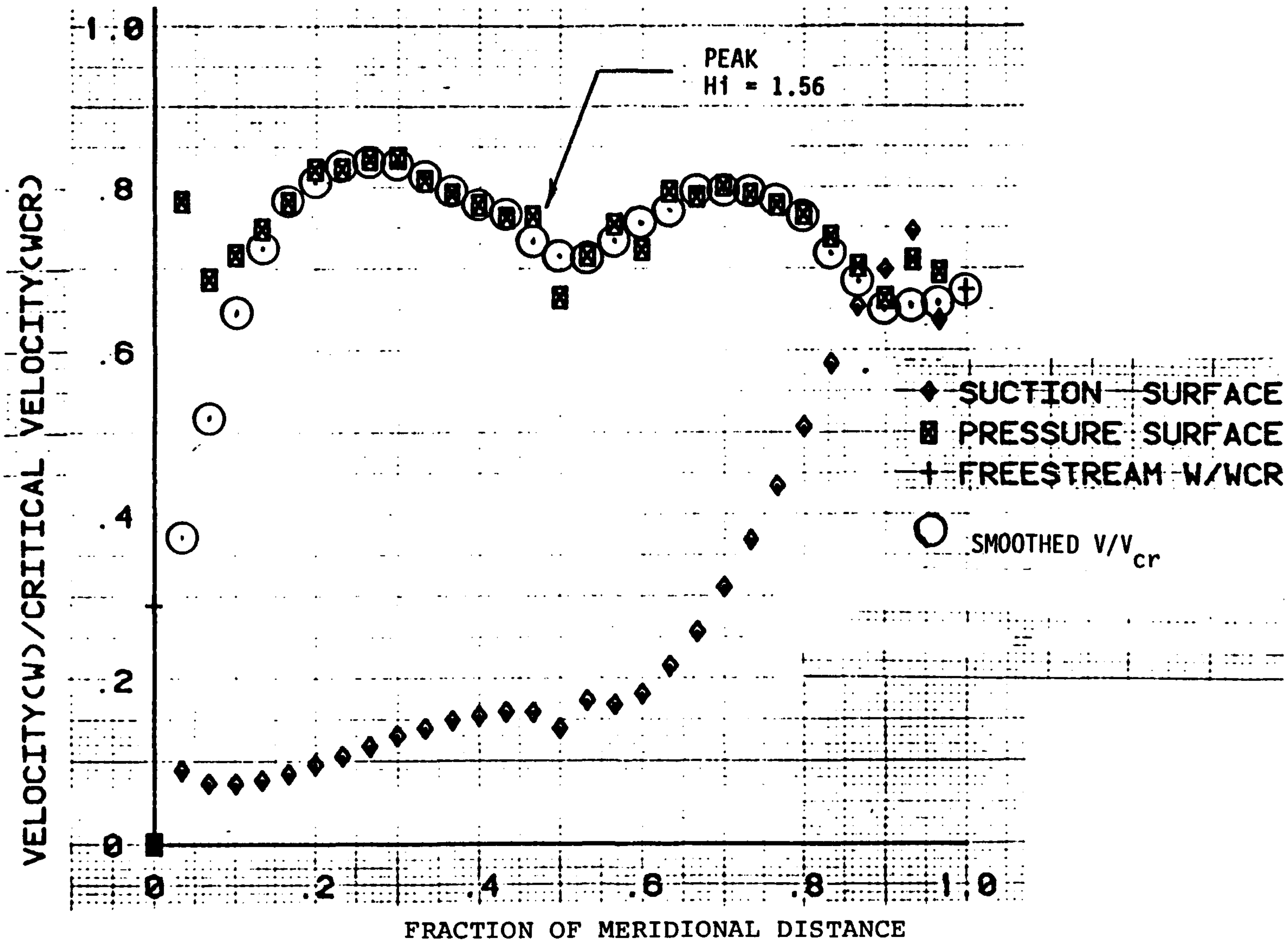


FIGURE 3.1-16 NASA HTRT ROTOR BOUNDARY LAYER ANALYSIS, MEAN STREAMLINE

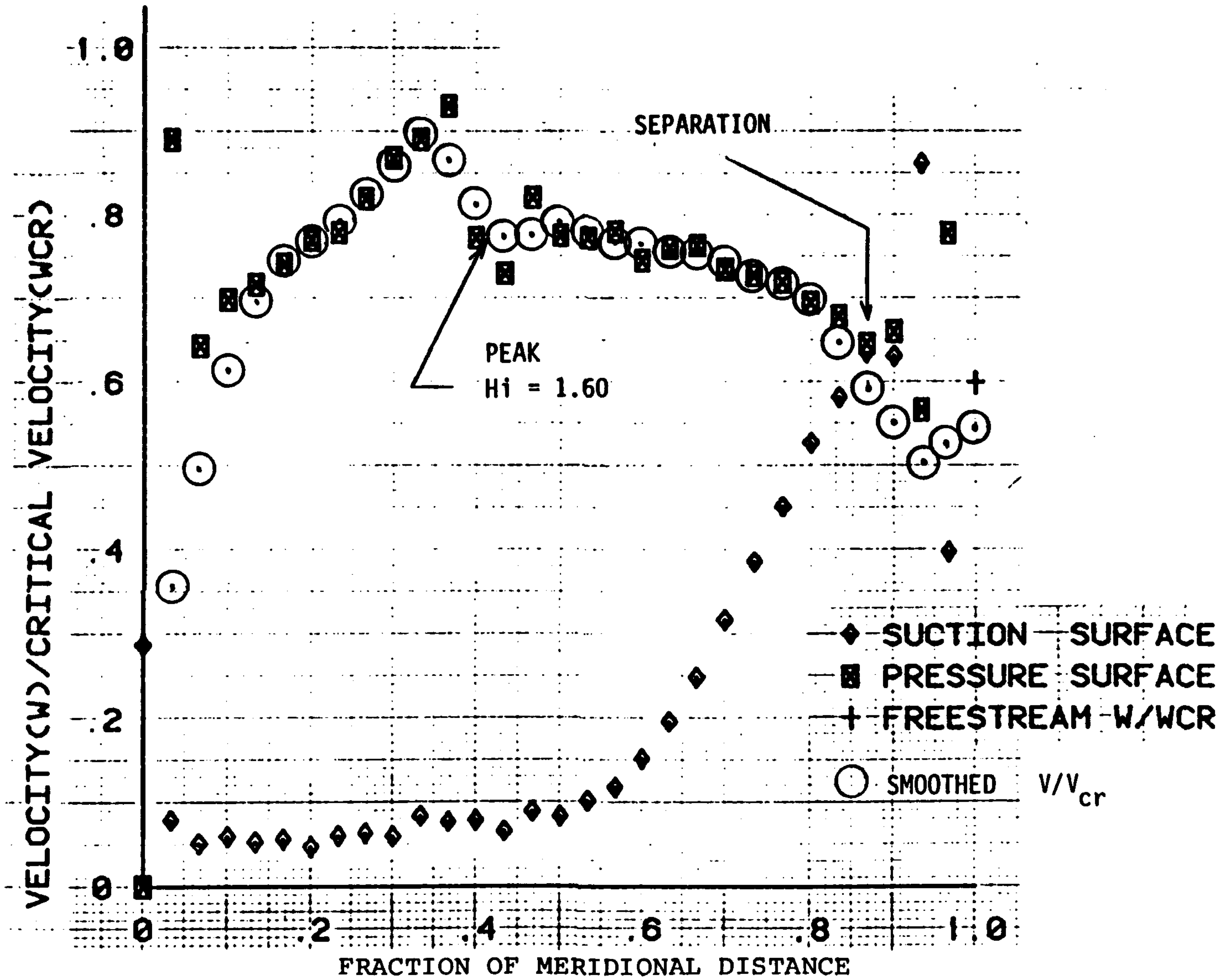


FIGURE 3.1-17 NASA HTRT ROTOR BOUNDARY LAYER ANALYSIS, SHROUD STREAMLINE

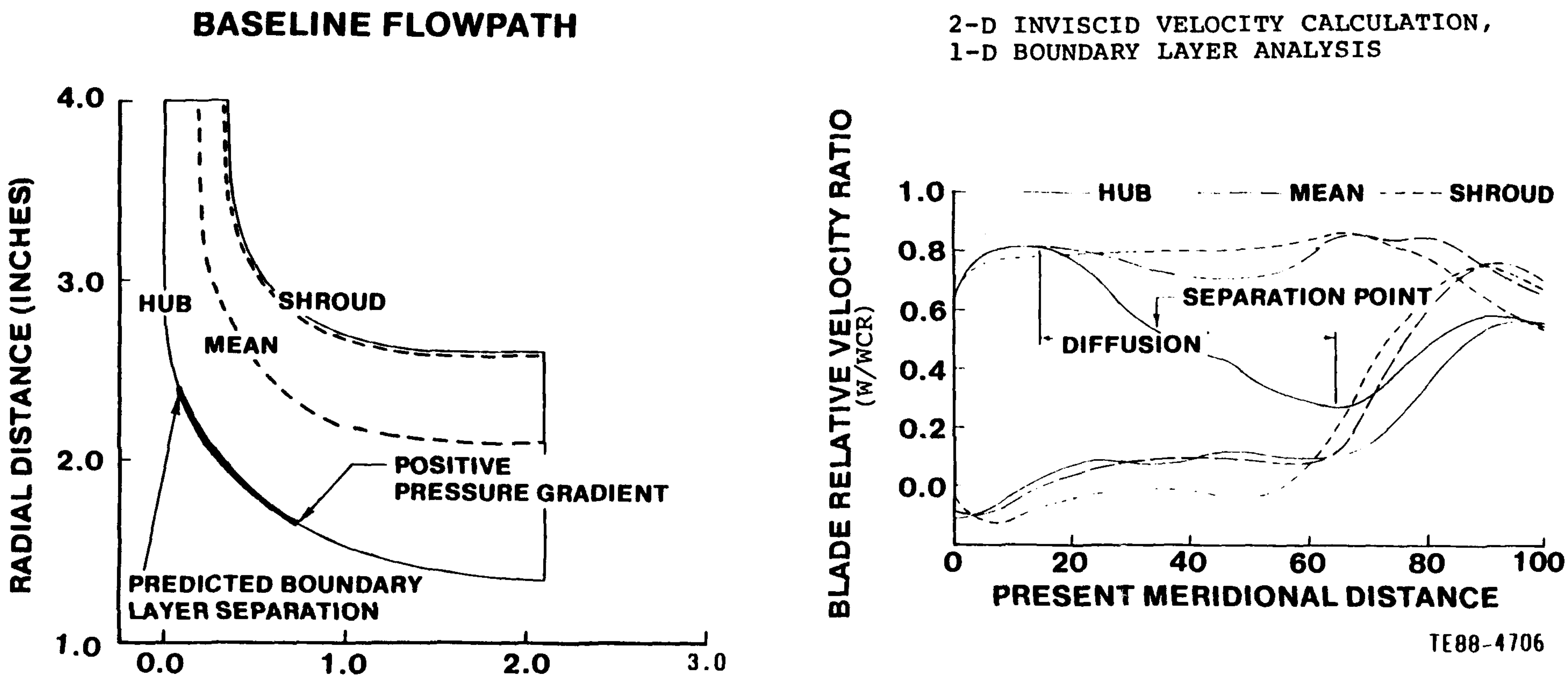


FIGURE 3.1-18 PREDICTED BLADE RELATIVE VELOCITIES FOR BASELINE ROTOR FLOWPATH

Radial filament blading eliminates bending stresses in the blade caused by rotational forces and thus reduces the overall blade stresses.

The one dimensional boundary layer analysis indicated the likelihood of boundary layer separation near the intersection of the hub and blade suction surfaces. This separated region was significantly larger than a similar region noted on the Task I rotor design as shown in Figure 3.1-19

In order to avoid this loss producing mechanism, the alternate hub contours of Figure 3.1-20 were examined for their potential in reducing the degree of diffusion. Results also shown on Figure 3.2-20 indicated that separation can be delayed or eliminated. Alterations to the mean and shroud streamline loadings with this hub contouring were found to be insignificant. However it was realized that the impact to the rotor and blade stress caused by this modification can be significant. Although blade stresses generally decrease with shortened blades, the potential exists for rotor disk stresses to rise. Thus, the addition of significant material to the disk, as in contour B, call for a comprehensive re-evaluation of the blade/disk stress picture tradeoffs. This analysis was beyond the scope of the study. For the purpose of this study, the improvements in hub diffusion offered by contour A were sufficiently improved over those of the baseline to warrant incorporation into the final rotor design.

### 3.1.3 Vane Aerodynamic Design

Design point performance of the vane was specified in Table 3.1-5. Table 3.1-8 presents the results of the design process along with a comparison with both the vane design results for the Task I turbine and the original NASA design for which the turbine research rig was designed.

Design of the blading was accomplished through the use of the Allison vane section generator. The resulting blade profile is presented in Figure 3.1-21. Vane velocity profiles are shown in Figure 3.1-22. Results of the 1-D boundary layer analysis shown in Figure 3.1-23 and 24 indicate a flow free of separation.

## 3.2 Rotor Coolant Passage Design

As part of the previously funded cooled radial turbine effort, a highly instrumented engine scale rotor was tested under warm turbine test conditions to evaluate it's cooling performance. Based on this work, the need for improvements in internal airfoil coolant passage design was identified as a next step in a cooled high temperature radial turbine fully meeting the requirements of advanced technology engines. A thorough consideration of the coolant flow path design constraints was found to be most important in achieving a successful design.

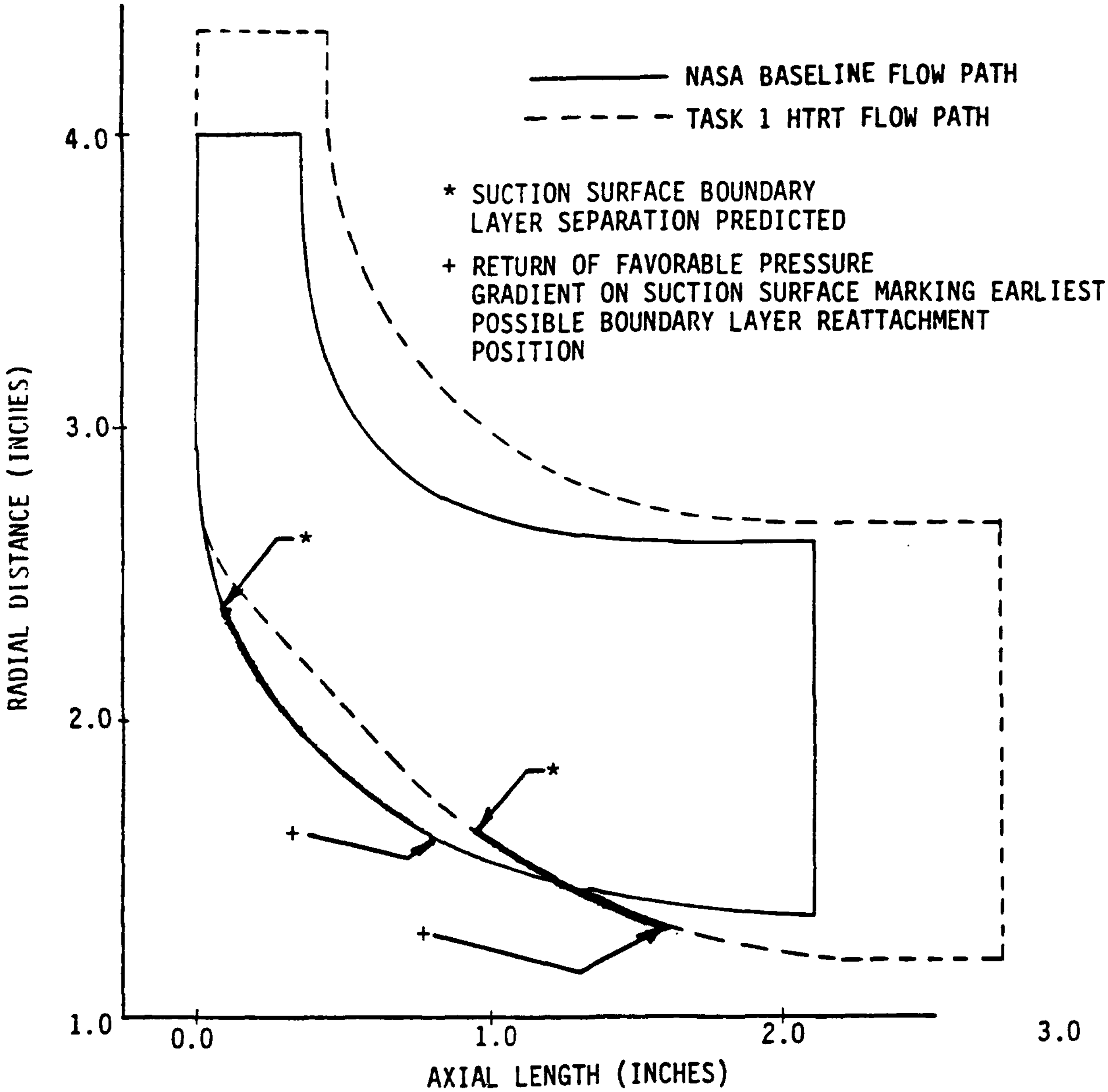


FIGURE 3.1-19 COMPARISON OF THE BASELINE FLOWPATH SEPARATED REGION WITH THAT OF THE TASK I ROTOR DESIGN

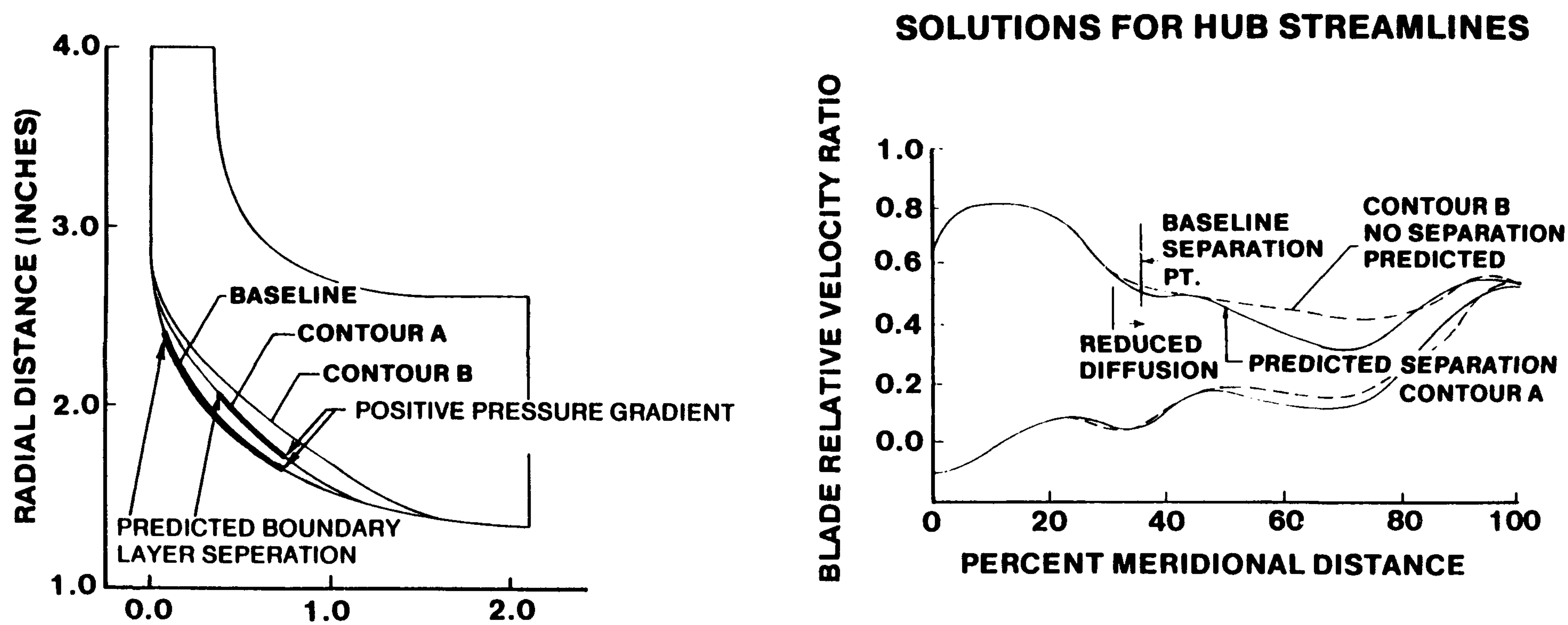


FIGURE 3.1-20 REVISED HUB CONTOURS TO REDUCE DIFFUSION CHARACTERISTICS

TABLE 3.1-8 COMPARISON OF VANE DESIGNS

| | NASA BASELINE | CURRENT DESIGN | TASK I DESIGN |
|---|---|---|---|
| TRAILING EDGE DIAMETER (IN) | 0.043 | 0.020 (CERAMIC) | 0.040 |
| LEADING EDGE DIAMETER (IN) | 0.307 | 0.300 (MINOR MODIFICATION) | 0.300 |
| THROAT DIMENSION (IN) | 0.500 | 0.449 (ROTOR MATCH) | 0.3927 |
| DESIGN FLOW EXIT ANGLE (DEGREES) | 73.9 | 74.7 (ROTOR MATCH) | 74.9 |
| OUTER RADIUS (IN) | 5.501 | 5.501 (UNCHANGED) | 5.629 |
| INNER RADIUS (IN) | 4.225 | 4.279 (DESIGN SOLIDITY) | 4.605 |
| NUMBER OF VANES | 15 | 15 (UNCHANGED) | 18 |
| PASSAGE WIDTH (IN) | 0.3439 | 0.3439 (UNCHANGED) | 0.4375 |
| ROTOR DIAMETER (IN) | 8.021 | 8.021 (UNCHANGED) | 8.710 |

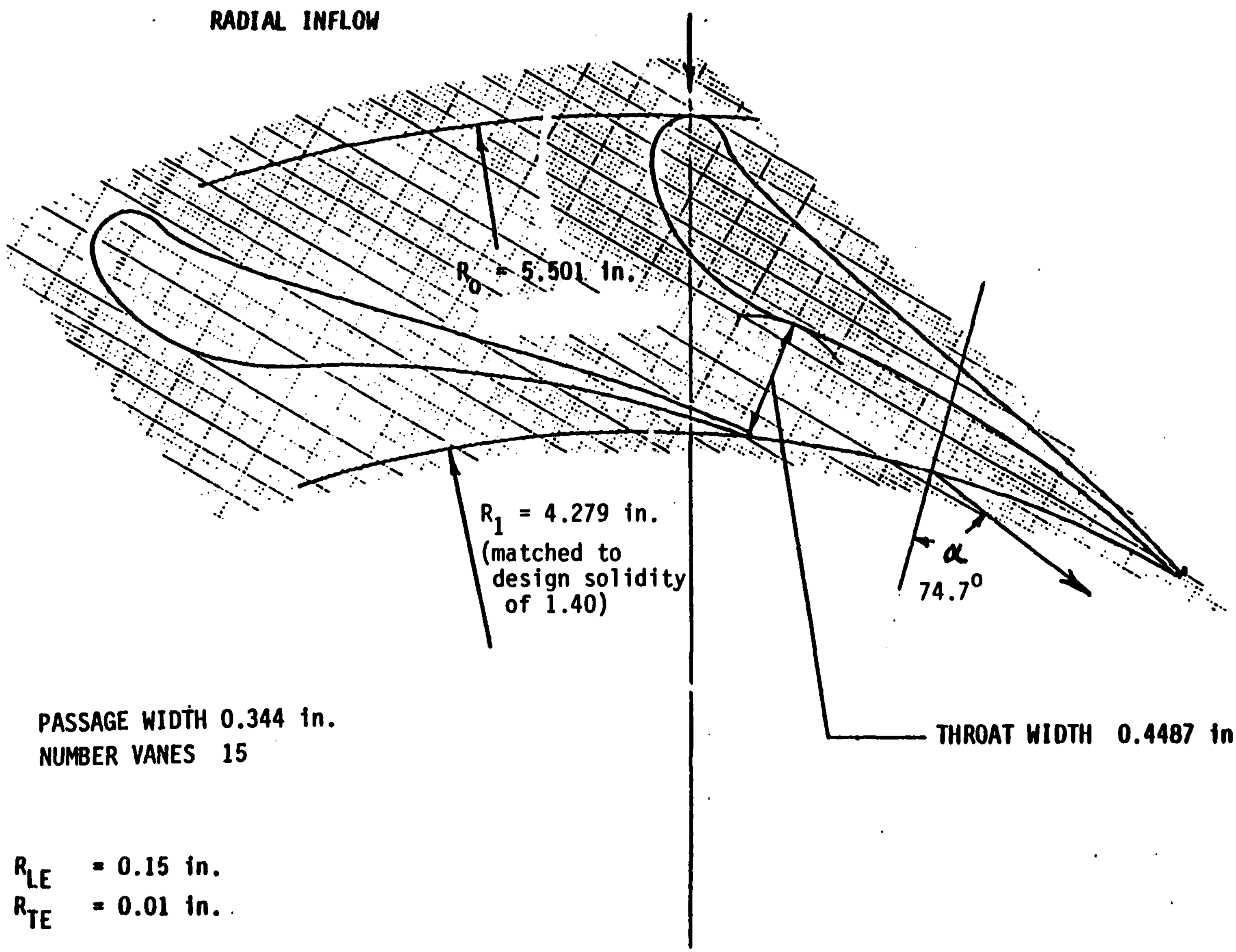


FIGURE 3.1-21 VANE DESIGN

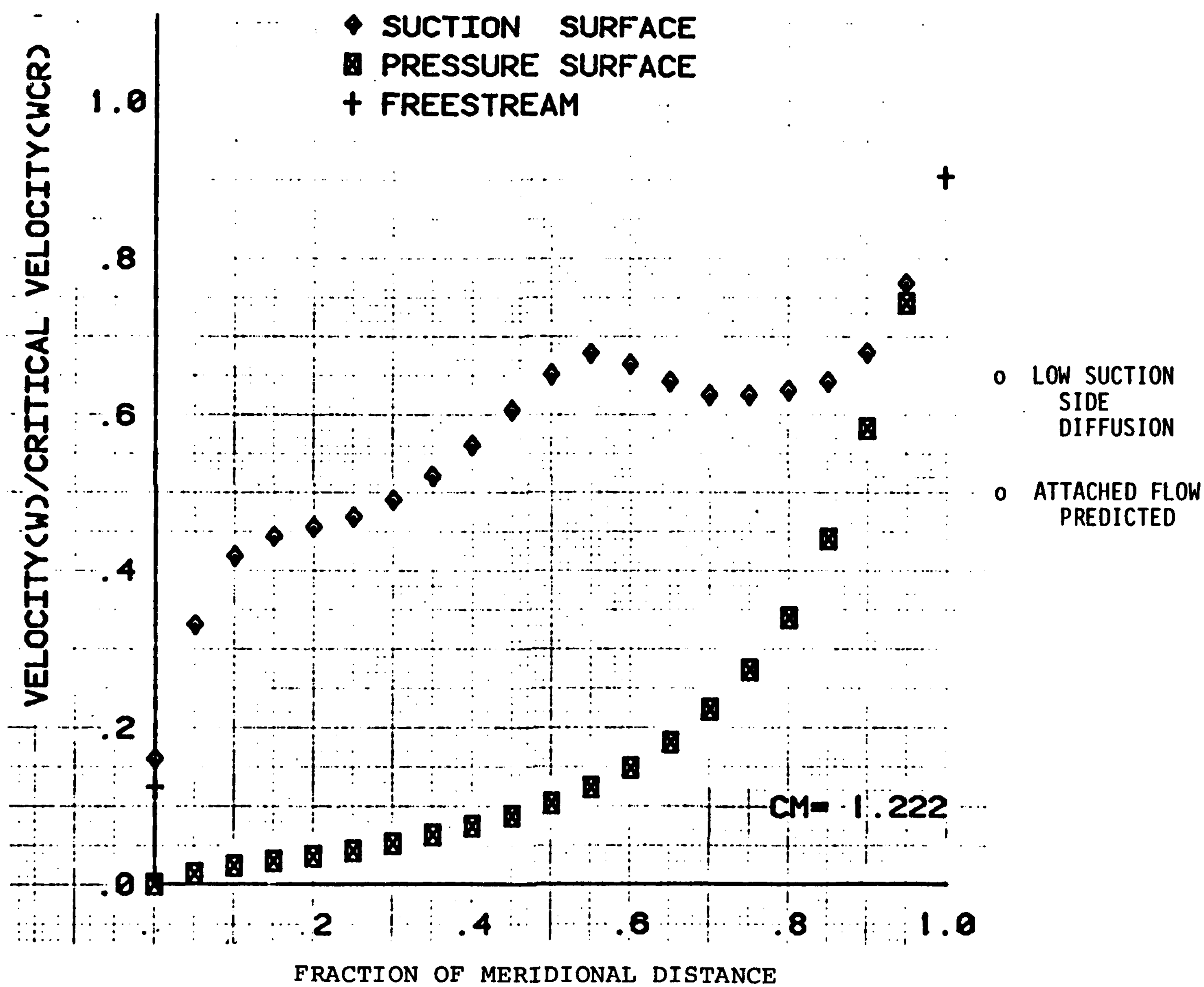


FIGURE 3.1-22 VANE VELOCITY PROFILE

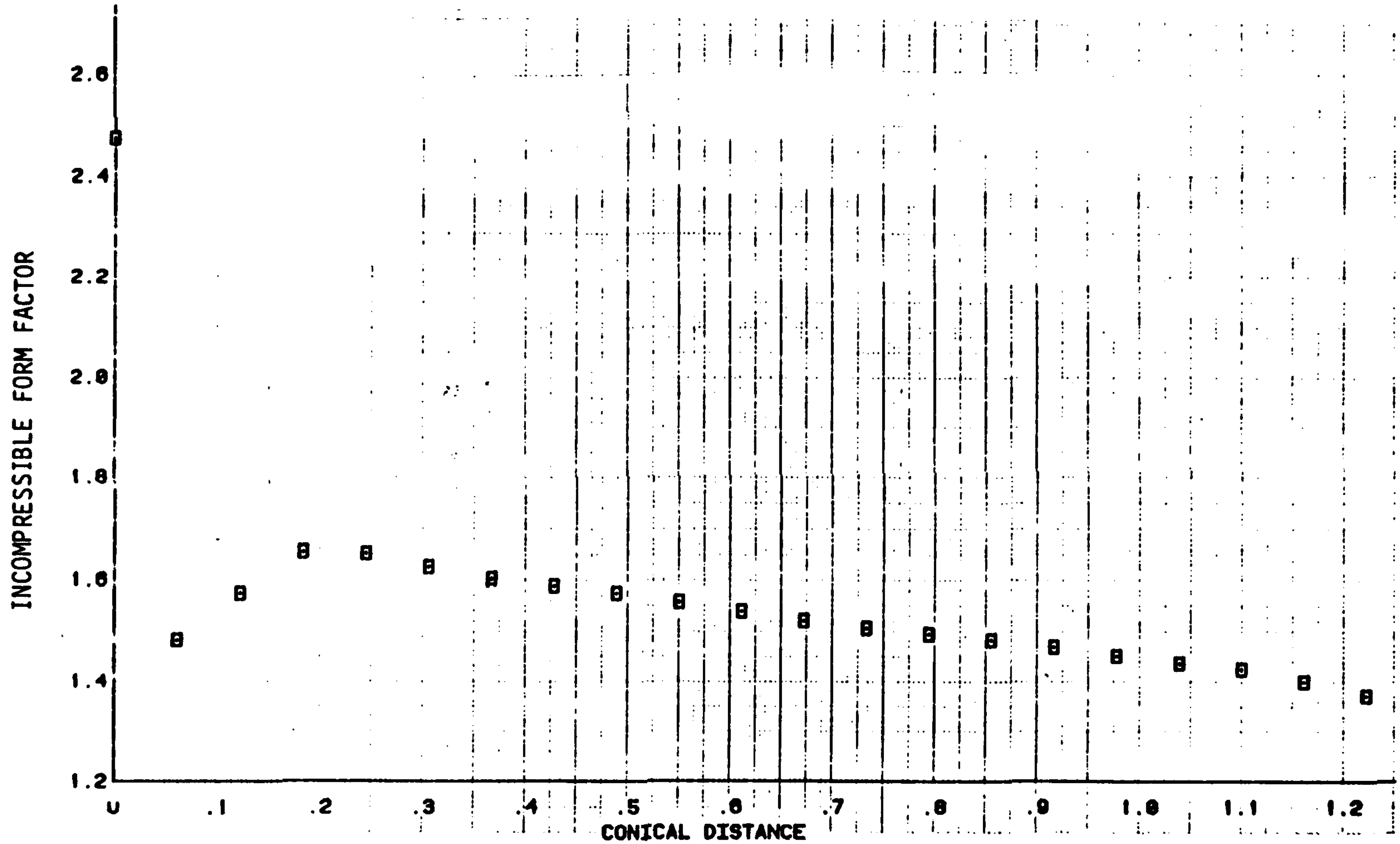


FIGURE 3.1-23 VANE PRESSURE SURFACE INCOMPRESSIBLE FORM FACTOR

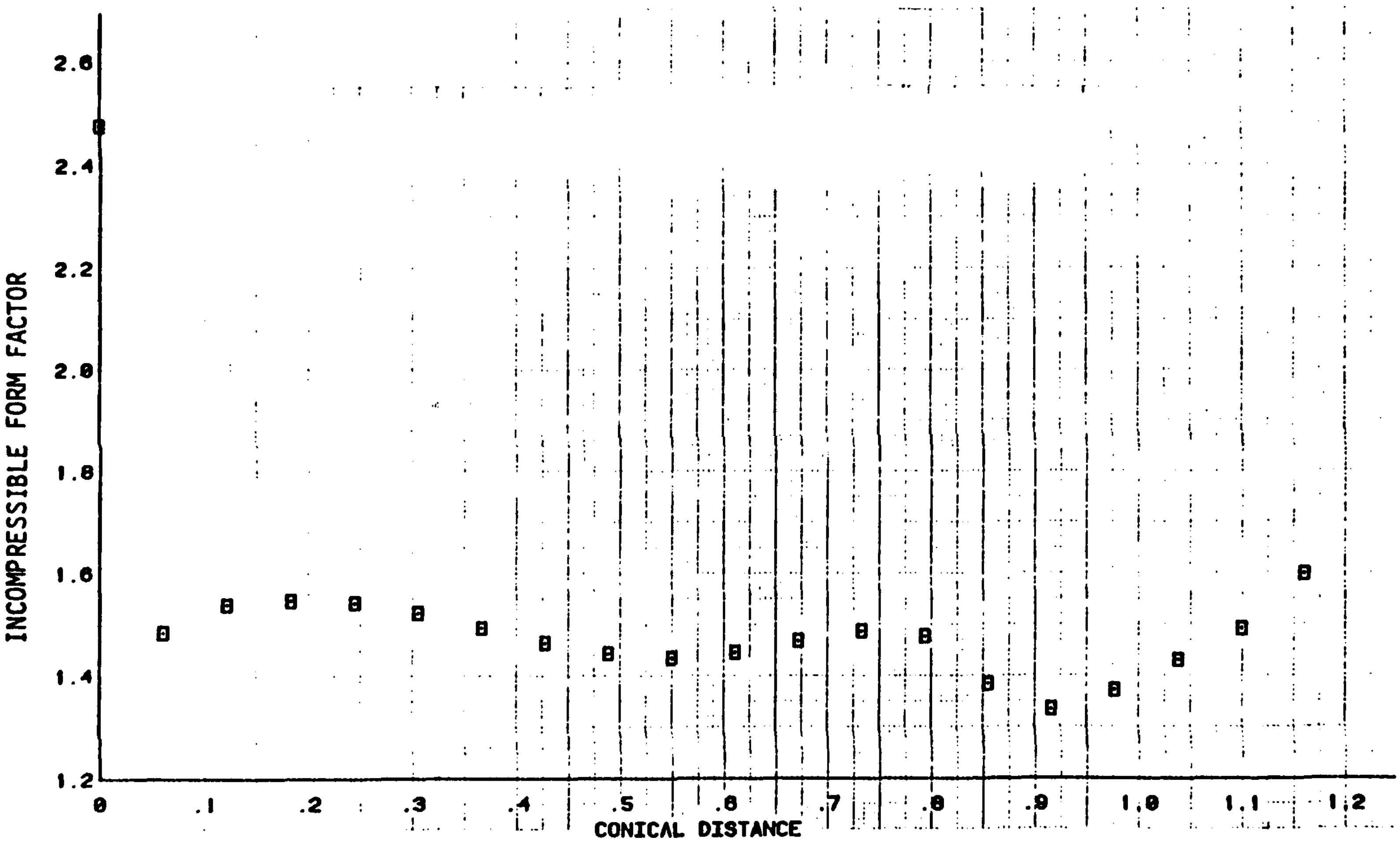


FIGURE 3.1-24 VANE SUCTION SURFACE INCOMPRESSIBLE FORM FACTOR

### 3.2.1 Coolant Passage Design Constraints

Design of the coolant passages within the the blade is constrained by three considerations:

- o blade internal heat transfer
- o coolant flow pressure losses
- o compatibility with fabrication methods.

Fabrication constraints are by far the most restrictive of the three constraints such that the design process, to a high degree, revolves around the limits placed upon coolant passage geometry. Fabrication is accomplished by the lost wax investment casting process which imposes several constraints on the cooling passage design.

Figure 3.2-1 illustrates the successfully fabricated coolant flow passageway of the previous program and compares it to the cooling path ultimately designed for the rotor considered here. A major feature of the previous design was the flow split between the inducer directed coolant flow and the flow directed to the hub section of the blade. The presence of this split resulted in an inherent uncertainty as to the actual distribution of coolant flow within the blade. This uncertainty is due in part to the lack of appropriate means to adequately inspect the internal structure of the final cast shell. Additional uncertainty arises in modeling the complexities of the coolant flowpath pressure loss characteristics in the presence of rotational forces setup within the blade. Uncertainties in the magnitude of coolant flow within the blade inducer region gave rise to difficulties in interpreting heat transfer data received from testing this rotor.

Fabrication of the rotor in this previous effort was, however, highly successful. Features of this design which contributed to it's success were: the position of the flow inlet on the rotor back-face, the pressure side discharge arrangement, and the internal tie between coolant passages at the flow split position. Also important to this program was the capability of securing the core during the fabrication process via protrusions through the shell at the inducer tip and the hub sections. Both openings are later closed by a braze process on the usable rotor casting.

Fabrication constraints which limit the allowable core passage geometries are in general based upon previous casting experience. These are summarized below:

- o minimum core cross sectional area (0.040 square inches)
- o maximum length of unsupported core section (dependent upon thickness of section)
- o minimum core and wall metal thicknesses (0.020inch)
- o minimum pin fin diameter (0.040 inch).

These criteria apply specifically to a nominal 8 inch diameter rotor. Heat transfer considerations in general call for complete coverage of the blade surface with adequate internal convective coefficients obtained via appropriate combinations of flow velocity, passage width, and wall surface roughness treatment.

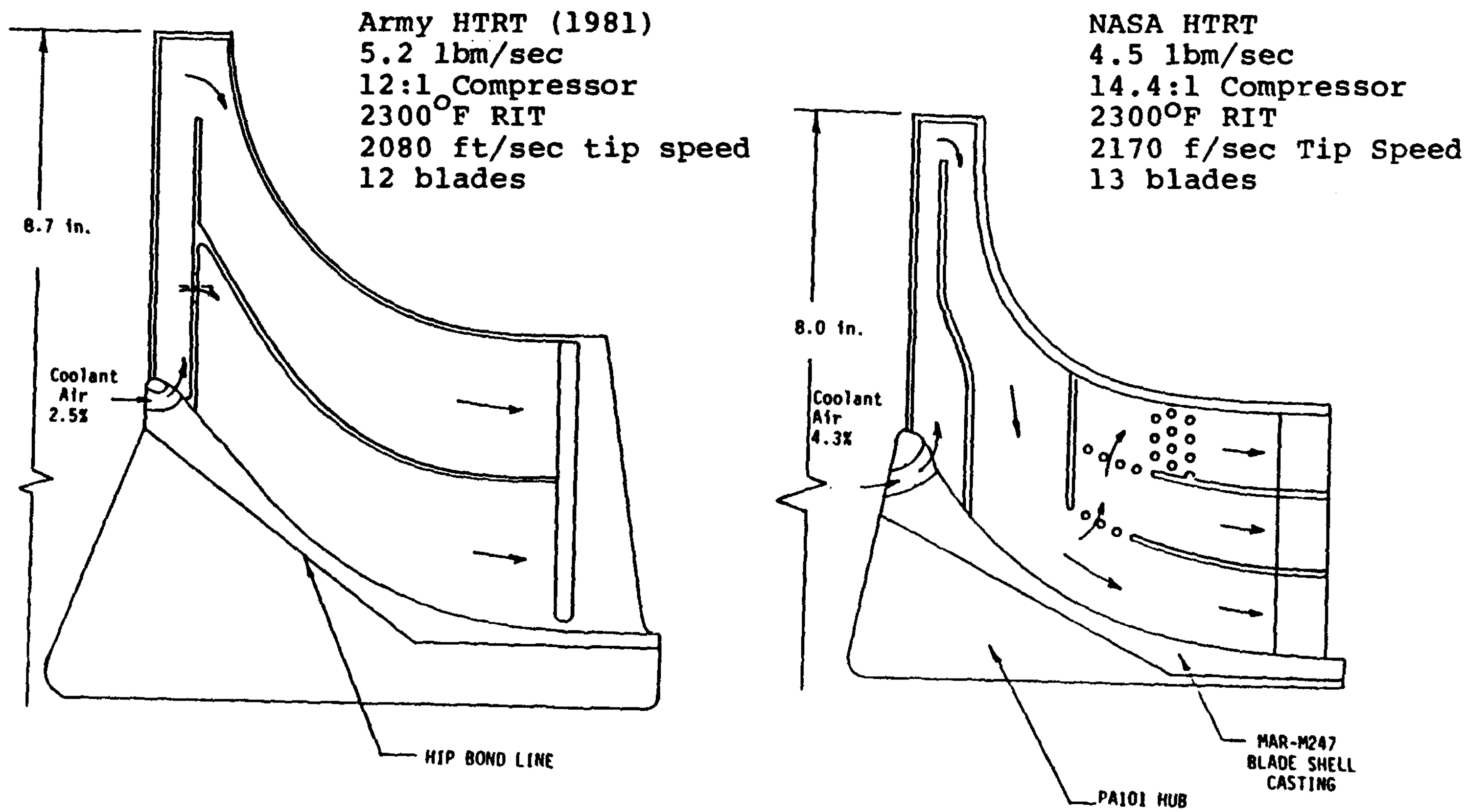


FIGURE 3.2-1 COMPARISON:PREVIOUS COOLANT PATH WITH PRESENT STUDY

Coolant flow pressure loss is limited by available coolant pressures from compressor bleed and the position at which the coolant air is discharged. It is the mutual satisfaction of these considerations which results in a successful design.

### 3.2.2 Selection of Coolant Passageway Configuration

The design process consisted of selecting cooling concepts, ranking of concepts according to compatibility with the established constraints, examining the ability of each to perform the required cooling, selecting the final conceptual scheme, and finally determining the detailed coolant flow path design. Figure 3.2-2 presents concepts initially examined along with perceived benefits and deficiencies. Due to the goal of the program to produce a rotor capable of heat transfer test under well defined conditions, the benefit of producing a design with well defined internal flow characteristics was emphasized.

Figure 3.2-1 presents the resulting concept used for the detailed design effort. Of key importance to this concept was eliminating the branching coolant flow within the important inducer section. It was, however, determined that branching was required within the exducer section in order to achieve an even distribution of coolant air discharge, thus providing cooling to the trailing edge region. Constraints on minimum wall and core thickness preclude the use of trailing edge injection without excessively thickened blade trailing edges. Thick trailing edges result in excessive turbine efficiency penalties due to high flow blockage.

### 3.2.3 Detailed Coolant Flow Path Design

Design of the detailed area distribution and branching coolant flow circuitry was accomplished using a detailed internal coolant flow model as indicated in Figure 3.2-3. The method utilizes 1 dimensional flow modeling within the blade passages via discreet elements which include frictional and bend losses, branching losses, and "pumping effects" (changes in pressure due to fluid movement within the rotating passage). Loss coefficients for each of the flow elements were determined from correlations available in the open literature. Wall and coolant temperature changes due to both heat transfer and rotational effects and coolant flow preswirling (tangential onboard injection) were also similarly modeled.

The flow solution summarized in Figure 3.2-4 demonstrated that pumping effects are extremely influential within the flow path. These forces cause significant compressions and expansions of the coolant flow with change in radius. Thus in order to achieve a uniform distribution of coolant air at the discharge, the circuitry employing pin fins and segmented exit passages was devised. The placement of pin fins within the coolant passage is designed to provide a well defined flow resistance in the radially outward direction to counter the pumping effect. The pumping force tends to drive the flow radially outward to the outer most coolant slot. The series nature of the resistance is designed to provide a cumulative resistance with increasing radius to counter the cumulative effects of rotation.

**ADVANTAGES:**

| Concept A | Concept B | Concept C |
|---|---|---|
| • POSITIVE INDUCER FLOW | • POSITIVE INDUCER FLOW<br>• GOOD FLOW DISTRIBUTION | • POSITIVE INDUCER FLOW<br>• ADJ. FLOW DISTRIBUTION |

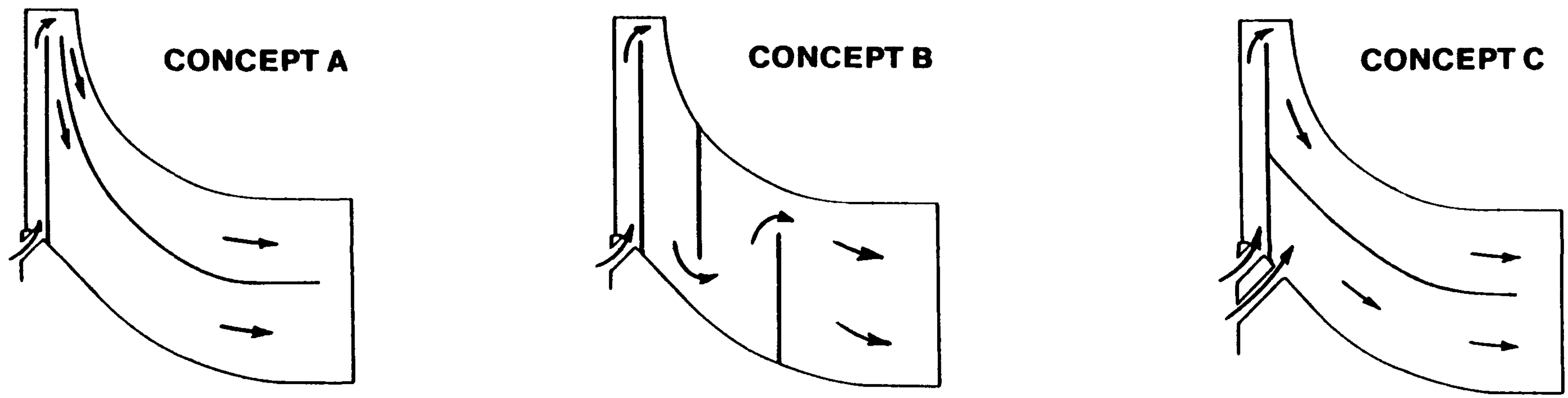


**DISADVANTAGES:**

| Concept A | Concept B | Concept C |
|---|---|---|
| • FLOW SPLIT NOT PREDICTABLE<br>• SLENDER CORE | • POOR CASTABILITY | • POOR CASTABILITY<br>• HUB COMPLEXITY |

FIGURE 3.2-2 COOLANT FLOWPATH CONCEPTS

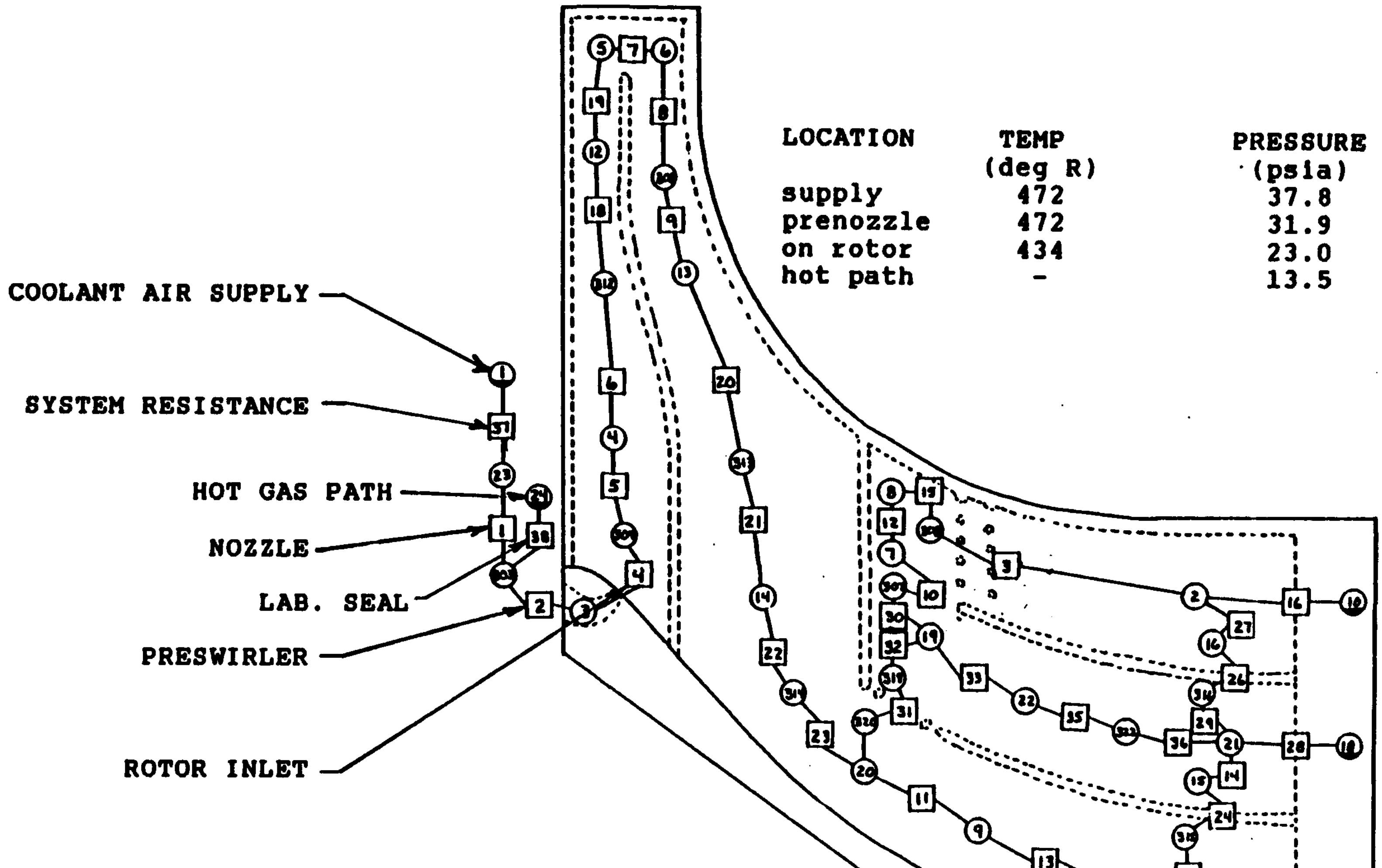


| LOCATION | TEMP (deg R) | PRESSURE (psia) |
|---|---|---|
| supply | 472 | 37.8 |
| prenozzle | 472 | 31.9 |
| on rotor | 434 | 23.0 |
| hot path | - | 13.5 |

SEAL FLOW 0.79%

BLADE INTERNAL FLOW 4.20%
(% of rotor inlet flow)

FIGURE 3.2-3 ROTOR INTERNAL COOLANT FLOWPATH MODEL

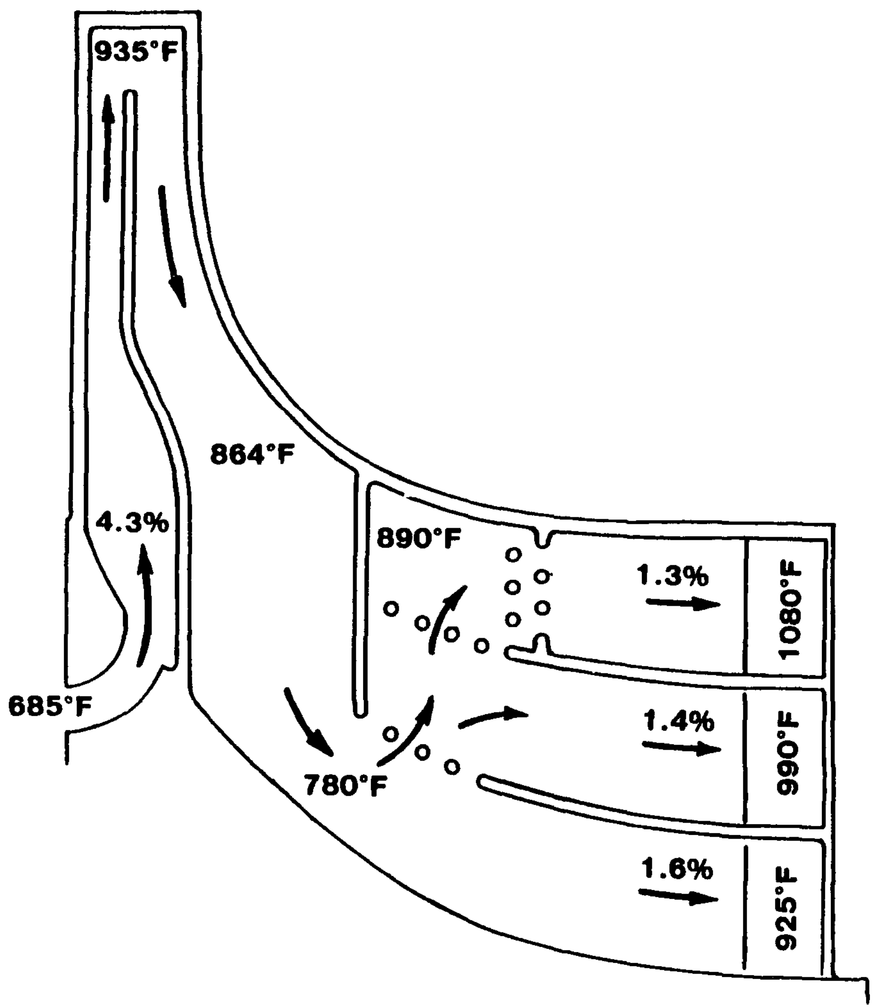


**INTERNAL FLOW MODEL INCLUDED EFFECTS OF**

- HEAT TRANSFER
- COMPRESSIBILITY
- FRICTION, TURNING, & BRANCHING
- ROTATION

**ADVANTAGES:**

- POSITIVE INDUCER FLOW
- GOOD FLOW DISTRIBUTION
- GOOD CASTABILITY

FIGURE 3.2-4 FINAL COOLANT FLOWPATH DESIGN

The rotational effects are sufficient to result in predicted temperature decreases in the bulk coolant flow for radially inward legs even though the fluid continues to pickup heat. Final design of the coolant flow path and determination of required coolant air flow rates was determined by an iterative process involving heat transfer analyses described in section 3.3 below.

An additional benefit is derived by selecting a design in which the entire coolant flow is routed through the rotor tip region. The design results in coolant passage tip region flow velocities giving high convective heat transfer coefficients. This eliminates the need for the geometric complexity of heat transfer enhancement through the use of discreet wall roughness.

Results of the design work resulted in the baffle and passage thickness pattern of Figure 3.2-5. Representation of slices of the blade showing final coolant passage width distributions are shown in Figure 3.2-6. The trailing edge discharge configuration selected closely follows cooled vane design technology and minimizes blade trailing edge thickness. The use of choked flow at the discharge point is, in this case, not feasible due to the minimum core size constraint. Blade angle distributions shown are the result of the comprehensive rotor aerodynamic design described above.

In addition, a preswirler was designed as a modification to the NASA test rig. The function of the preswirler is to efficiently bring the coolant air up to wheel speed and hence provide coolant air to the blade at the lowest possible temperatures, a benefit to either an engine or a rig design. The basic rig without preswirler is shown in Figure 3.2-7. The details of the preswirler design are presented in Figure 3.2-8 and 9.

## 3.3 Heat Transfer and Stress Analysis Results

As part of the detailed design process, 2-D and quasi 3-D finite element heat transfer and stress analyses were made of the engine rotor. Coolant flow values and coolant passage geometry were selected to give acceptable temperatures and material strengths within the dual property rotor in meeting rotor life requirements. Analysis techniques parallel those of the Task I effort previously reported.

### 3.3.1 Heat Transfer Results

A comprehensive analysis of the rotor design at 2300 $^{o}$F (program requirements) was completed. Figure 3.3-1 presents metal temperatures at design conditions for the 2-D analysis. The results indicated that cooling was adequate in terms of peak blade (50 degrees below Task 1 values) and hub temperature (below 1200°F) requirements. Figure 3.3-2 gives similar results for the analysis of the transient analysis used for LCF determination. In addition heat transfer calculations evaluating design feasibility at 2500°F were also completed. Results of the 2-D heat transfer analysis are shown in Figure 3.3-3. Rotor internal blade cooling was set at 4.3% of rotor inlet flow. In addition, a 1% hub film cooling and a 0.5% bore cooling was included.

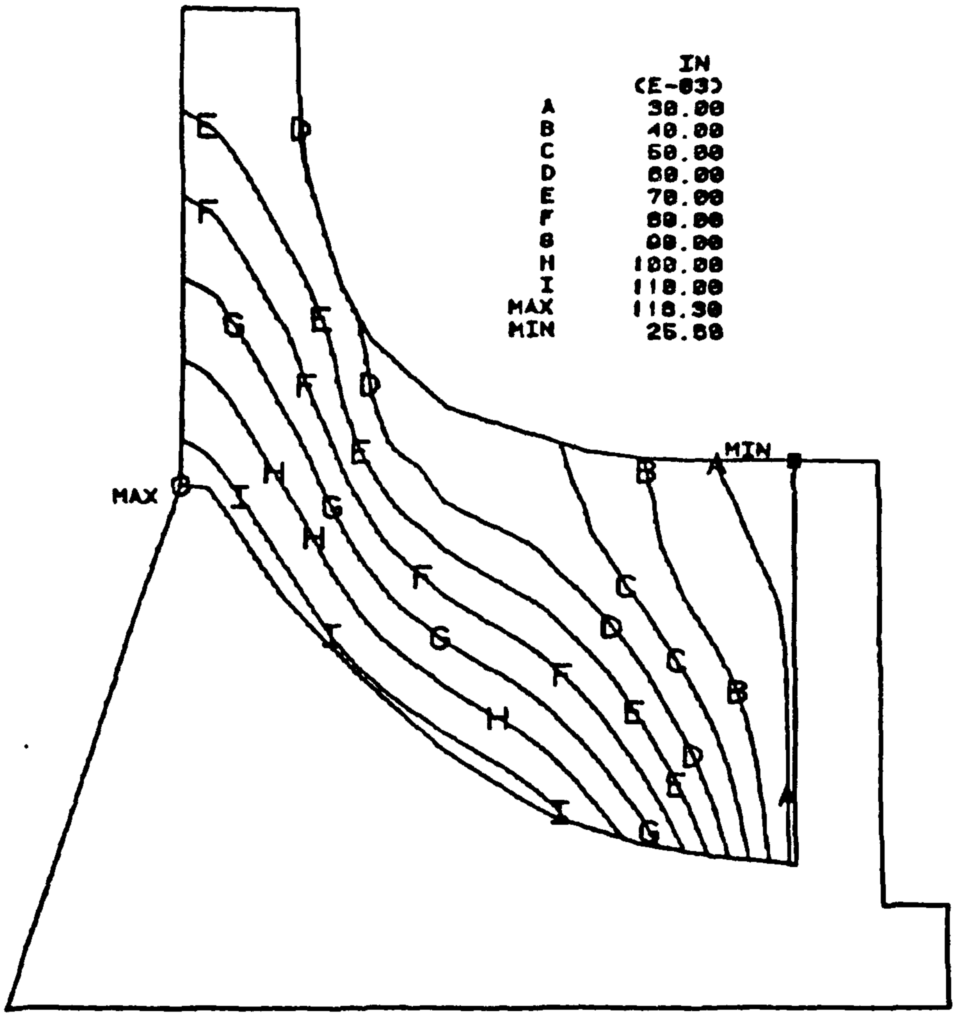


FIGURE 3.2-5 NASA HTRT COOLANT FLOWPATH
NORMAL THICKNESS DISTRIBUTION

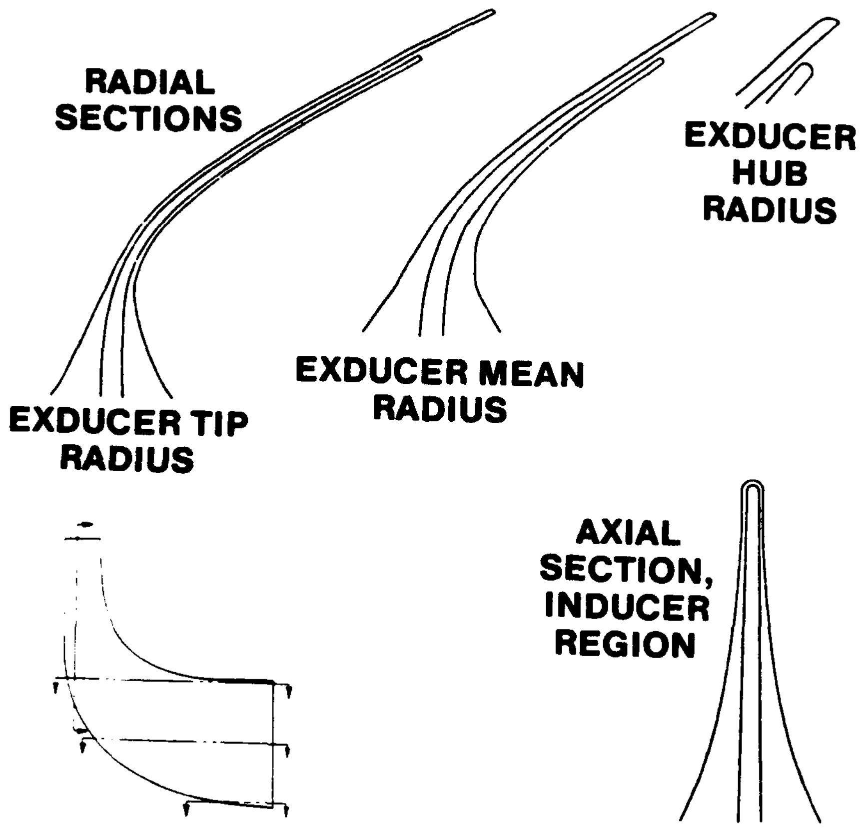


FIGURE 3.2-6 COOLANT FLOWPATH WITHIN BLADE

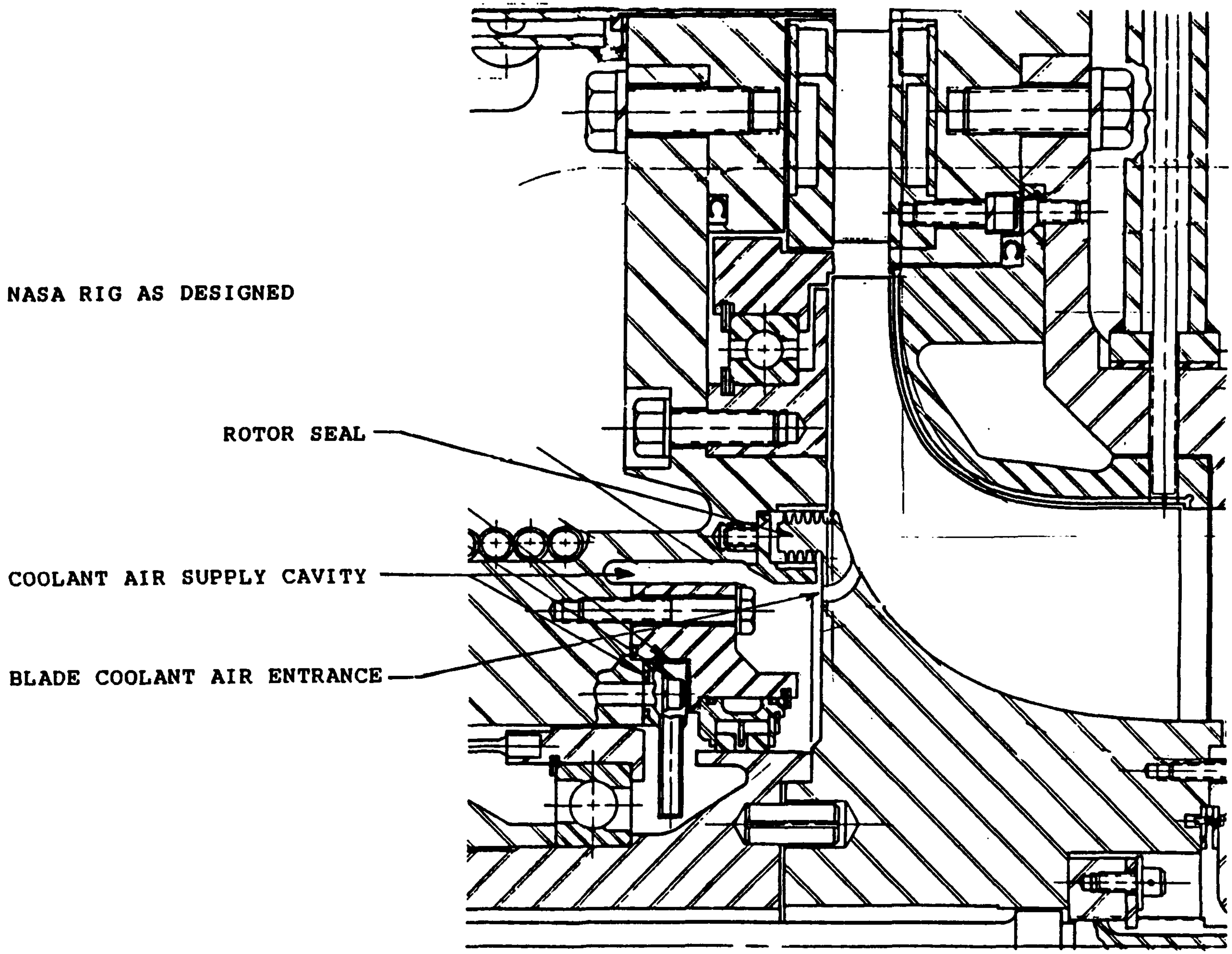


FIGURE 3.2-7 NASA COOLED HTRT RIG

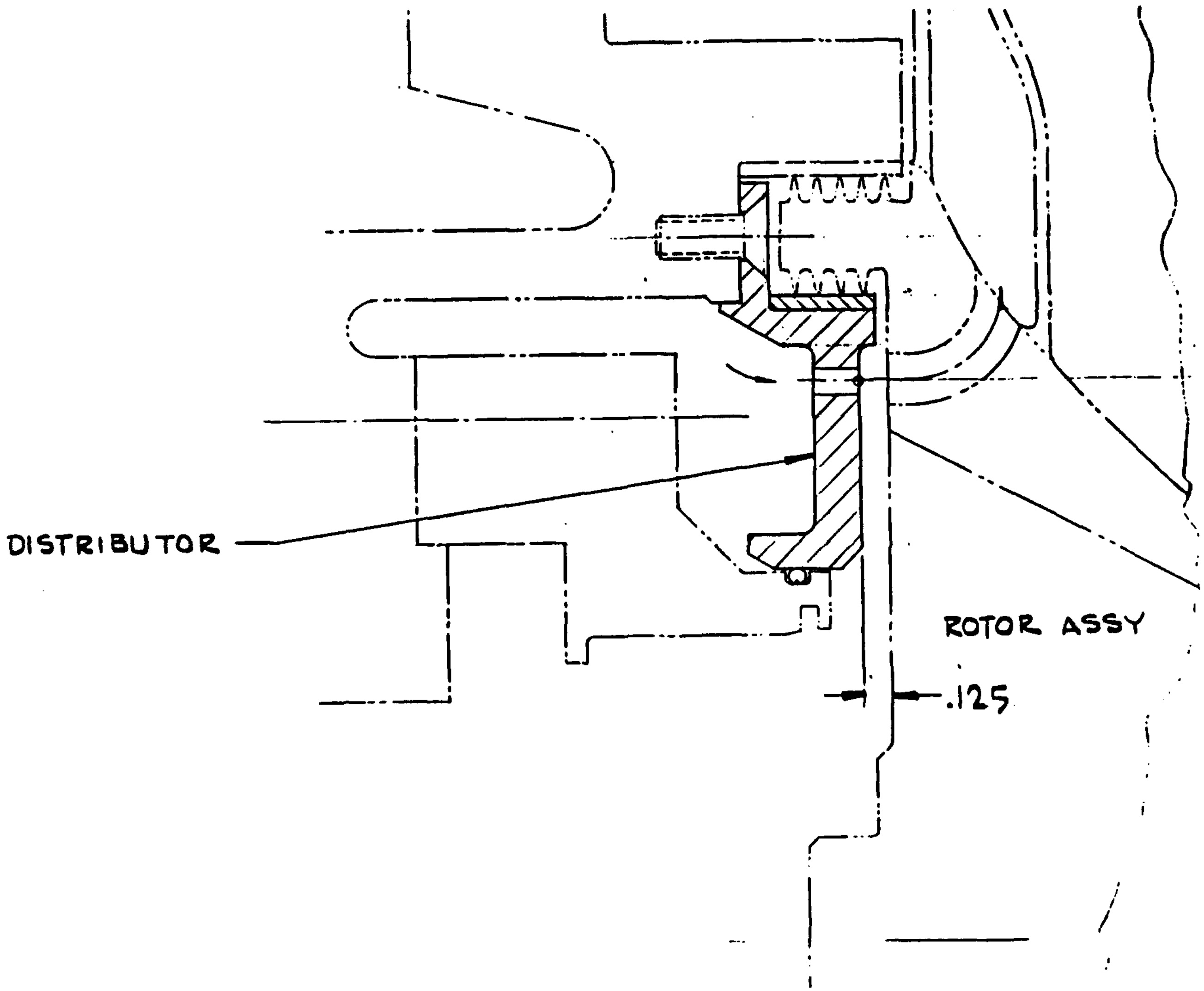


FIGURE 3.2-8 PRESWIRLER DESIGN MODIFICATION TO NASA RIG

PRESWIRLER DETAILS

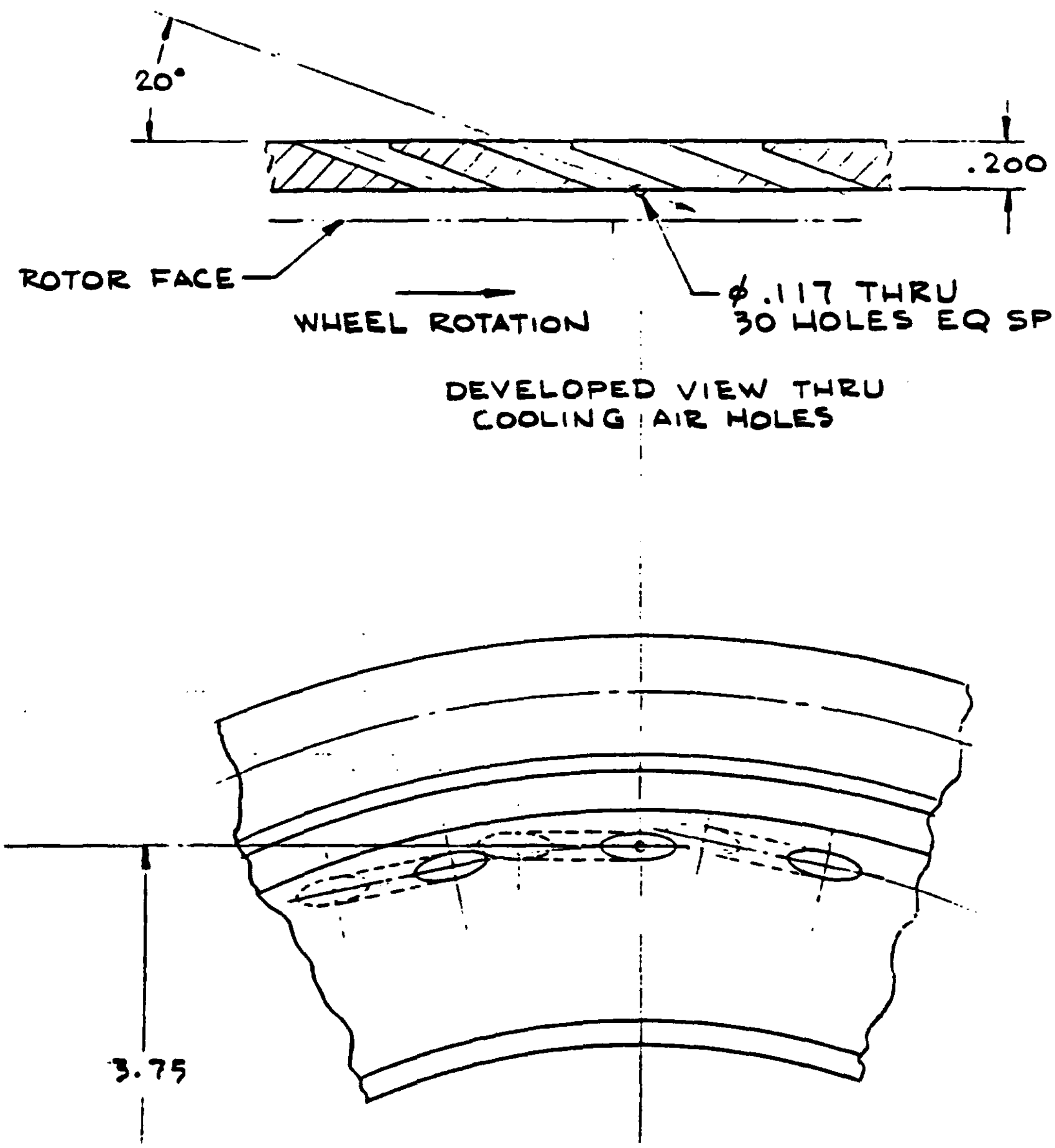


FIGURE 3.2-9 PRESWIRLER DETAILS

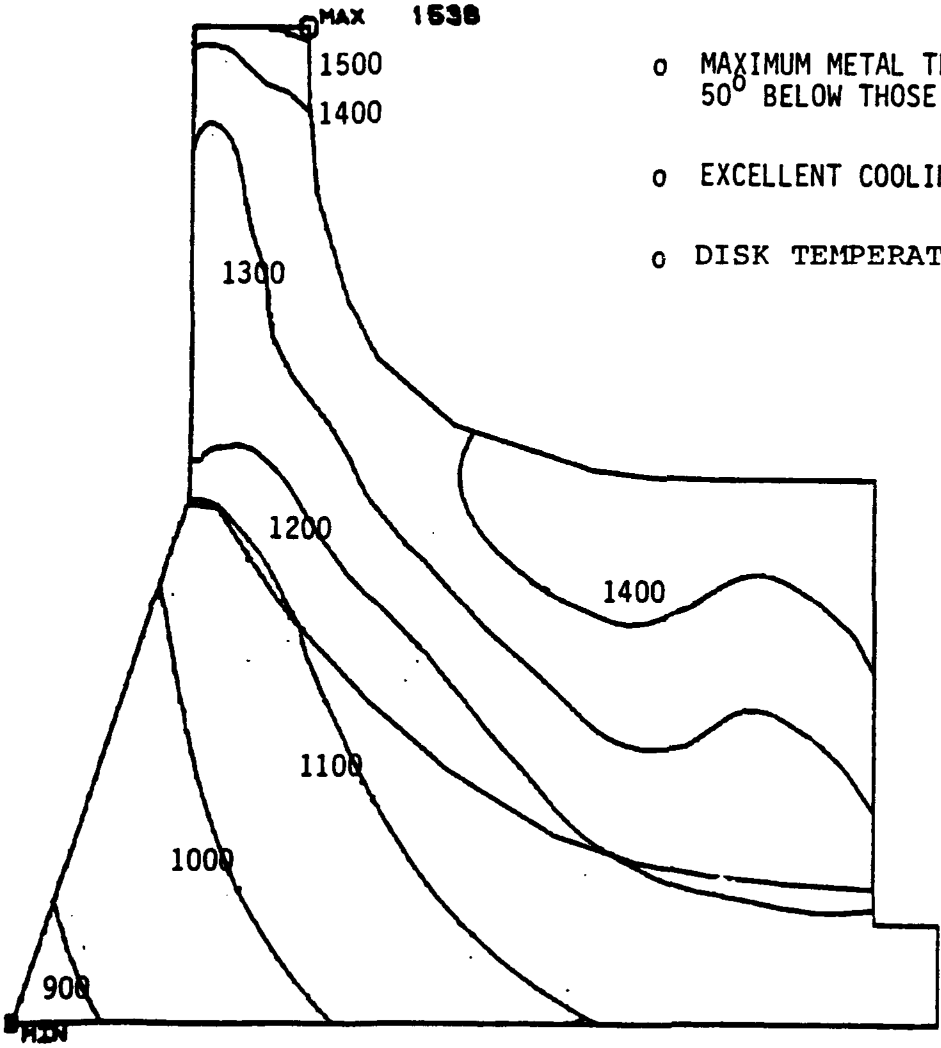


- MAXIMUM METAL TEMPERATURES 50° BELOW THOSE FOR TASK I DESIGN
- EXCELLENT COOLING OF INDUCER REGION
- DISK TEMPERATURE ≤ 1200°F

FIGURE 3.3-1 STEADY STATE BLADE METAL TEMPERATURES AT DESIGN CONDITIONS, RIT = 2300°F

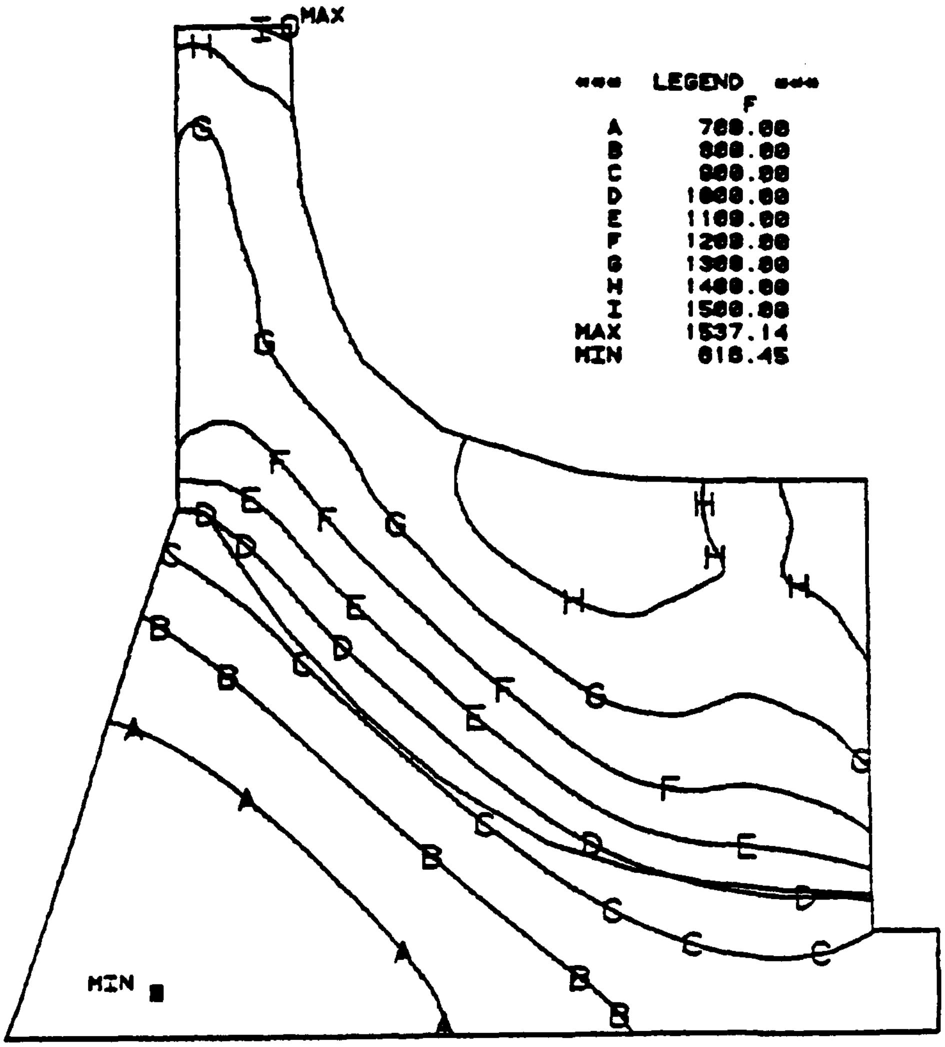


FIGURE 3.3-2 IDLE TO IRP TRANSIENT TEMPERATURE PROFILE
AT TIME = 20 sec.

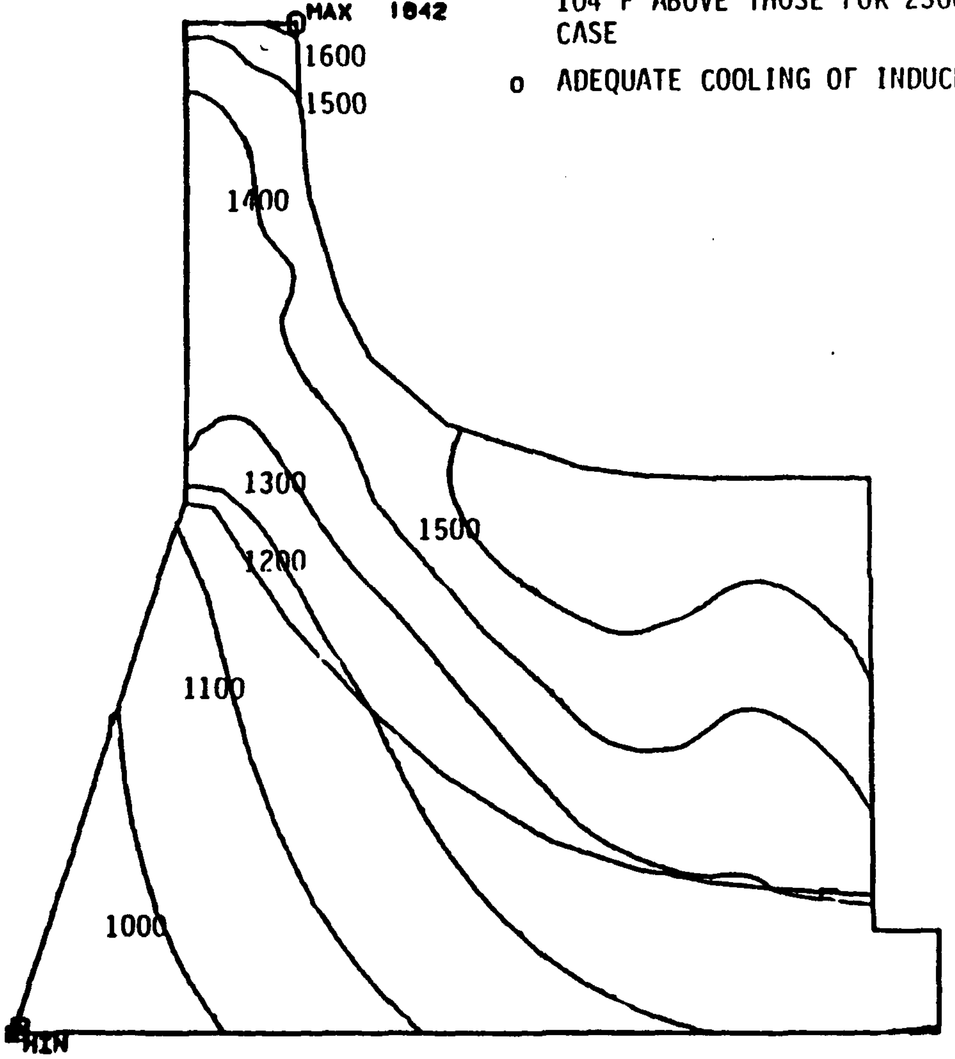


o MAXIMUM METAL TEMPERATURES 104°F ABOVE THOSE FOR 2300°F CASE

o ADEQUATE COOLING OF INDUCER REGION

FIGURE 3.3-3 STEADY STATE BLADE METAL TEMPERATURES AT 2500°F RIT

Significant features of these heat transfer results are the uniformity of blade temperatures, with a peak value of 1642 $^{o}F$, adequate for the Mar M247 material in the tip region. Peak temperatures within the PA101 material are in the 1260 $^{o}F$ range ensuring retainment of suitable material properties within the hub. Thermal gradients within the hub are relatively low giving rise to low steady state thermal stresses in the hub.

### 3.3.2 Stress Analysis Results

Determination of low cycle fatigue (LCF) life is of prime concern for a radial turbine rotor particularly with a center bore hole. LCF life assessment was made by modeling transient heat transfer performance of the rotor during the period of acceleration from idle to design point conditions. Results for the time interval giving rise to maximum thermal gradients within the rotor serve as input to the stress analysis. Stress modeling based upon results for the 2500 F case are shown in Figure 3.3-4. As expected, maximum stresses existed at the hub bore. A summary of the results of the complete stress analysis is shown in Table 3.3-1. The results show that the rotor exceeds all life requirements based on anticipated 10 year advances in metal technology.

## 3.4 Test Rig Rotor Scaling

Analysis of heat transfer test results from the previous Army sponsored effort demonstrated the need for a test rotor capable of measuring the hot gas heat transfer conditions imposed on a radial turbine rotor. A key component to this work is the comprehensive testing of the final rotor design. This testing is designed to demonstrate turbine aerodynamic performance and coolant flow path performance. At the same time it will provide fundamental data on heat transfer requirements of the radial turbine blading.

Warm turbine testing will be accomplished utilizing a 1.4 X scaled up rotor operated with turbine inlet temperatures near 600 $^{o}F$. Scaling on key turbine parameters; isentropic spouting velocity ratio and Reynolds number, results in a test conditions as shown in Table 3.4-1 for the 14.4 inch diameter rotor.

A limited analysis was made of test conditions for which the radial turbine may be operated in a warm air facilities to simulate engine operating conditions. Figures 3.4-1 through 4 present convection coefficients and adiabatic wall temperatures for the test conditions. Calculated metal temperatures are shown in Figure 3.4-5. Coolant air temperatures are shown in Figure 3.4-6.

TABLE 3.3-1 SUMMARY OF ROTOR LIFE CRITERIA AT TWO ROTOR INLET TEMPERATURES

ROTOR LIFE CRITERIA ARE SATISFIED AT 2500°F RIT

SUMMARY OF STRESS ANALYSIS RESULTS

| CRITERIA ( $3\sigma$ ) | REQUIRED | COMPUTED 2300°F | COMPUTED 2500°F |
|---|---|---|---|
| .2 CREEP | 1,000 HRS | 10,870 HRS | >1,900 HRS |
| BURST SPEED | 71,300 RPM (130%) | 79,300 HRS | 79,300 HRS |
| LOW CYCLE FATIGUE | 6,000 CYCLES | 8,398 CYCLES | 6,367 CYCLES |
| | | (3,880 CYCLES W/O 10% MATERIALS IMPROVEMENT) | (3,248 CYCLES W/O 10% MATERIALS IMPROVEMENT) |

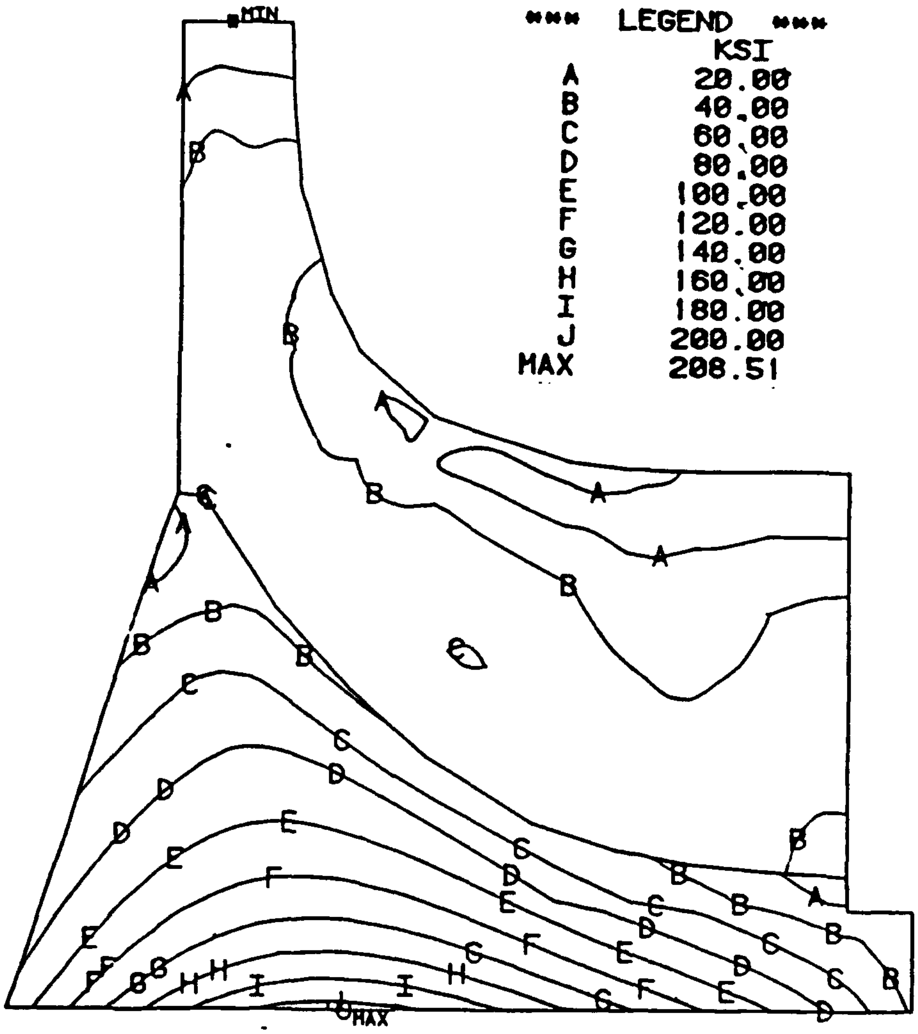


FIGURE 3.3-4 IDLE TO IRP TRANSIENT EQUIVALENT STRESS FOR 2500$^{o}$F RIT

TABLE 3.4-1 TEST RIG CONDITIONS MODELING ENGINE ROTOR PERFORMANCE

| PARAMETERS | ENGINE | RIG |
|---|---|---|
| ROTOR INLET TOTAL TEMPERATURE $^{o}F$ | | 600 |
| ROTOR EXIT TOTAL TEMPERATURE $^{o}F$ | 1674 | 306 |
| INLET TOTAL PRESSURE - psia | 200 | 37.8 |
| ROTOR EXIT TOTAL PRESSURE - psia | 54.6 | 9.5 |
| EQUIVALENT FLOW - lbm/sec | 0.799 | 2.567 |
| ACTUAL FLOW - lbm/sec | 4.559 | 4.593 |
| EQUIVALENT SPEED - RPM | 27,262 | 15,146 |
| ACTUAL SPEED - RPM | 61,900 | 21,574 |
| EXPANSION RATIO, T-T | 3.66 | 3.97 |
| $U_T/\sqrt{2gJ\Delta h_{IS}}$ | 0.661 | 0.661 |
| POWER - HP | 1191 | 471 |
| TORQUE - ft-lbf | 102 | 116 |
| REYNOLDS NUMBER | $3.81 \times 10^5$ | $2.81 \times 10^5$ |
| SPECIFIC SPEED | 62.2 | 62.9 |
| ROTOR DIAMETER - in. | 8.021 | 14.4 |
| ACTUAL ROTOR COOLANT FLOW-lbm/sec | 0.196 (4.3%) | 0.193 |
| ROTOR COOLANT SUPPLY TEMP - $^{o}F$ | 769 | 12 |
| $\Delta H/\theta_c$ - Btu/lbm | 34.9 | |

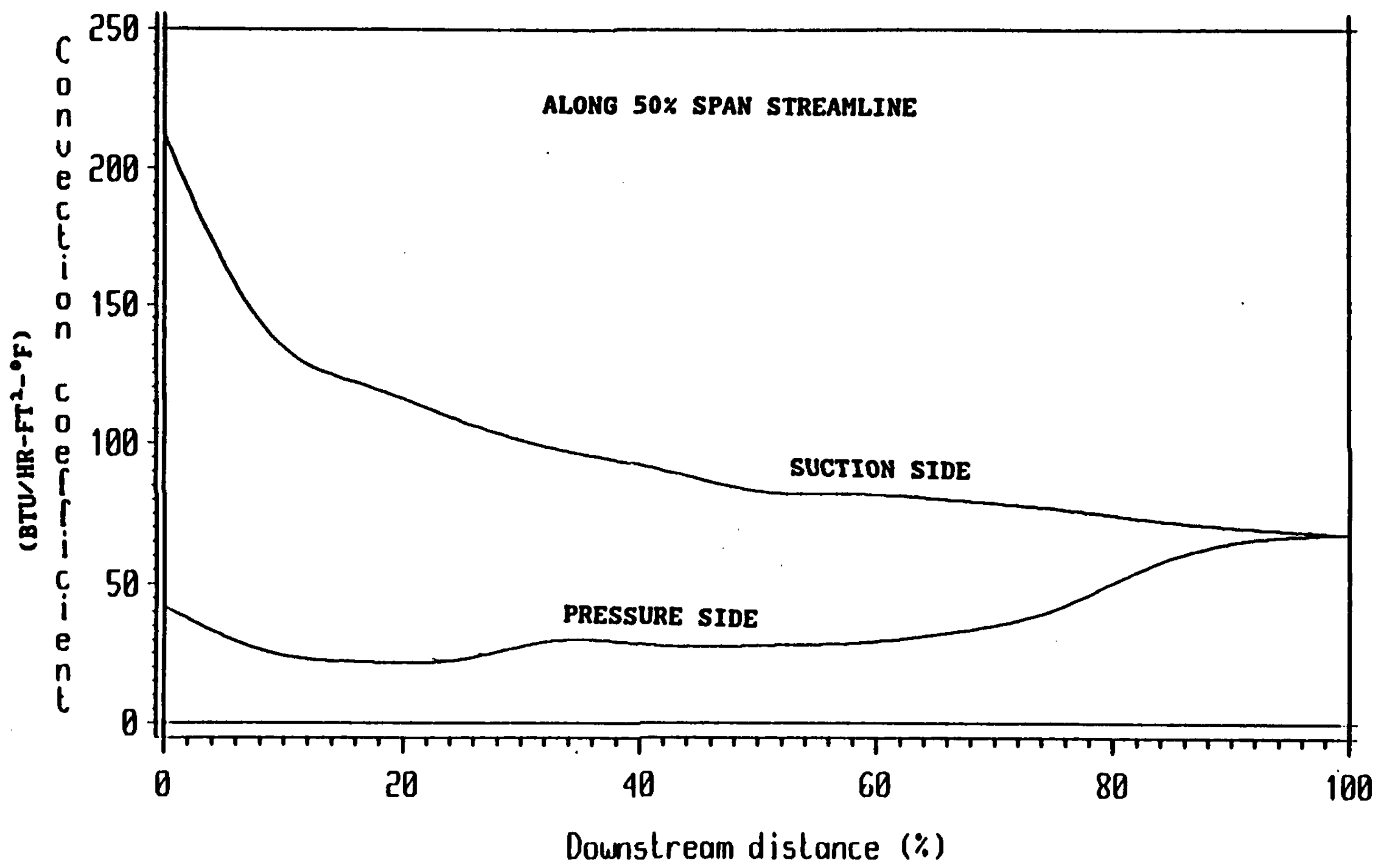


FIGURE 3.4-1 HOT SIDE GAS PATH CONVECTION COEFFICIENTS, RIG TEST CONDITIONS

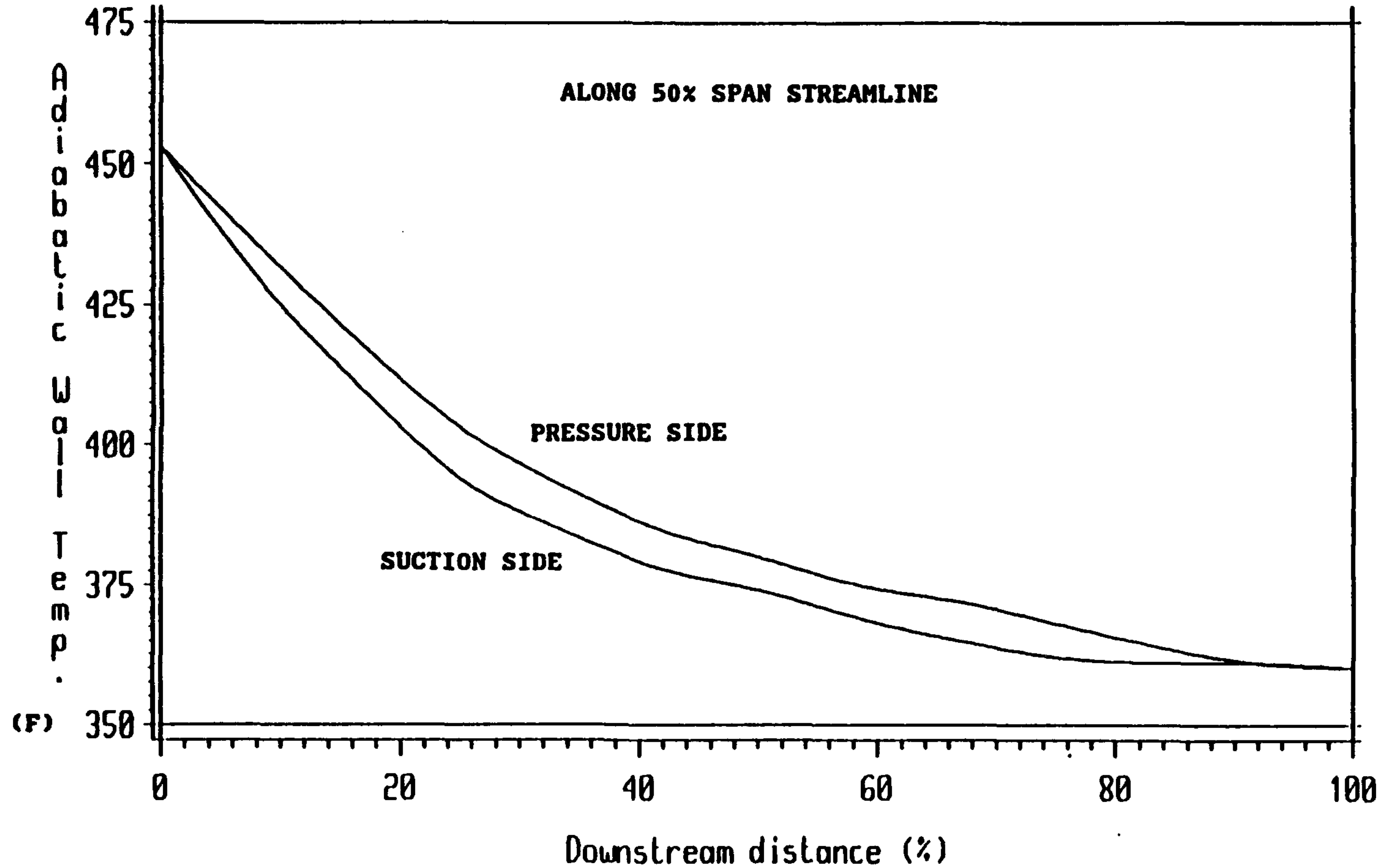


FIGURE 3.4-2 GAS PATH ADIABATIC WALL TEMPERATURES, RIG TEST CONDITIONS

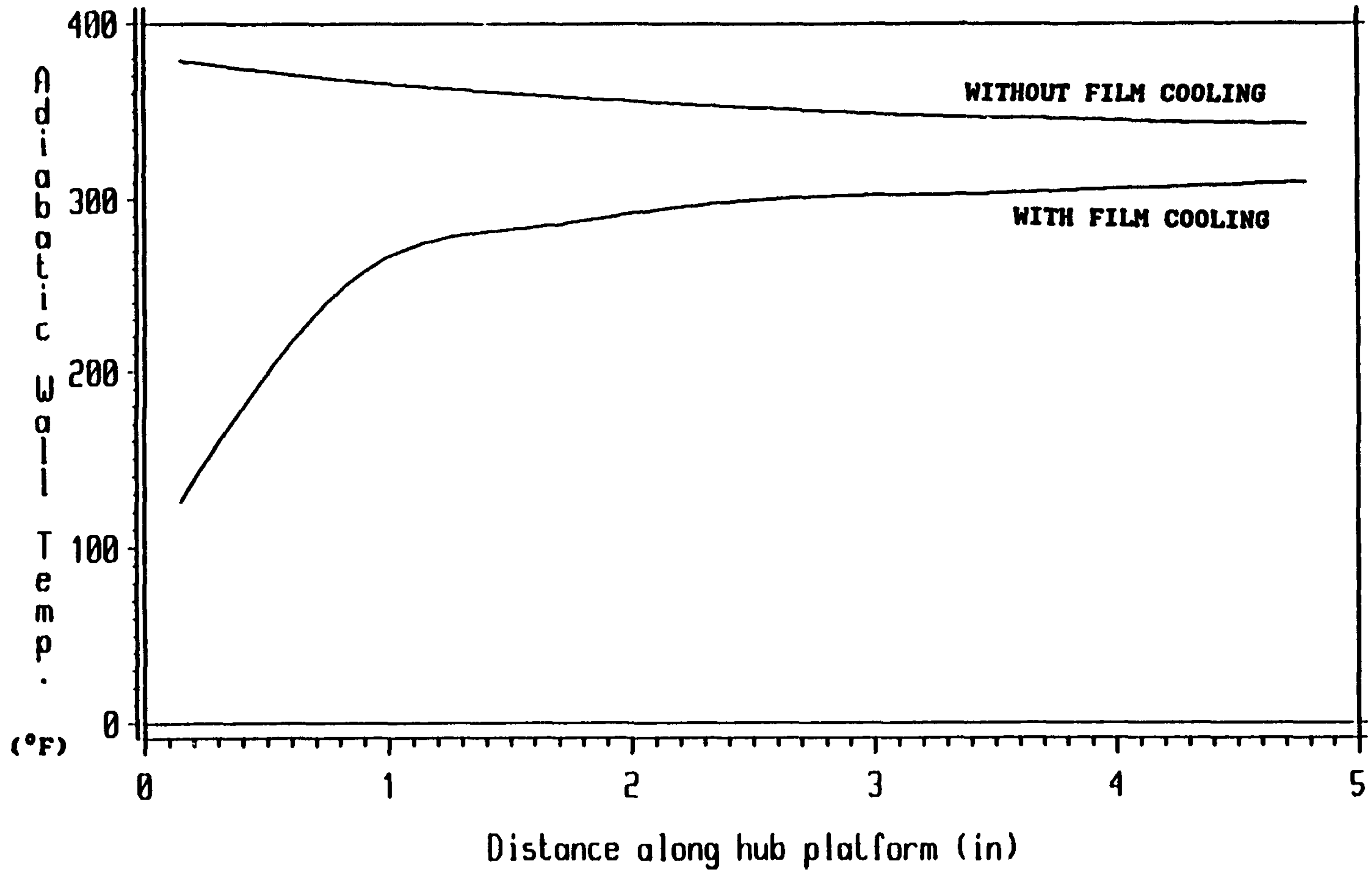


FIGURE 3.4-3 HUB PLATFORM ADIABATIC WALL TEMPERATURES, RIG TEST CONDITIONS

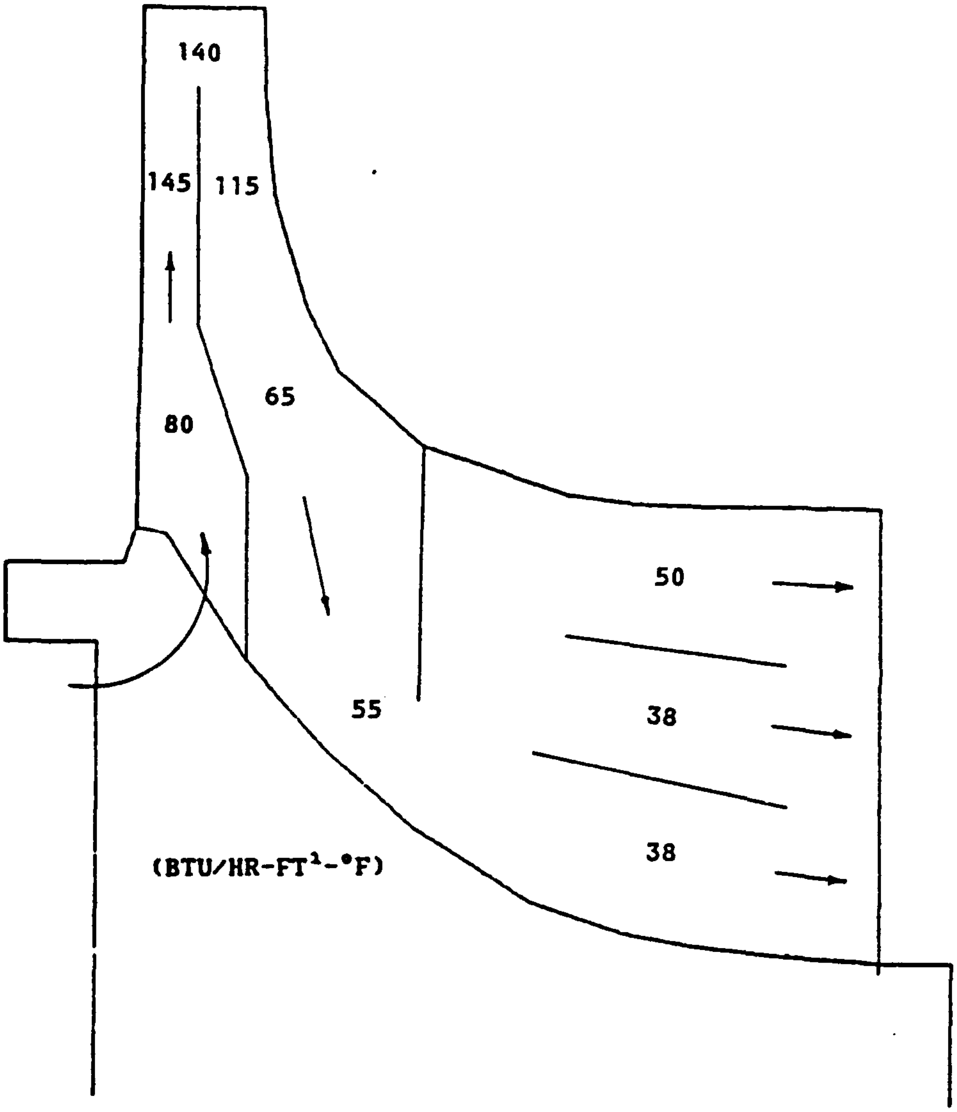


FIGURE 3.4-4 INTERNAL COOLING CONVECTION COEFFICIENTS, RIG TEST CONDITIONS

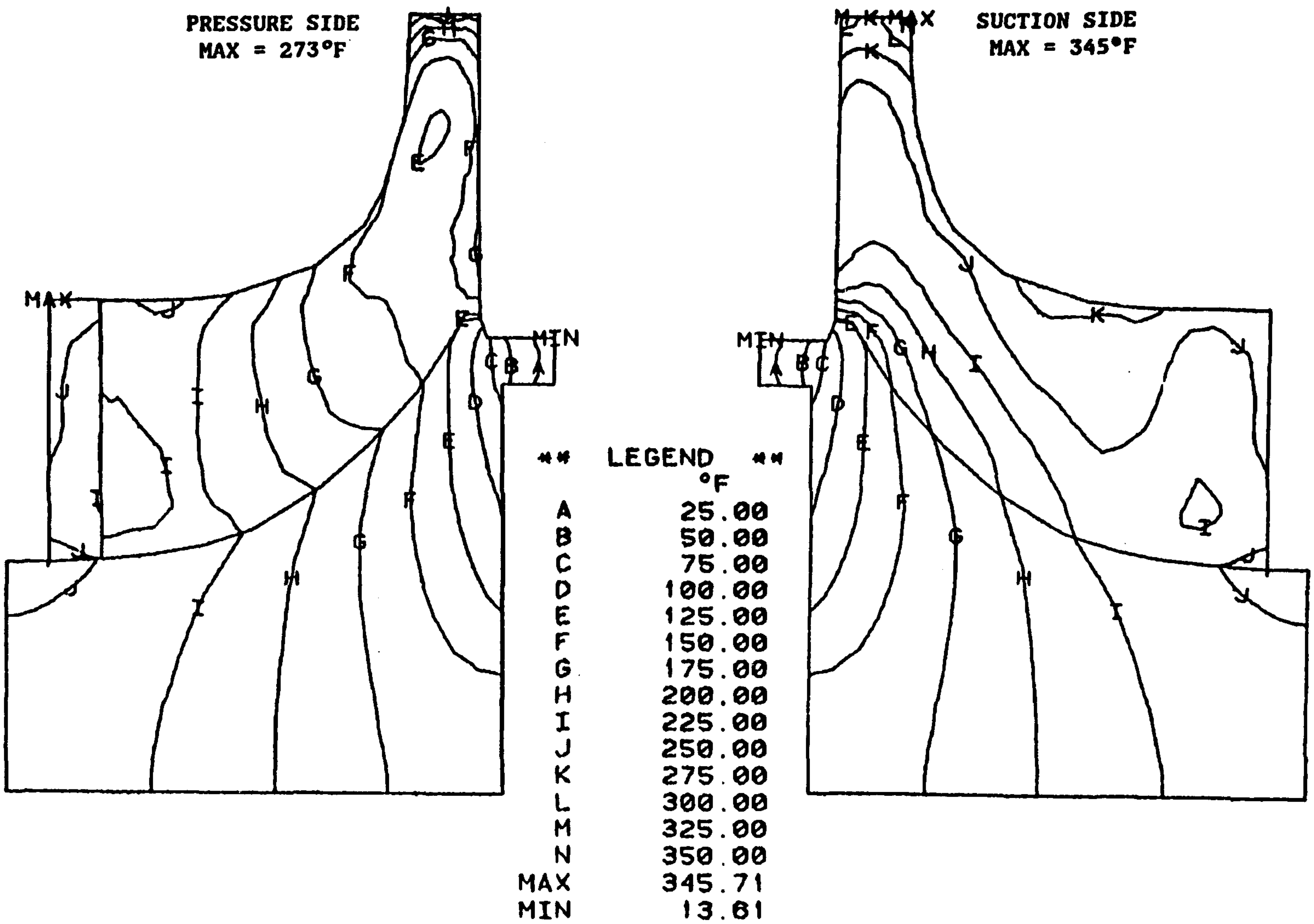


FIGURE 3.4-5 CALCULATED METAL TEMPERATURES, RIG TEST CONDITIONS

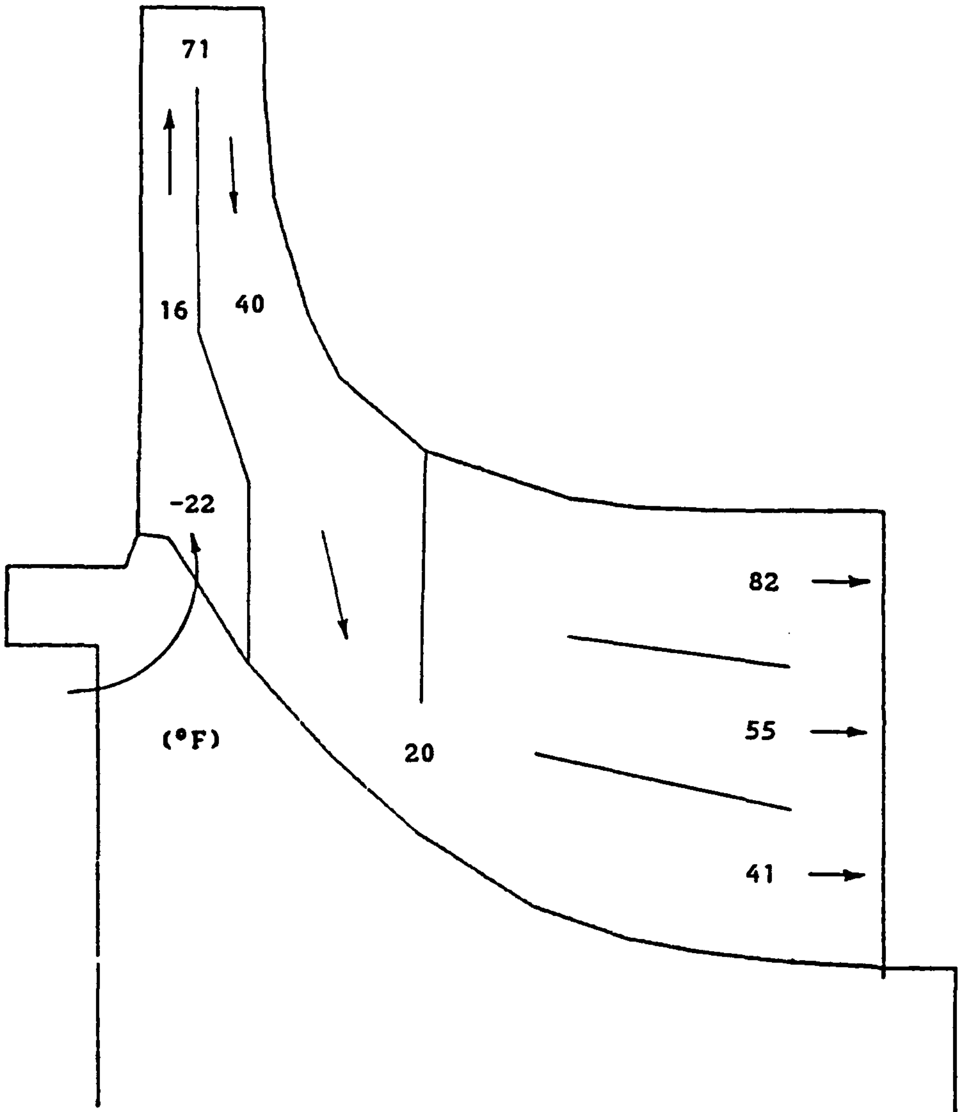


FIGURE 3.4-6 CALCULATED COOLANT TEMPERATURES, RIG TEST CONDITIONS

## 3.5 Test Rotor Fabrication

Two 13 bladed test rotors were fabricated. A solid rotor, fabricated without coolant passages, provides the capability of detailed aerodynamic testing including rotating static pressure measurements and is shown in Figure 4.5-1. A cooled or "hollow" rotor, fabricated with cooled passages in place, was designed for extensive heat transfer testing. Because of the large number and type of rotor instrumentation, two test rotors are required. Both rig rotors are designed to be compatible with the NASA Lewis Research Center's warm turbine test facility. Because of the reduced rotor stress loading at rig operating conditions, both rotors are designed to be single alloy castings, thus omitting the required fabrication of the PA101 hub and use of the HIP-bonding process. Fabrication of the cooled rotor was determined to be completely compatible with this fabrication technique.

Fabrication of the hollow rotor was accomplished using the ceramic cores of the type shown in Figure 3.5-2. Details of the coolant flow path within the highly wrapped blade are shown for both the blade pressure and suction surfaces. The wax replica of the cooled rotor with cores in place is shown in Figure 3.5-3. Core-mold attachment points are shown at the inducer tip and coolant discharge slot. Also shown are ceramic protrusions at the coolant inlet locations. A second view is shown in Figure 3.5-4.

Figures 3.5-5 and 6 show the final machined casting with integral cooling passages. A better appreciation of the cooling passages with in the casting is gained in Figures 3.5-7 through 11 showing a casting cut to reveal the interior geometry. It should be noted that the rotor cut to reveal interior geometry differs in one minor detail to the delivered rotor shown in Figure 3.5-5. The two "half-pins" in the second row of pin fins in the outer passage of the exducer were omitted in the rotor of Figure 3.5-7 through 11. This change in core tooling was made during late attempts to improve fabrication accuracy which proved unnecessary. No rotors cast in this late serial number group were final machined.

## 3.6 Rotor Spin Test

Prior to deliver of the machined solid bladed and air cooled metal rotors, a spin test was conducted to demonstrate mechanical integrity. Figures 3.6-1 and 2 show the rotor after successful test. The rough balance slots and spin arbor are shown.

## 4.0 Conclusions

An advanced air cooled metal rotor has been designed. A combination of series and parallel branched internal flow channels carrying coolant air flow of 4.3%, adequately cools the rotor for an inlet temperature of 2500°F. All fabrication limitations were considered in developing the successful design. Predicted rotor aerodynamics were enhanced through tailoring of blade angle distribution and hub contour shape to achieve improved blade loading distributions at the hub, mean, and shroud streamline positions.

Heat transfer and stress examinations indicate that the resulting design of the cooled metal radial turbine rotor is capable of meeting all rotor life and efficiency requirements. Hence the design of a cooled metallic radial turbine capable of operation at rotor inlet temperatures of 2500°F has been successfully completed.

The rotor is compatible with requirements of an advanced turbine engine utilizing a 14:1 compressor pressure ratio and a 2500°F rotor inlet temperature. Further effort shows promise in improving turbine efficiency through the comprehensive study of hub contour modification. Modification should be driven by aerodynamic performance improvement and developed in conjunction with heat transfer and stress optimization analyses.

FIGURE 3.5-1  FINAL MACHINED SOLID TURBINE ROTOR

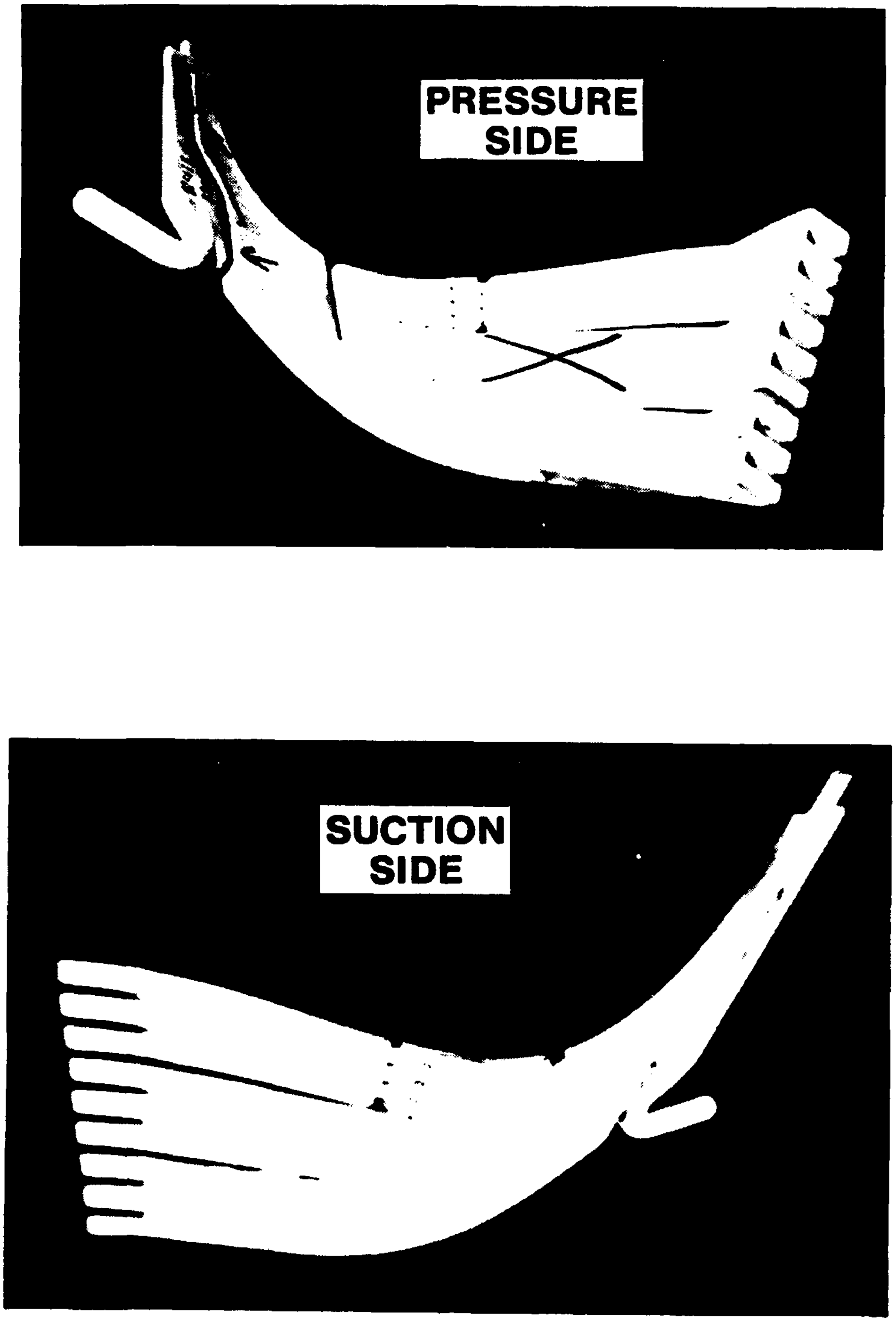


FIGURE 3.5-2 CERAMIC CORES USED TO CAST COOLANT FLOW PASSAGES

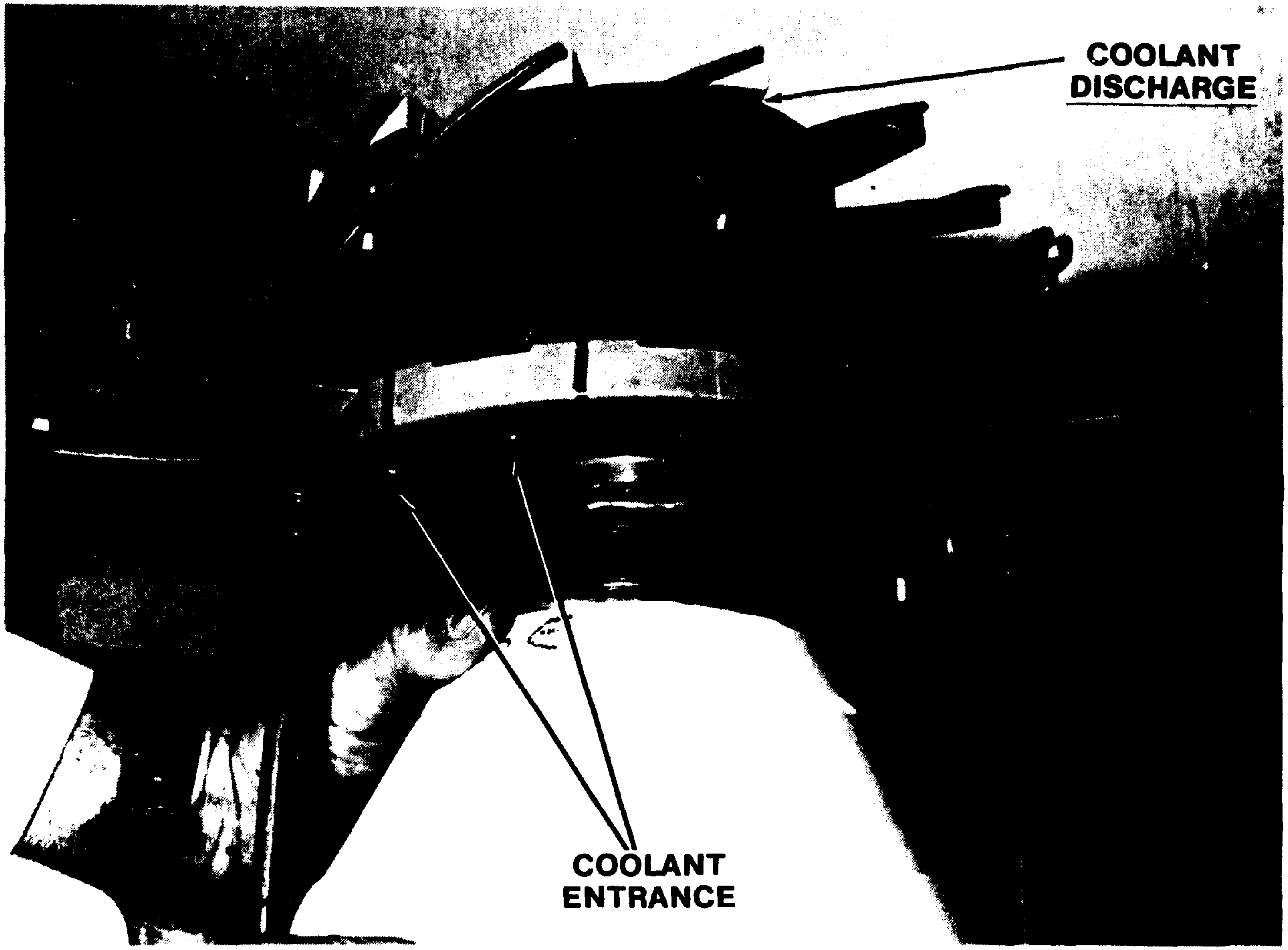


FIGURE 3.5-3  WAX REPLICA OF COOLED ROTOR

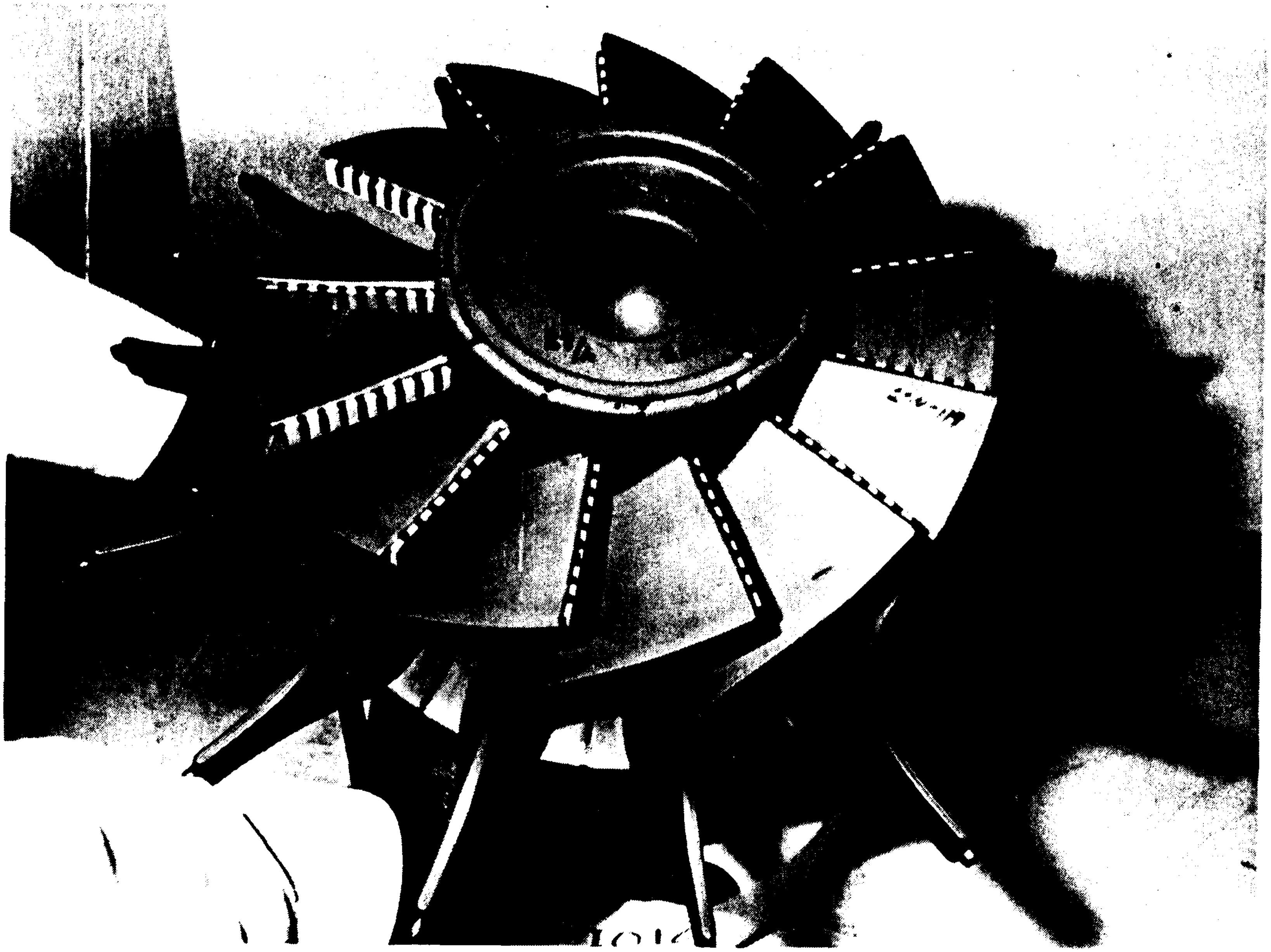

FIGURE 3.5- 4 WAX REPLICA OF COOLED ROTOR, EXDUCER END

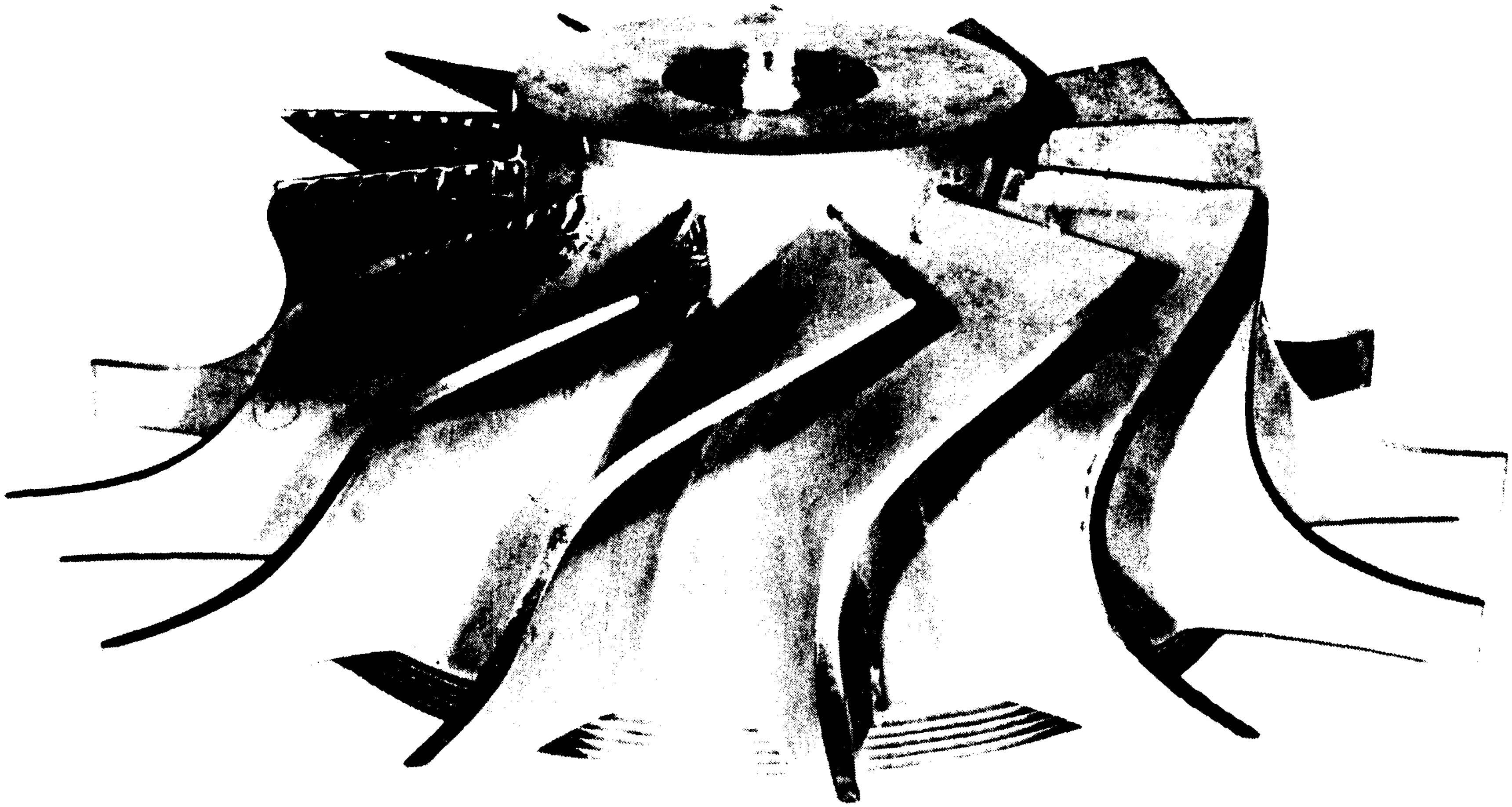

FIGURE 3.5-5 FINAL MACHINED AIR-COOLED TURBINE ROTOR

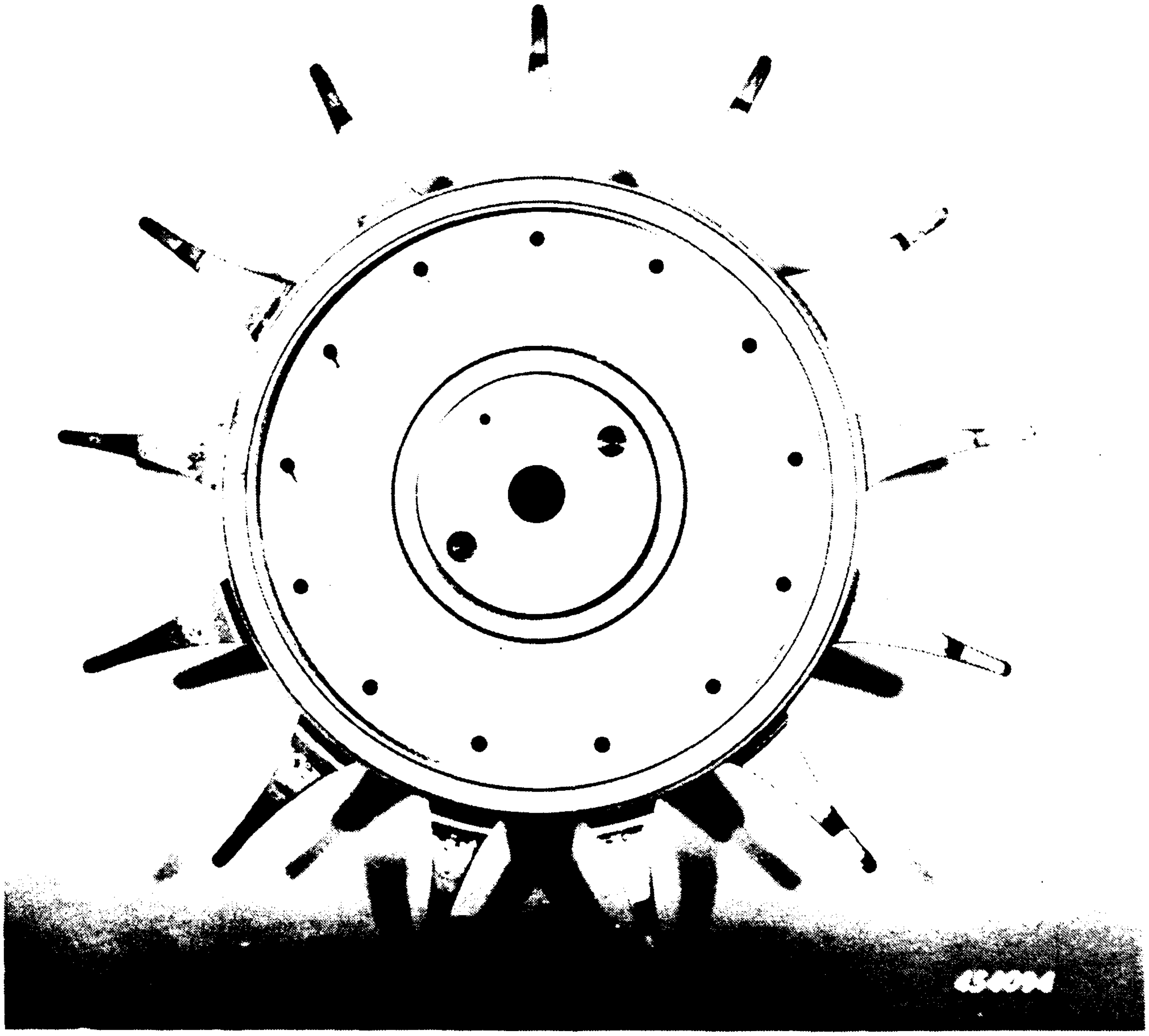

FIGURE 3.5-6 FINAL MACHINED AIR-COOLED TURBINE ROTOR

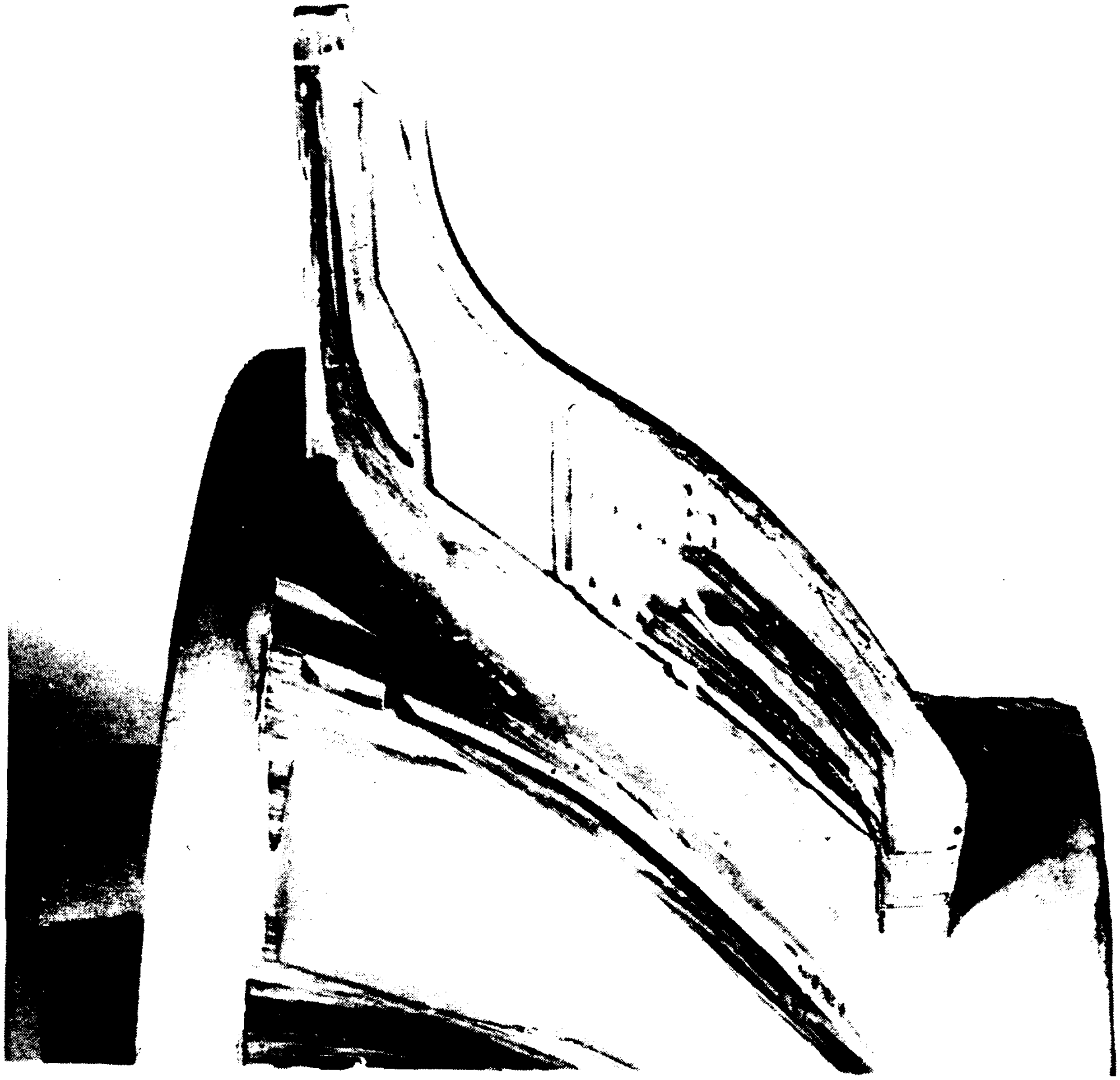

FIGURE 3.5-7 SECTIONED CASTING, PRESSURE SIDE

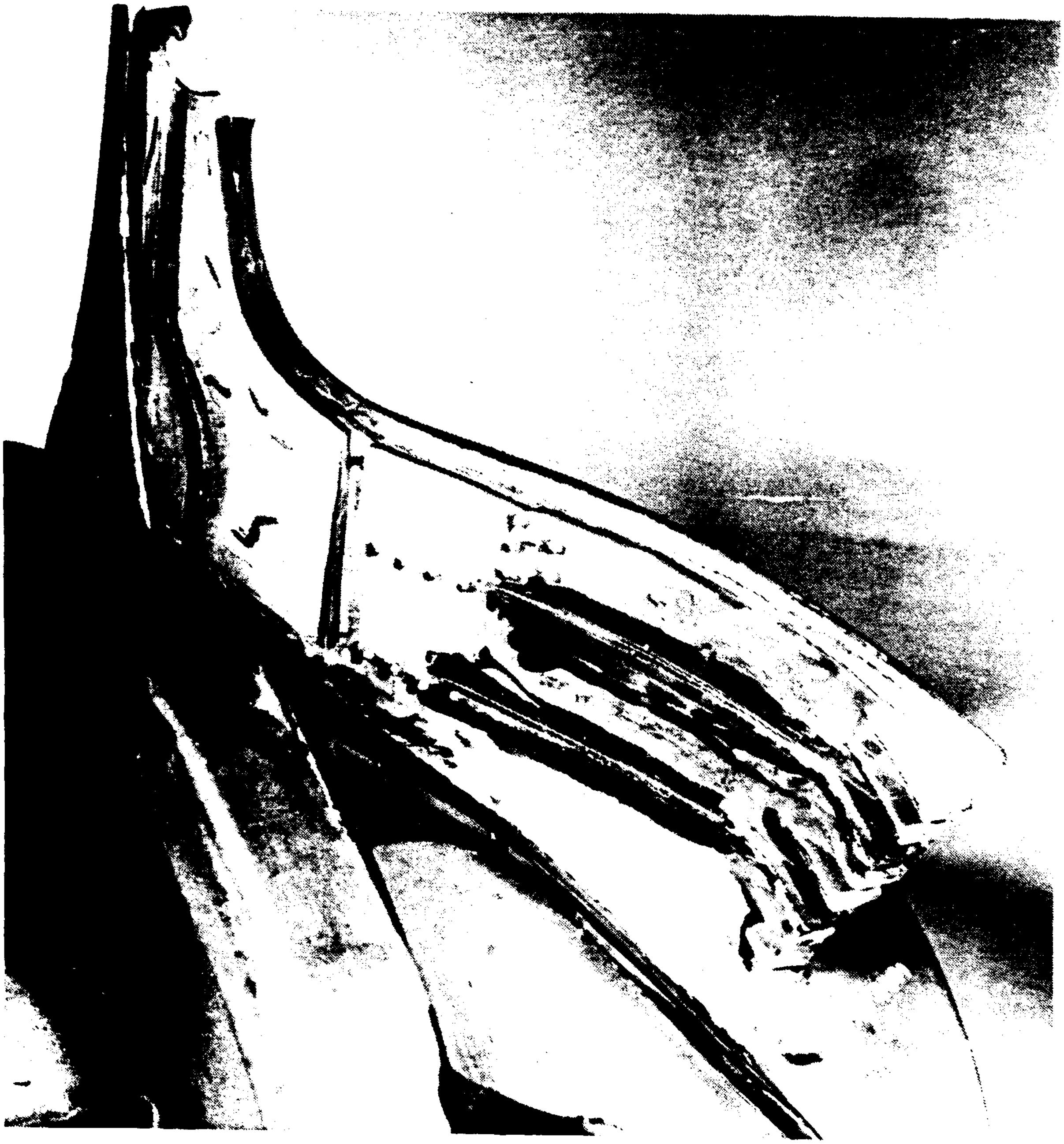

FIGURE 3.5-8 SECTIONED CASTING, PRESSURE SIDE

FIGURE 3.5-9 SECTIONED CASTING, SUCTION SIDE

FIGURE 3.5-10 SECTIONED CASTING, SUCTION SIDE

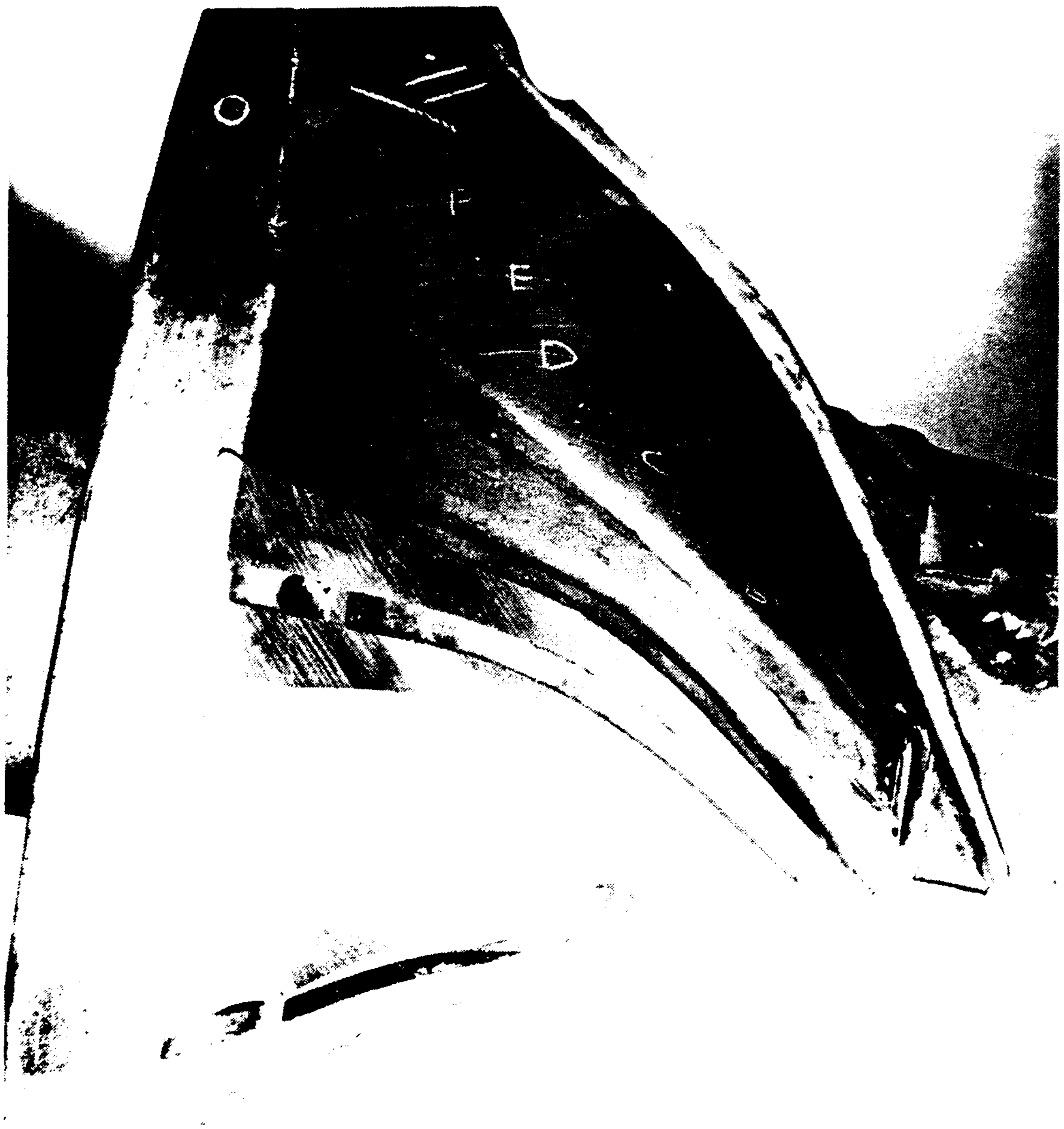

FIGURE 3.5-11  SECTIONED CASTING, BLADE HUB

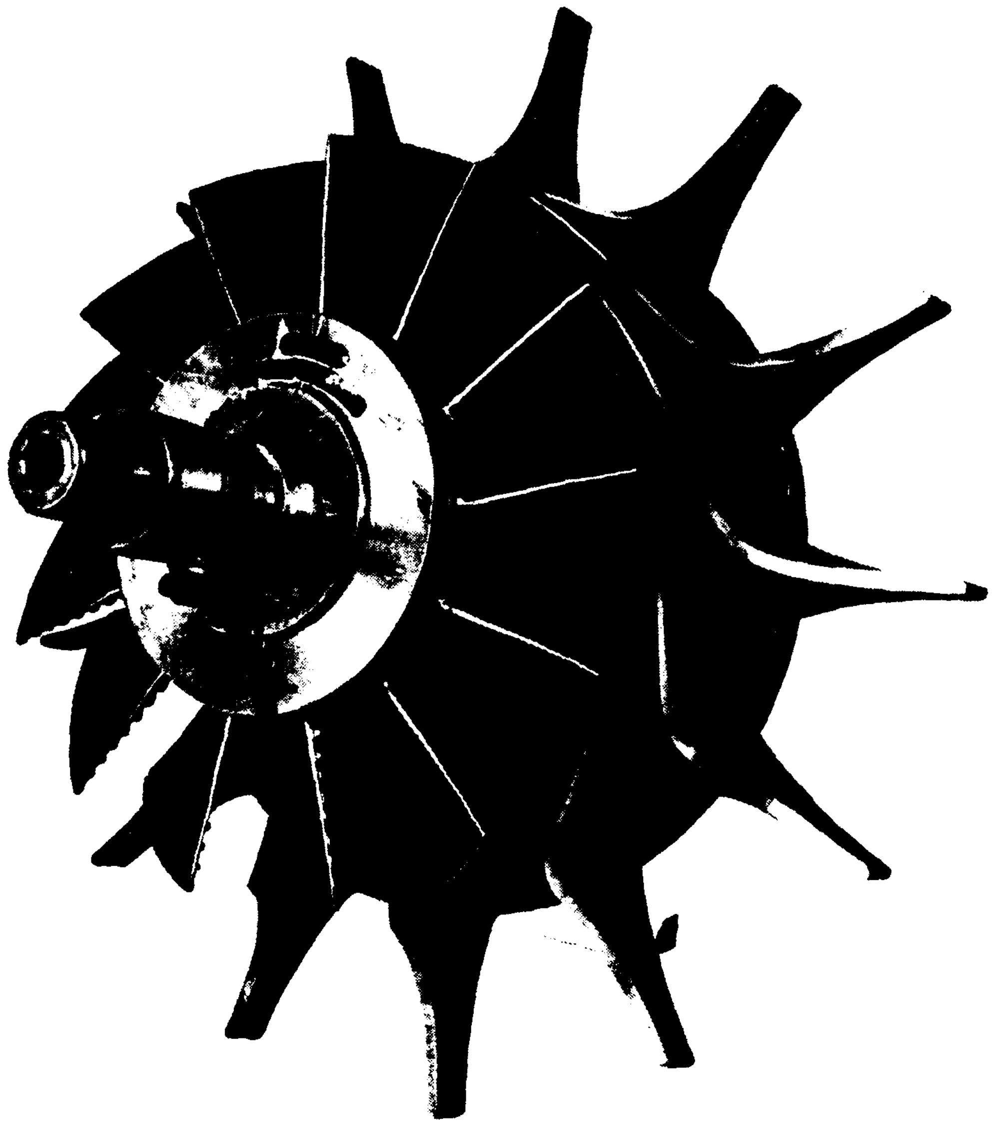

FIGURE 3.6-1 AIR-COOLED ROTOR, POST SPIN TEST

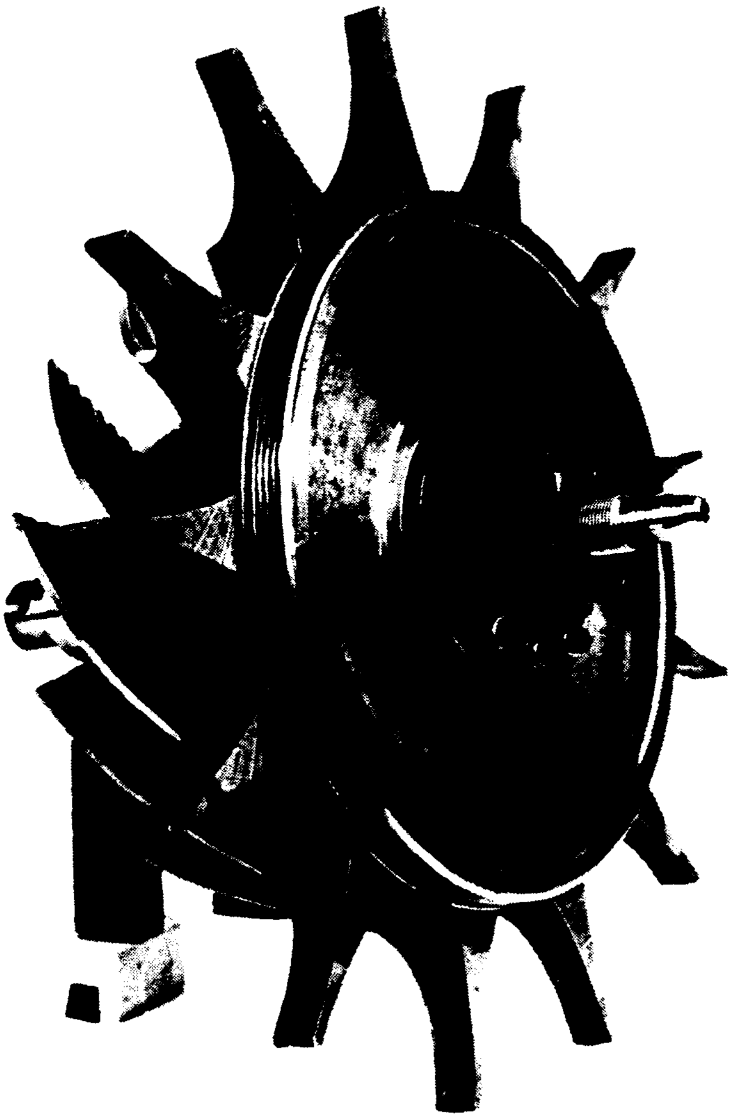

FIGURE 3.6-2 AIR-COOLED ROTOR - POST SPIN TEST

## 5.0 References


1. Snyder, P. H., "Cooled High-Temperature Radial Turbine Program, I - First Turbine Design", NASA CR-179606, May 1987.

2. Snyder, P. H., and Roelke, R. J., "The Design of an Air-Cooled Metalic High Temperature Radial Turbine", Journal of Propulsion and Power, Vol 26, No. 3, May-June 1990, pages 283-288.

3. Monson, D. S., and Ewing, B. A., "High-Temperature Radial Turbine Demonstration", USAAVRADCOM-TR-80-D-6, April 1980.

DISTRIBUTION LIST

COOLED HIGH-TEMPERATURE RADIAL TURBINE PROGRAM
II - FINAL REPORT
NAS3-24230

| | Number of Copies |
|---|---|
| NASA Lewis Research Center<br>21000 Brookpark Road<br>Attn: Report Control, MS 60-1<br>Cleveland, OH 44135 | 1 |
| NASA Lewis Research Center<br>21000 Brookpark Road<br>Attn: Library, MS 60-3<br>Cleveland, OH 44135 | 2 |
| NASA Lewis Research Center<br>21000 Brookpark Road<br>Attn: TU Office, MS 7-3<br>Cleveland, OH 44135 | 1 |
| NASA Lewis Research Center<br>21000 Brookpark Road<br>Attn: J. A. Ziemianski, MS 86-1<br>Cleveland, OH 44135 | 1 |
| NASA Lewis Research Center<br>21000 Brookpark Road<br>Attn: C. L. Ball, MS 86-1<br>Cleveland, OH 44135 | 1 |
| NASA Lewis Research Center<br>21000 Brookpark Road<br>Attn: W. Girard, MS 500-305<br>Cleveland, OH 44135 | 1 |
| NASA Lewis Research Center<br>21000 Brookpark Road<br>Attn: L. J. Bober, MS 77-6<br>Cleveland, OH 44135 | 1 |

## COOLED HIGH-TEMPERATURE RADIAL TURBINE PROGRAM
## DISTRIBUTION LIST

| | Number of Copies |
|---|---|
| NASA Lewis Research Center<br>21000 Brookpark Road<br>Attn: K. C. Civinskas, MS 77-6<br>Cleveland, OH 44135 | 10 |
| NASA Lewis Research Center<br>21000 Brookpark Road<br>Attn: P. L. Meitner, MS 77-12<br>Cleveland, OH 44135 | 1 |
| NASA Lewis Research Center<br>21000 Brookpark Road<br>Attn: R. W. Niedzwiecki, MS 77-10<br>Cleveland, OH 44135 | 1 |
| NASA Lewis Research Center<br>21000 Brookpark Road<br>Attn: R. Stabe, MS 6-9<br>Cleveland, OH 44135 | 1 |
| NASA Lewis Research Center<br>21000 Brookpark Road<br>Attn: D. DiCicco, MS 6-9<br>Cleveland, OH 44135 | 1 |
| NASA Lewis Research Center<br>21000 Brookpark Road<br>Attn: R. Gaugler, MS 5-11<br>Cleveland, OH 44135 | 1 |
| NASA Lewis Research Center<br>21000 Brookpark Road<br>Attn: D. C. Mikkelson, MS AAC-1<br>Cleveland, OH 44135 | 1 |

## COOLED HIGH-TEMPERATURE RADIAL TURBINE PROGRAM
## DISTRIBUTION LIST

| | Number of Copies |
|---|---|
| Sverdrup Technology, Inc.<br>Lewis Research Center Group<br>2001 Aerospace Parkway<br>Attn: L. Tirres<br>Brookpark, OH 44142 | 1 |
| Sverdrup Technology, Inc.<br>Lewis Research Center Group<br>2001 Aerospace Parkway<br>Attn: P. S. Simonyi<br>Brookpark, OH 44142 | 1 |
| Sverdrup Technology, Inc.<br>Lewis Research Center Group<br>2001 Aerospace Parkway<br>Attn: L. Tran<br>Brookpark, OH 44142 | 1 |
| NASA Headquarters<br>Attn: RP/N. Nijhawan<br>Washington, D.C. 20546 | 1 |
| NASA Headquarters<br>Attn: RP/J. R. Facey<br>Washington, D.C. 20546 | 1 |
| NASA Scientific and Technical Information Facility<br>P. O. Box 8757<br>Attn: Acquisition Branch<br>Baltimore/Washington International Airport<br>Baltimore, MD 21240 | 25 |
| Director<br>Aviation Applied Technology Directorate<br>U.S. Army Aviation Research and<br>Technology Activity - AVSCOM<br>Attn: SAVRT-TY-AT<br>Ft. Eustis, VA 23604-5577 | 2 |

## COOLED HIGH-TEMPERATURE RADIAL TURBINE PROGRAM
## DISTRIBUTION LIST

| | Number of Copies |
|---|---|
| Director<br>Aviation Applied Technology Directorate<br>U.S. Army Aviation Research and<br>Technology Activity - AVSCOM<br>Attn: SAVRT-TY-ATP (Sandra Hoff)<br>Ft. Eustis, VA 23604-5577 | 1 |
| Director<br>Advanced Systems Research Office - AVSCOM<br>Attn: SAVRT-R (Library)<br>M/S 219-3<br>Ames Research Center<br>Moffet Field, CA 94035-1000 | 1 |
| Commander<br>U.S. Army Aviation Systems Command<br>Attn: AMSAV - N<br>4300 Goodfellow Boulevard<br>St. Louis, MO 63120-1798 | 1 |
| Commander<br>U.S. Army Aviation Systems Command<br>Attn: AMSAV-EQP<br>4300 Goodfellow Boulevard<br>St. Louis, MO 63120-1798 | 1 |
| Commander<br>U.S. Army Aviation Systems Command<br>Attn: AMSAV-DIL (Ms. Feng)<br>4300 Goodfellow Boulevard<br>St. Louis, MO 63120-1798 | 4 |
| Commander<br>U.S. Army Mobility Equipment R&D Command<br>Attn: STRBE-ZT (Mr. T. Lovelace)<br>Ft. Belvoir, VA 22060 | 1 |

## COOLED HIGH-TEMPERATURE RADIAL TURBINE PROGRAM
## DISTRIBUTION LIST

| | Number of Copies |
|---|---|
| Director<br>U.S. Army Tank-Automotive R&D Command<br>Attn: AMSTA-RGE (Dr. R. Munt)<br>Warren, MI 48090 | 1 |
| The Pentagon<br>Room 1809, OSD/OUSDR&E (ET)<br>Attn: Dr. Donald Dix<br>Staff Specialist for Propulsion<br>Washington, D.C. 20301 | 1 |
| Director<br>Army Research Office<br>Attn: Dr. R. Singleton<br>P. O. Box 12211<br>Research Triangle Park, NC 27709-2211 | 1 |
| Commandant<br>U.S. Military Academy<br>Attn: Chief, Department of Mechanics<br>West Point, NY 10996 | 1 |
| Commander<br>Southwest Research Institute<br>U.S. Army Fuels and Lubricants<br>Research Laboratory<br>P. O. Drawer 28510<br>San Antonio, TX 78284 | 1 |
| Department of the Army<br>Aviation Systems Division<br>ODCSRDA (DAMA-WSA, R. Ballard)<br>Room B454, The Pentagon<br>Washington, D.C. 20310 | 1 |
| U.S. Army Materiel Systems Analysis Activity<br>Attn: DRXSY-MP (Mr. Herbert Cohen)<br>Aberdeen Proving Ground, MD 21005 | 1 |

## COOLED HIGH-TEMPERATURE RADIAL TURBINE PROGRAM
## DISTRIBUTION LIST

| | Number of Copies |
|---|---|
| Director, Turbopropulsion Laboratory<br>Code 67Sf<br>Naval Postgraduate School<br>Monterey, CA 93940 | 1 |
| U.S. Department of Energy<br>1000 Independence Avenue<br>Attn: Mr. Richard Alpaugh<br>Washington, D.C. 20585 | 1 |
| ORI, Inc.<br>1375 Piccard Drive<br>Attn: Mr. Bill Cleary<br>Associate Division Director<br>Rockville, MD 20850 | 1 |
| U.S. Army Aberdeen Proving Ground<br>Installation Support Activity<br>Attn: AMXSY-MP<br>Aberdeen Proving Ground, MD 21005 | 1 |
| Wright Research and Development Center<br>Attn: Robert E. Gray<br>Mail Code POTC<br>Dayton, OH 45433 | 1 |
| Wright Research and Development Center<br>Attn: W. Troha<br>Mail Code POTC<br>Dayton, OH 45433 | 1 |
| General Electric Aircraft Engines<br>Attn: B. Gregory, MS A322<br>One Neumann Way<br>Cincinnati, OH 45215-6301 | 1 |

COOLED HIGH-TEMPERATURE RADIAL TURBINE PROGRAM
DISTRIBUTION LIST

| | Number of Copies |
|---|---|
| General Electric Aircraft Engines<br>Attn: D. Evans, MS A34034<br>1000 Western Avenue<br>Lynn, MA 01910 | 1 |
| Allison Gas Turbine Division<br>General Motors Corporation<br>Attn: P. Tramm<br>P. O. Box 420<br>Indianapolis, IN 46206-0420 | 1 |
| Allison Gas Turbine Division<br>General Motors Corporation<br>Attn: P. Snyder<br>P. O. Box 420<br>Indianapolis, IN 46206-0420 | 10 |
| United Technologies Research Center<br>Attn: B. Johnson<br>Silver Lane<br>East Hartford, CT 06108 | 1 |
| United Technologies Research Center<br>Attn: R. Dring, MS 16<br>Silver Lane<br>East Hartford, CT 06108 | 1 |
| United Technologies Research Center<br>Attn: M. Blair, MS 16<br>Silver Lane<br>East Hartford, CT 06108 | 1 |
| Pratt & Whitney<br>Government Engine Business<br>Attn: F. Huber, MS 715-92<br>P. O. Box 109600<br>West Palm Beach, FL 33410 | 1 |

COOLED HIGH-TEMPERATURE TURBINE PROGRAM
DISTRIBUTION LIST

| | Number of Copies |
|---|---|
| Pratt & Whitney<br>Government Engine Business<br>Attn: A. Fredmonski, MS 715-92<br>P. O. Box 109600<br>West Palm Beach, FL 33410 | 1 |
| Pratt & Whitney<br>Commercial Engine Business<br>Attn: O. Sharma, MS 163-01<br>400 Main Street<br>East Hartford, CT 06108 | 1 |
| Pratt & Whitney<br>Commercial Engine Business<br>Attn: S. Tanrikut, MS 163-01<br>400 Main Street<br>East Hartford, CT 06108 | 1 |
| Pratt & Whitney Canada, Inc.<br>Attn: U. Okapuu<br>C. P. 10<br>Longueuil, Quebec J4K 4X9<br>CANADA | 1 |
| Garrett Engine Division<br>Attn: Bill Waterman<br>P. O. Box 5217<br>Phoenix, AZ 85010 | 1 |
| Sundstrand Corp.<br>Attn: Colin Rodgers<br>P. O. Box 85757<br>San Diego, CA 92186-5757 | 1 |
| Textron Lycoming<br>Attn: Rick Bozzola<br>550 Main Street<br>Stratford, CT 06497-2452 | 1 |

COOLED HIGH-TEMPERATURE RADIAL TURBINE PROGRAM
DISTRIBUTION LIST

| | Number of Copies |
|---|---|
| Textron Lycoming<br>Attn: George Minkkinen<br>550 Main Street<br>Stratford, CT 06497-2452 | 1 |
| Teledyne CAE<br>Attn: Eli Benstein<br>1330 Laskey Road<br>P. O. Box 6971<br>Toledo, OH 43612 | 1 |
| Teledyne CAE<br>Attn: Casimir Rogo<br>1330 Laskey Road<br>P. O. Box 6971<br>Toledo, OH 43612 | 1 |
| Williams International<br>Attn: Ron Pampreen<br>2280 W. Maple Road<br>P. O. Box 200<br>Walled Lake, MI 48088 | 1 |